Universidade Federal do Rio de Janeiro

Centro de Ciências da Saúde

Faculdade de medicina

Hospital Universitário Clementino Fraga Filho

Instituto de Cardiologia Edson Saad

Programa de Pós-Graduação em Medicina Cardiologia

Validação de Estratégias para Redução de Radiação na Cintilografia Miocárdica de Perfusão (CMP): Protocolo Rápido com Baixa Dose em Gama-Câmara CZT e Valor Prognóstico da CMP em Pacientes com DAC Conhecida e Alta Capacidade de exercício

Thaís Ribeiro Peclat Monteiro

Rio de Janeiro

Outubro/2019

Validação de Estratégias para Redução de Radiação na Cintilografia Miocárdica de Perfusão (CMP): Protocolo Rápido com Baixa Dose em Gama-Câmara CZT e Valor Prognóstico da CMP em Pacientes com DAC Conhecida e Alta Capacidade de exercício

Thaís Ribeiro Peclat Monteiro

Tese de doutorado apresentada ao Programa de Pós-Graduação em Medicina (Cardiologia) do Departamento de Clínica Médica da Faculdade de Medicina e do Instituto do Coração Edson Saad da Universidade Federal do Rio de Janeiro, como requisito final para obtenção de grau de Doutora em Cardiologia.

Orientador: Ronaldo de Souza Leão Lima

Rio de Janeiro

Outubro/2019

Validação de Estratégias para Redução de Radiação na Cintilografia Miocárdica de Perfusão (CMP): Protocolo Rápido com Baixa Dose em Gama-Câmara CZT e Valor Prognóstico da CMP em Pacientes com DAC Conhecida e Alta Capacidade de exercício

Thaís Ribeiro Peclat Monteiro

ORIENTADOR: Prof. Ronaldo de Souza Leão Lima

Tese de Doutorado apresentada ao Programa de Pós-Graduação em Medicina (Cardiologia) do Departamento de Clínica Médica da Faculdade de Medicina e do Instituto do Coração Edson Saad da Universidade Federal do Rio de Janeiro, como requisito final para obtenção de grau de Doutora em Cardiologia.

Aprovada por:

_____

Presidente, Prof. Dr. Paolo Blanco Villela

_____

Prof. Dr. Paulo Henrique Rosado de Castro

_____

Dr. Gustavo Luiz Gouvêa de Almeida jr

Rio de Janeiro

Outubro/2019

FICHA CATALOGRÁFICA

RESUMO

Validação de Estratégias para Redução de Radiação na Cintilografia Miocárdica de Perfusão (CMP): Protocolo Rápido com Baixa Dose em Gama-Câmara CZT e Valor Prognóstico da CMP em Pacientes com DAC Conhecida e Alta Capacidade de exercício

Thaís Ribeiro Peclat Monteiro

ORIENTADOR: Prof. Ronaldo de Souza Leão Lima

Resumo da Tese de Doutorado submetida ao Programa de Pós-Graduação em Medicina (Cardiologia) do Departamento de Clínica Médica da Faculdade de Medicina e do Instituto do Coração Edson Saad da Universidade Federal do Rio de Janeiro, como requisito final para obtenção de grau de Doutora em Cardiologia.

Introdução: O aumento da exposição à radiação de origem médica tem se destacado de forma relevante na atualidade. A Cintilografia miocárdica de perfusão (CMP) é um dos principais métodos diagnósticos e prognósticos utilizados na doença arterial coronariana (DAC). Apesar de sua ampla adoção, este método apresenta a desvantagem de depender do uso de radiofármacos. A fim de garantir a adequação deste método de imagem ao príncipio de exposição mínima à radiação determinado pelos órgãos competentes, foi estabelecido um conjunto de estratégias. Entre outros, elas objetivam a utilização de protocolos com redução da dose e a melhoria do critério de indicação da CMP para pacientes com DAC conhecida que atingiram ≥ 10 METs. **Objetivo**: Validar o valor prognóstico do uso de um protocolo rápido e com baixa dose em gama-câmara (GC) CZT e da CMP em pacientes com DAC conhecida e alta capacidade de exercício, a fim de melhor adequar o uso da CMP em relação a estas estratégias. **Métodos:** Para avaliação do valor prognóstico da GC CZT, foi analisada uma coorte de 2930 pacientes submetidos à CMP nesta GC, entre 2011 e 2012. Para comparação do valor prognóstico desta GC com as tradicionais, 6128 pacientes submetidos ao exame entre 2008 e 2012, foram estudados, sendo separados em dois grupos de 1777 pacientes de acordo com a GC usada, equiparados através de escore de propensão. Por fim, desta mesma coorte, 926 pacientes com DAC conhecida e submetidos à CMP, entre 2008 e 2012, com estresse por exercício pelo protocolo de Bruce, foram analisados. O protocolo em GC CZT foi de 1 dia, com uso de 99mTC-sestamibi, começando com repouso (185-222 MBq) seguido pelo estresse (666–740 MBq). Os tempos de aquisição foram, respectivamente, de 6 e 3 min. Na GC Anger, foi utilizado protocolo de dois dias, com estresse (10-12 mCi) e repouso (15-18 mCi) adquiridos em 6 minutos. A CMP foi classificada em normal e anormal e a soma dos escores de estresse, repouso e diferença (SSS, SRS, SDS), calculados. Eventos duros foram considerados infarto agudo do miocárdio (IAM) não-fatal e morte por todas as causas **Resultados:** A dosimetria média utilizada nos exames em GC CZT foi de 6 mSv e o tempo médio total de exame

foi de 48±13 min. A taxa anual de evento duro e revascularização tardia foram maiores em pacientes com maior extensão de defeito e isquemia. Pacientes com DAC conhecida e ≥ 10 METs com exame anormal tiveram maior taxa anualizada de eventos duros em comparação com aqueles com exames normais no mesmo grupo. **Conclusão:** Um protocolo mais rápido e com menor radiação em GC CZT manteve a habilidade de estratificar pacientes com maior risco de eventos, mostrando prognóstico similar ao obtido em GC Anger. A CMP foi capaz de estratificar pacientes com DAC conhecida que atingiram ≥ 10 METs para a ocorrência de IAM não-fatal e morte por todas as causas.

ABSTRACT

Validation of Radiation Reduction Strategies on Myocardial Perfusion Imaging (MPI): A Fast, Low-Dose Protocol in a CZT Gamma Camera and the Prognostic Value of MPI in Patients with Known CAD and High Exercise Capacity

Thaís Ribeiro Peclat Monteiro

ORIENTADOR: Prof. Ronaldo de Souza Leão Lima

Abstract da Tese de Doutorado submetida ao Programa de Pós-Graduação em Medicina (Cardiologia) do Departamento de Clínica Médica da Faculdade de Medicina e do Instituto do Coração Edson Saad da Universidade Federal do Rio de Janeiro, como requisito final para obtenção de grau de Doutora em Cardiologia.

Introduction: Increased exposure to radiation of medical origin has been prominently highlighted nowadays. Myocardial perfusion imaging (MPI) is one of the main diagnostic and prognostic methods used in coronary artery disease (CAD). Despite its wide adoption, this method has the disadvantage of relying on the use of radiopharmaceuticals. In order to ensure the adequacy of this imaging method to the principle of minimum radiation exposure determined by the competent agencies, a set of strategies was defined. Among others, they aim at the use of lower dose protocols and the improvement of MPI indication criteria for patients with known CAD who achieved ≥ 10 METs. **Objective:** To validate the prognostic value of the use of a fast, low-dose gamma camera (GC) CZT and MPI protocol in patients with known CAD and high exercise capacity, in order to better match the use of MPI to these strategies. **Methods:** To assess the prognostic value of the CZT GC, a cohort of 2930 patients who underwent CMP in this GC between 2011 and 2012 was analyzed. These were studied and divided into two groups of 1777 patients according to the used GC, matched by propensity score. Finally, from this same cohort, 926 patients with known CAD who underwent exercise MPI using the Bruce protocol, between 2008 and 2012, were analyzed. The CZT GC protocol was 1 day, using 99mTC-sestamibi, starting with rest (185-222 MBq) followed by stress (666–740 MBq). The acquisition times were, respectively, 6 and 3

min. With the Anger GC, we used a two-day protocol, with stress (10-12 mCi) and rest (15-18 mCi) acquired within 6 minutes. The MPI was classified as normal and abnormal and the sum of stress, rest and difference (SSS, SRS, SDS) scores calculated. Hard events were considered nonfatal acute myocardial infarction (MI) and all-cause mortality. **Results:** The mean dosimetry used in CZT GC scans was 6 mSv and the total mean examination time was 48 ± 13 min. The annual rate of hard events and late revascularizations were higher in patients with greater extent of defect and ischemia. Patients with known CAD and ≥ 10 METs with abnormal scans had a higher annualized rate of hard events compared with those with normal scans in the same group. **Conclusion:** A faster and lower radiation dose protocol in GC CZT maintained the ability to stratify patients at higher risk of events, showing similar prognosis to that obtained in Anger GC. MPI was able to stratify patients with known CAD who reached ≥ 10 METs for nonfatal MI and all-cause mortality.

LISTA DE FIGURAS

Introduçao e revisão de literatura:

Artigo 1:

Artigo 2:

Artigo 3:

LISTA DE TABELAS

Introduçao e revisão de literatura:

Artigo 1:

Artigo 2:

Artigo 3:

LISTA DE ABREVIATURAS E SIGLAS

Termos em lingua portuguesa:

CMP Cintilografia miocárdica de perfusão

DAC Doença arterial coronariana

DCV Doenças cardiovasculares

GC Gamacâmara

IAM Infarto agudo do miocárdio

SCA Síndrome coronariana aguda

SCC Síndrome coronariana crônica

SUS Sistema Único de Saúde

TE Teste ergométrico

Gy Gray

SI Sistema internacional

Sv Sievert

Termos em língua inglesa

ALARA As low as reasonable achievable

BMI Body mass index

CABG Coronary artery bypass graft

CAD Coronary artery Disease

ECG electrocardiography

EF Ejection Fraction

LVEF Left ventricle Ejection Fraction

MAPHR Maximum age-predicted heart rate

METs Metabolic Equivalents

MI Myocardial Infarction

MPI Myocardial perfusion imaging

MPS Myocardial perfusion SPECT

SDS Summed difference scores

SPECT single photon emission computed tomography

SRS Summed rest scores

SSS Summed stress scores

PCI Percutaneous coronary intervention

TPD Total Perfusion Defect

UNSCEAR United Nations Scientific Committee on the Effecys of Atomic Radiation

ASNC American Society of Nuclear Cardiology

SUMÁRIO

1 Introdução e revisão da literatura

1.1 Doença Arterial Coronariana

1.1.1 Epidemiologia e relevância

A doença arterial coronariana (DAC) é o tipo mais comum de doença cardiovascular (DCV) e representa um grave problema de saúde pública tanto em países desenvolvidos quanto em países subdesenvolvidos, devido a sua alta morbimortalidade.

Estima-se que 153,5 milhões de pessoas vivam com DAC em todo o mundo, com prevalência maior em homens (86,5 milhões)[1]. Segundo estatísticas publicadas pela American Heart Association em 2019, a prevalência de DAC nos Estados Unidos é de 6,7% em adultos acima de 20 anos de idade, aproximadamente 18,2 milhões de pessoas. De acordo com este mesmo órgão, calcula-se que um infarto agudo do miocárdio (IAM) ocorra, aproximadamente, a cada 40 segundos, com incidência de 605.000 novos casos e 200.000 casos recorrentes. Desse total, estima-se que 170.000 sejam silenciosos[2].

Apesar da mortalidade por DAC estar em constante declínio ao longo das últimas quatro décadas[2; 3], em geral atribuído aos diversos avanços ocorridos na medicina no tangente à prevenção, diagnóstico, prognóstico e tratamento, ela permanece como líder das causas de morte no mundo[1]. Nos Estados Unidos, a DAC é responsável por um terço das mortes que ocorrem em pessoas acima de 35 anos[4]. No Brasil, as DCV foram responsáveis por 31,2% das mortes em 2015 e também apresentam declínio em relação a dados de 1990[5]. Devido a sua relevante morbimortalidade, a DAC gera altos custos ao sistema de saúde mundial. Os custos diretos estimados gerados pela DAC nos Estados Unidos entre 2014 e 2015 foi de US$109,4 bilhões segundo dados obtidos atraves do Medical Expenditure Panel Survey, gerado pelo National Heart, Lung, and Blood Institute. Ademais, projeta-se um aumento de aproximadamente 100% nos custos

médicos relacionados a DAC entre 2015 e 2030 [2]. No Brasil, foi estimado um custo direto de R$ 500 milhões associado a IAM em 2011 sob a perspectiva do Sistema Único de Saúde (SUS). Quando considerados custos diretos e indiretos (reabilitação, efeitos sociais da doença crônica, etc.) o custo foi de R$ 3,8 bilhões neste mesmo ano[6].

1.1.2 Fisiopatologia e classificação

A DAC ocorre por consequência do depósito e acúmulo de placas de ateroma na parede interna das artérias coronárias, resultando em progressiva diminuição do lúmen ou alteração do tônus arterial. A aterosclerose é uma doença inflamatória crônica, progressiva e dinâmica e sua manifestação clínica na DAC mostra-se de forma correspondente ao seu caráter patológico, apresentando-se sob as formas subclínica, estável ou aguda.

A fase subaguda caracteriza-se por um estágio assintomático no qual a lesão ateromatosa está presente, porém não provoca redução significativa do lúmen arterial de forma a afetar o duplo produto cardíaco. A DAC aguda está presente no contexto das síndromes coronarianas agudas (SCA) que abrangem o IAM com e sem supradesnivelamento de ST e a angina instável. Estes ocorrem tipicamente devido a um processo agudo de aterotrombose secundário a ruptura ou erosão de uma placa de ateroma. A DAC estável é considerada aquela na qual há DAC suspeita com presença de sintomas anginosos estáveis ou DAC conhecida, porém com sintomatologia controlada ou estabilizada através de tratamento clínico otimizado. Em diretriz publicada recentemente, a European Society of Cardiology (ESC)[7] revisou o termo "estável", optando por adotar a terminologia "crônica". Segundo este documento, os grupos de pacientes considerados como portadores da síndrome coronariana crônica (SCC) são:

- Pacientes com DAC suspeita ou sintomas de angina estável e/ou dispneia;
- Pacientes com DAC suspeita e início recente de insuficiência cardíaca ou disfunção de ventrículo esquerdo;
- Pacientes com DAC conhecida (SCA e/ou revascularização prévia) assintomáticos ou com sintomas estáveis;
- Pacientes sintomáticos com suspeita de angina vasoespástica ou doença microvascular;
- Pacientes assintomáticos nos quais DAC é encontrada em exames solicitados como *screening*.

1.1.3 Abordagem diagnóstica e estratificação de risco na DAC crônica

A definição do teste a ser usado para diagnóstico de DAC crônica varia em função da probabilidade pré-teste de o paciente ter a doença. Em pacientes nos quais o diagnóstico de DAC é incerto ou não pode ser excluído apenas com avaliação clínica, o uso de testes não-invasivos é recomendado para estabelecimento do diagnóstico e estratificação de risco. A decisão por encaminhamento direto para a coronariocineangiografia (CAT) é reservada para pacientes com alto risco, irresponsivos a terapia médica ou com angina a leves esforços.

A Cintilografia miocárdica de perfusão (CMP) é um dos principais testes não-invasivos para avaliação de DAC, apresentando importância tanto no cenário de DAC suspeita (nova ou por mudança de estágio de uma doença conhecida estável) quanto para estratificação de risco em pacientes com DAC conhecida. Além de sua importância pelo estabelecido valor diagnóstico e prognóstico, a CMP se destaca por ser um teste funcional, capaz de detectar mudanças mínimas no fluxo coronariano. Dentre os testes não-invasivos, a CMP é recomendada em pacientes com intermediária a alta

probabilidade pré-teste (classe I, nivel de evidencia A), não havendo benefício estabelecido na realização do exame em pacientes com baixo risco pré-teste.

1.2 Cintilografia Miocárdica de perfusão

1.2.1 Origem da Cardiologia Nuclear

Foi Hermann Blumgart, auxiliado por Otto C. Yens, em 1925, o responsável pelas pioneiras descobertas envolvendo radioatividade e cardiologia. Utilizando, elegantemente, radônio dissolvido em soro como marcador radionuclídeo e uma câmara Wilson modificada como detector, suas invenções permitiram os primeiros estudos hemodinâmicos não invasivos, capazes de, ainda que sem formação de imagem, medir o tempo da circulação sanguínea de um membro superior ao outro [8]. Pouco depois, na década de 1940, Myron Prinzmetal desenvolveu o conceito da radiocardiografia, permitindo a medição do débito cardíaco, volume sanguíneo e tempo de trânsito circulatório através de uma sonda de iodeto de sódio marcada com albumina. As descobertas de Blumgart e Prinzmetal foram a base inicial para os posteriores estudos hemodinâmico em modelos fisiológicos e patológicos, nas décadas de 1950 e 1960 [9]. Contudo, Hal O Anger foi quem, em 1957, revolucionou a radiologia e propiciou o surgimento da cardiologia nuclear como especialidade, ao inventar a primeira câmara de cintilação. A gamacâmara (GC) Anger possibilitou a obtenção de imagens com alta resolução, dinâmicas e capazes de capturar todo um órgão em uma mesma imagem, essas sendo suas mais significativas vantagens em relação ao scanner retilíneo inventado por Benedict Cassen, poucos anos antes.

O modelo de GC desenvolvido por Anger é utilizado até os dias de hoje e consiste em um colimador de chumbo capaz de focalizar a radiação gama proveniente do corpo do paciente sobre placas formadas por cristais detectores de iodeto de sódio,

que cintilam ao receber esta radiação. A cintilação é então captada por tubos fotomultiplicadores capazes de amplificar o sinal recebido e o transformar em pulso eletrônico, que é então reconhecido por um computador acoplado a GC. O somatório da contagem dos pulsos eletrônicos determina a quantidade da presença do fármaco utilizado em cada ponto da imagem[10].

1.2.2 Estabelecimento do valor diagnostico e prognostico da CMP

Foi em 1973 que o conceito de isquemia induzida por exercício foi capturado em imagem por Zaret, Strauss e colegas. Estes demonstraram pela primeira vez a heterogeneidade de distribuição do radiotraçador após estresse físico e sua reversão nas imagens obtidas em repouso. No mesmo ano, a introdução do Tálio-201 como radiotraçador de baixa energia possibilitou uma série de avanços no desenvolvimento da cardiologia nuclear, que culminariam no estabelecimento do valor diagnóstico da CMP [11; 12; 13; 14].

Ao estabelecerem de forma pioneira a capacidade de estratificação de risco de IAM com uso de Tálio, Gibson e Beller inauguraram, em 1983, uma nova era de descobertas no campo da imagem cardiovascular[15]. Foi a partir de então, que o valor prognóstico da CMP passou a ser amplamente investigado, em concomitância com o surgimento de sucessivas tecnologias que aperfeiçoaram a qualidade e complexidade da CMP, como o SPECT e o ECG-gated.

Em função de ser um método não invasivo, capaz de fornecer informação funcional e territorial e com valor diagnóstico e prognóstico estabelecidos, a CMP se tornou o exame com melhor custo-benefício tanto para a população de pacientes com risco intermediário de DAC suspeita quanto para acompanhamento de pacientes com DAC conhecida[16]. Com isso, se tornou um método cada vez mais difundido, apesar do

surgimento de novas modalidades de imagem cardiovascular. Apenas nos Estados Unidos, em 2008, foi realizado um total de 8,5 milhões de CMP, representando um crescimento de 370% em comparação ao ano de 2004[17].

1.3 Radiação e Cintilografia Miocárdica de perfusão

O aumento na realização de exames de CMP foi concomitante à elevação do uso de radiação em outras áreas da medicina, criando uma preocupação relacionada aos efeitos consequentes a esse aumento.

1.3.1 Radiação Absorvida, Equivalente e Efetiva

Para entendermos os efeitos da radiação e os protocolos de regulação da mesma, é necessário pontuar os princípios pelos quais ela é medida e definida. Algumas das definições básicas necessárias para este entendimento são as de radiação absorvida, equivalente e efetiva.

Radiação absorvida é a quantidade de energia absorvida por unidade de massa por qualquer tipo de material e é representada pela unidade gray (Gy) no Sistema Internacional de Unidades (SI). Ainda que exposto a mesma quantidade de energia, cada tipo de tecido pode apresentar uma resposta biológica diferente. A dose de radiação que um tecido biológico absorve, ajustada pelo nível de sensibilidade do tecido ao tipo de radiação empregada, é chamada de dose equivalente. O risco de radiação para o paciente é medido a partir da dose efetiva, que representa o somatório das doses equivalentes. Ambas são representadas pela unidade Sievert (Sv) no SI.

Após a administração de um radiofármaco a um paciente, não é possível medir diretamente a dose a que um tecido ou órgão foi especificamente exposto. Em geral, é feito um cálculo baseado em um modelo computadorizado[9].

1.3.2 Riscos associados à radiação

Hermann Muller foi o primeiro cientista a demonstrar, em 1927, a associação entre a exposição à radiação e à mutação genética e o câncer. Foi ele quem determinou, conforme expresso em seu discurso como ganhador do prêmio Nobel por esses achados, que o risco imposto pela radiação é diretamente proporcional à dosimetria a que se é exposto, não havendo uma dose limiar[18; 19; 20].

A partir do princípio estabelecido por Hermann, configurou-se um modelo de dose-resposta para calcular a probabilidade de ocorrência de efeitos estocásticos a saúde, chamado *Linear no-threshold model* (LNT). Efeitos estocásticos são aqueles que ocorrem ao acaso e cuja probabilidade é proporcional a dose, porém a severidade independe da mesma. O modelo LNT assume que a radiação tem potencial de causar injúria em qualquer dosagem e que a soma de pequenas exposições tem efeito equivalente a uma única exposição de maior dose.

Apesar de haver escassa evidência da acurácia do modelo em relação aos efeitos relacionados à baixa dose de radiação, na década de 1970, o modelo LNT foi aceito como padrão na prática de proteção contra a radiação. No entanto, a aplicação desse modelo para baixas dosagens manteve-se controversa na comunidade científica, com diversos trabalhos que suportam[21; 22] e que se opõe[23] ao seu uso como padrão. Em função dessa falta de consenso, o *United States Congress Joint Committee on Atomic Energy* estabeleceu, como princípio das políticas de proteção a radiação, o conceito "*As Low As Reasonably Achievable*" (ALARA), o que determinou o emprego de todos os esforços razoáveis para manter as exposições à radiação ionizante tão baixas quanto possível, corroborando assim o modelo LNT.

1.3.3 Riscos associados à radiação na cardiologia nuclear

Ao se considerar o uso de métodos de imagem que envolvem o uso de radiação, é preciso balancear os riscos, a curto e médio prazo, relacionados à doença em investigação; e os riscos a longo prazo associados a exposição do paciente à radiação [24]. Ao mesmo tempo em que a CMP é um método de imagem capaz de obter informação funcional e anatômica do coração, ela exige que o paciente seja exposto a doses de radiação que produzem um potencial risco à saúde a longo prazo.

De acordo com o *United Nations Scientific Committee on the Effects of Atomic Radiation* (UNSCEAR) entre os anos de 1980 e 1982 a radiação dose efetiva não-médica per capita era de 3 mSv por ano, enquanto a médica era de 0.54 mSv por ano. No ano de 2006, a dose efetiva não médica permaneceu constante, enquanto a de origem médica tornou-se 6 vezes maior (3mSv). Deste total, a radiação advinda da cardiologia nuclear correspondeu a 10,5%, 10 vezes maior do que sua representatividade na década de 1980 [25], conforme mostrado na Figura 1.

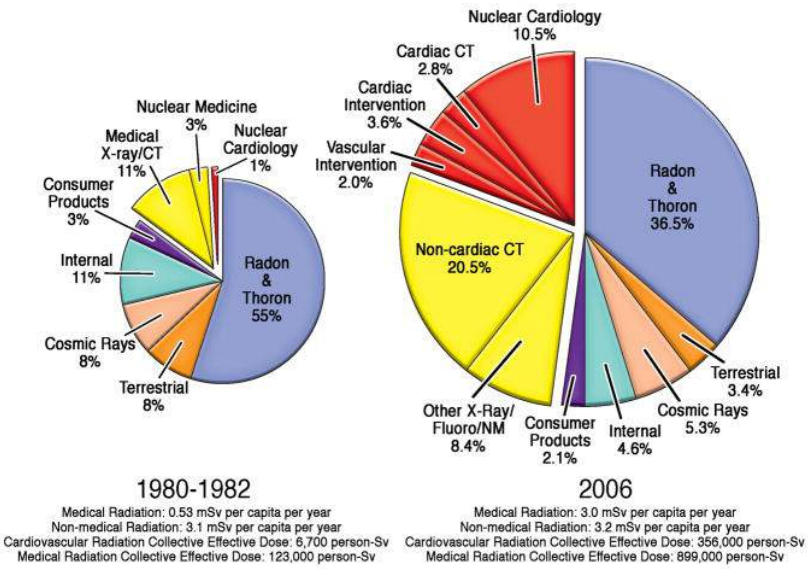

Figura 1 Aumento da participação da cardiologia nuclear como fonte de radiação

Atualmente o valor de dose efetiva estabelecido como baixo pelo UNSCEAR é de 100 mSv. Em 2016, a *American Society of Nuclear Cardiology* (ASNC) estabeleceu a recomendação do uso de protocolos consoantes com o princípio ALARA, como mostrado na Tabela 1. Além disso, determina como objetivo crucial o uso ≤ 9mSv em pelo menos 50% dos exames realizados nos laboratórios de imagem. No mesmo ano em que estabeleceu essa diretriz, a ASNC reforça seu comprometimento com esta meta - emitindo nota exigindo a otimização das doses de radiação, em resposta à heterogeneidade na implementação dessa diretriz no mundo[26,27].

Tabela 1 Protocolos atuais em Cintilografia miocárdica de perfusão: Radiofármacos recomendados e suas respectivas doses efetivas.

	First injection				Second injection				Total Dose (mSv)	Total dose if Stress only (mSv)
	Given at	Activity (mCi)	Activity (MBq)	Dose (mSv)	Given at	Activity (mCi)	Activity (MBq)	Dose (mSv)		
Tc-99m protocols										
Tc-99m one-day stress-first/ stress-only	Stress	8-12	296-444	2.0-3.0	(Rest)	24-36	888-1332	7.0-10.5	9.0-13.5	2.0-3.0
Tc-99m one-day rest/stress	Rest	8-12	296-444	2.3-3.5	Stress	24-36	888-1332	6.1-9.1	8.4-12.6	n/a
Tc-99m two-day stress/rest	Stress	8-12	296-444	2.0-3.0	(Rest)	8-12	888-1332	2.3-3.5	4.3-6.5	2.0-3.0
Tc-99m two-day stress/rest—large patient	Stress	18-30	666-1110	4.5-7.6	(Rest)	18-30	666-1110	5.2-8.7	9.8-16.3	4.5-7.6
Tc-99m two-day rest/stress	Rest	8-12	296-444	2.3-3.5	Stress	8-12	296-444	2.0-3.0	4.3-6.5	n/a
Tc-99m two-day rest/stress large patient	Rest	18-30	666-1110	5.2-8.7	Stress	18-30	666-1110	4.5-7.6	9.8-16.3	n/a
Tl-201 protocols										
Tl-201 stress/redistribution rest	Stress	2.5-3.5	92.5-129.5	10.9-15.3	n/a	n/a	n/a	n/a	10.9-15.3	10.9-15.3
Tl-201 stress/redistribution rest/ reinjection	Stress	2.5-3.5	92.5-129.5	10.9-15.3	Rest	1-2	37-74	4.4-8.8	15.3-24.1	n/a
Tl-201 rest/redistribution	Rest	2.5-3.5	92.5-129.5	10.9-15.3	n/a	n/a	n/a	n/a	10.9-15.3	n/a
Dual-isotope Tl-201 rest/Tc-99m stress	Rest	2.5-3.5	92.5-129.5	10.9-15.3	Stress	8-12	296-444	2.0-3.0	13.0-18.3	n/a
Dual-isotope Tl-201 rest/Tc-99m stress—large patient	Rest	3.0-3.5	111-129.5	13.1-15.3	Stress	18-30	666-1110	4.5-7.6	17.7-22.9	n/a
I-123 protocol										
MIBG	Rest	10	370	4.6	n/a	n/a	n/a	n/a	4.6	n/a
Newer technology reduced-dose protocols										
Tc-99m one-day stress-first/ stress-only	Stress	4-6	148-222	1.0-1.5	(Rest)	12-18	444-666	3.5-5.2	4.5-6.7	1.0-1.5
Tc-99m one-day rest/stress	Rest	4-6	148-222	1.2-1.7	Stress	12-18	444-666	3.0-4.5	4.2-6.3	n/a
Tc-99m two-day stress/rest	Stress	4-6	148-222	1.0-1.5	(Rest)	4-6	148-222	1.2-1.7	2.2-3.3	1.0-1.5
Tc-99m two-day stress/rest—large patient	Stress	9-15	333-555	2.3-3.8	(Rest)	9-15	333-555	2.6-4.4	4.9-8.1	2.3-3.8
Tc-99m two-day rest/stress	Rest	4-6	148-222	1.2-1.7	Stress	4-6	148-222	1.0-1.5	2.2-3.3	n/a
Tc-99m two-day rest/stress—large patient	Rest	9-15	333-555	2.6-4.4	Stress	9-15	333-555	2.3-3.8	4.9-8.1	n/a

1.3.4 As novas tecnologias na CMP e a busca por estratégias de redução de radiação

Anos antes do estabelecimento de novas diretrizes relacionadas à otimização do uso de radiação na CMP, a preocupação com o fenômeno do aumento da exposição mundial à radiação médica já existia. Esta figurava como alvo primário na busca por novas tecnologias no campo da imagem cardiovascular, assim como nas publicações científicas correlatas.

Dentre estas inovações, destacaram-se os avanços nos *softwares* de reconstrução da imagem cintilográfica. Contrapondo-se aos algoritmos tradicionais, como o *Filtered backprojection* (FBP), estes novos algoritmos foram desenvolvidos para melhorar a relação sinal-ruído e aumentar a resolução da imagem. Para isso, utilizam métodos de recuperação de resolução e técnicas de otimização matemática iterativas, a fim de compensar as limitações impostas por fatores intrínsecos ao tipo de GC utilizado[28]. Por consequência, tornaram possível a aquisição de imagens de qualidade equivalente às obtidas com algoritmos de reconstrução mais tradicionais, utilizando um menor tempo de exame[29,30] e menor dosimetria. A utilização destes novos algoritmos não altera o valor prognóstico da CMP[31].

Paralelamente, os avanços na pesquisa também incluíram inovações no equipamento que compõe a GC. Em especial, podemos citar a utilização de detectores de Telureto de Cadmio e Zinco (do inglês, Cadmium-Zinc-Telluret [CZT]), que revolucionou o padrão de formação do pulso eletrônico - até então baseada no mesmo princípio, desde o advento das GCs Anger.

A GC com utilização de detectores CZT, conhecida como GC CZT, é formada por um colimador e por arranjos de detectores de estado sólido compostos por cristais

de CZT. Estes detectores apresentam maior sensibilidade à radiação gama quando comparados aos cristais de iodeto de sódio. Ademais, são capazes de converter diretamente o fóton de radiação gama emitido pelo paciente em pulso eletrônico, dispensando o uso de tubos fotomultiplicadores e sendo, por isso, mais compactos. Essa característica permitiu a construção de GCs dedicadas a captação de imagens cardíacas[32; 33].

As GC CZT podem apresentar uma sensibilidade ao fóton até 8 vezes maior[33] que as GCs tradicionais, como mostrado na Figura 2, reduzindo assim o tempo de aquisição de forma significativa. Com isso, a GC CZT proporciona uma maior tolerância do paciente ao teste, diminuindo os artefatos de técnica relacionados à movimentação do mesmo, além de facilitar a realização do exame em duas posições - supina e prona. Tudo isso associado à possibilidade de um aumento de até 1.7 a 2.5 vezes da resolução [34], gera imagens de melhor qualidade quando comparadas às geradas em GCs tradicionais.

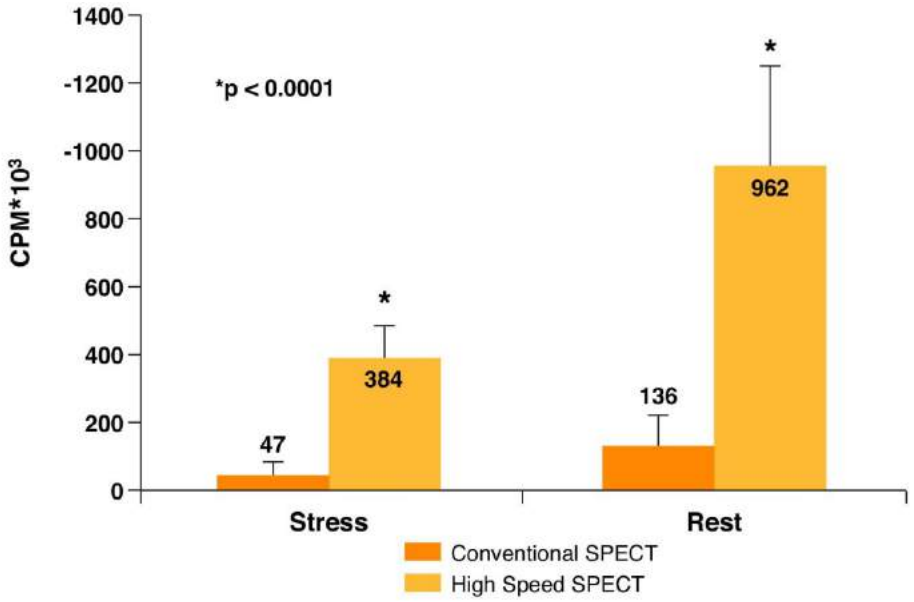

Figura 2 Comparação da sensibilidade entre a GC CZT e GCs tradicionais

O advento da GC CZT possibilitando exames ultrarrápidos suscitou o aprofundamento da discussão a respeito da possibilidade de reduzir a dosimetria em detrimento da redução do tempo de exame [35,36,37,38]. Do ponto de vista físico, a redução do tempo ou da dose resultam no mesmo somatório de contagem de pulsos eletrônicos. Portanto, é possível obter uma redução de dose proporcional à redução de tempo, se mantido o tempo padrão utilizado em protocolos tradicionais. A flexibilidade da manipulação da proporção tempo-dosimetria, propicia a existência de diferentes protocolos com resultados teoricamente equivalentes, conforme mostrado na Figura 3. A Figura 4 expõe o impacto dos diferentes protocolos na dose efetiva[39].

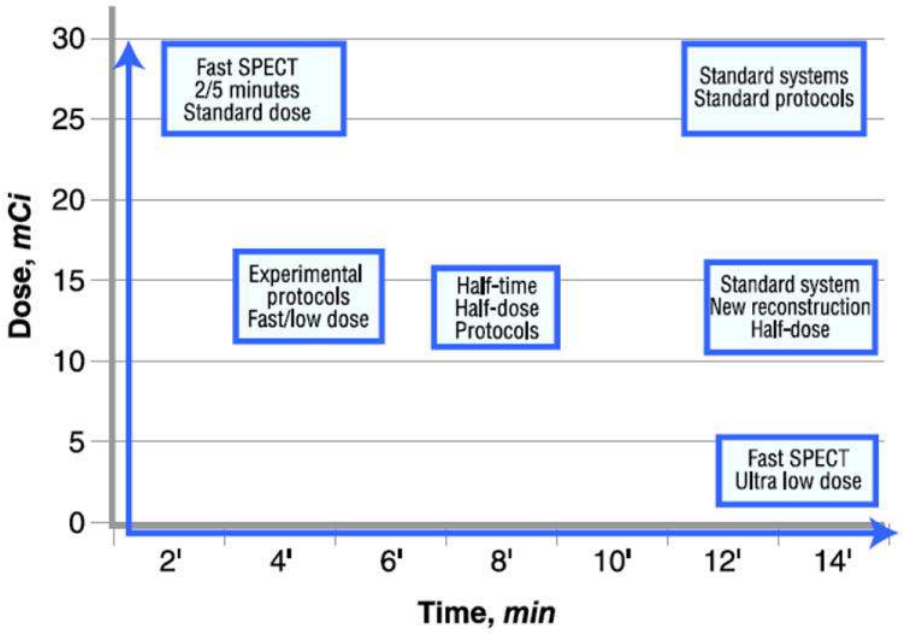

Figura 3 Relação entre a dose e o tempo de captura de imagens e possíveis novos protocolos investigativos utilizando as novas tecnologias da cintilografia miocárdica de perfusão

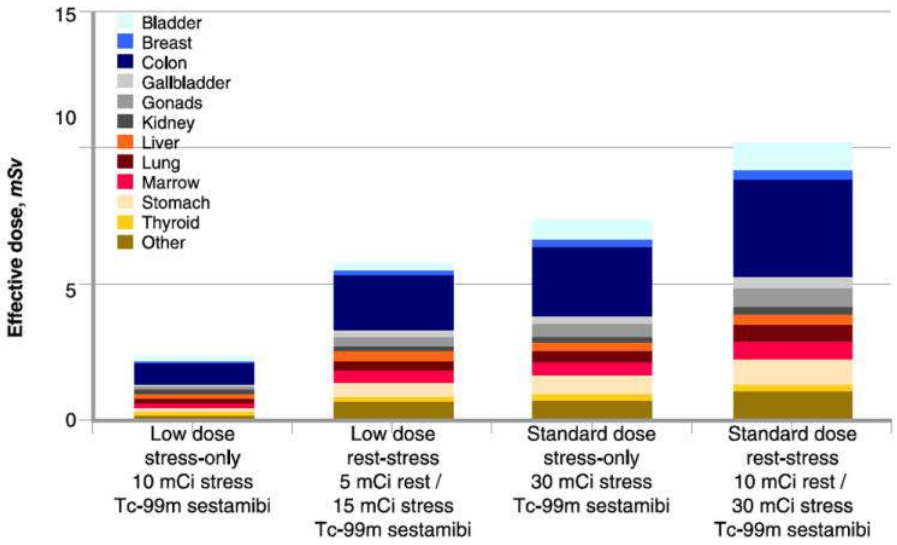

Figura 4 Efeito de diferentes protocolos na dose efetiva

Estabelecida a capacidade das GC CZT em usar menos tempo e dose, sem comprometer a qualidade da imagem gerada e a acurácia diagnóstica do método, questiona-se se o mesmo ocorreria com seu valor prognóstico quando da implementação desses novos protocolos. Até o momento, a comparação realizada entre os dois tipos de GCs somente fez uso do protocolo tradicional de dosimetria e tempo, confirmando neste caso a equivalência do valor prognóstico[40]. Resta, no entanto, avaliar se o valor prognóstico é mantido quando se faz uso do potencial de redução de dose e tempo das GC CZT.

Além dos avanços tecnológicos, outras estratégias para redução da exposição à radiação foram apresentadas em diretriz recente publicado pela ESC[7]. Dentre estas, destaca-se a seleção ótima do tipo de teste mais adequado para cada paciente e situação, baseando-se na probabilidade pré-teste e características intrínsecas a cada tipo de teste. Essa recomendação suscita a discussão do quão apropriadamente a CMP é aplicada.

Apesar de tanto a CMP quanto o teste ergométrico (TE) serem indicados para população de intermediário risco para DAC, sabe-se que a CMP apresenta uma sensibilidade maior para a detecção de isquemia[41]. Aliado a isso, a CMP é capaz de adicionar outras informações funcionais muitas vezes aliadas na decisão clínica. Por consequência, pode haver uma inclinação por parte da equipe médica em encaminhar o paciente - com intermediário risco para a CMP, subutilizando o TE. Além de gerar mais custos ao sistema de saúde, esta prática expõe o paciente a um risco desnecessário à radiação. Esta situação ressalta a relevância de se confirmar que fatores devem ser considerados para a escolha entre a CMP e o TE.

2 Motivação e Justificativa

A DAC é a principal doença cardiovascular e tem fundamental relevância epidemiológica devido à sua morbimortalidade. Nesse cenário, a CMP se estabeleceu como um dos principais métodos diagnósticos e prognósticos na avaliação de pacientes com DAC suspeita e conhecida, levando ao aumento da utilização desse método de imagem. Este novo cenário associado à utilização dos protocolos de dosimetria tracionais, opõem-se ao princípio de exposição mínima necessária à radiação. Diante disto é notória a necessidade de avaliar mecanismos que reduzam o tempo do exame, a dosagem do fármaco radioativo utilizado nele ou a sua frequência de realização.

O advento das GC CZT iniciou uma nova era na cardiologia nuclear, possibilitando a aplicação de diferentes protocolos e flexibilizando o tempo de aquisição das imagens e a dose de radiofármaco utilizado na CMP. No entanto, o valor prognóstico da CMP sendo realizada com um protocolo mais rápido e com menor dose nessa GC não foi estabelecido, tampouco comparado ao utilizado nas GC tradicionais. O estabelecimento deste valor traz benefícios tanto na perspectiva do paciente, por ser submetido a um

exame mais confortável e sob menor dosimetria, quanto da equipe médica, por assegurar a confiabilidade do resultado obtido na estratificação de risco do paciente.

No tangente à redução da frequência de utilização da CMP, tornou-se determinante certificar-se de que os critérios de adequação do teste para os diferentes subgrupos de pacientes com risco intermediário de DAC eram apropriados. Nesse sentido, um grupo que tem despertado a atenção da comunidade médica científica são os pacientes com alta capacidade de exercício.

A capacidade de exercício é um preditor estabelecido de mortalidade[42; 43; 44; 45; 46; 47] e, nas duas últimas décadas, vários autores discutiram se esse parâmetro seria suficiente para apoiar a decisão clínica. Pacientes que atingiram ≥10 equivalentes metabólicos (METs) demonstraram ter excelente prognóstico, com baixas taxas de eventos cardiovasculares e baixa prevalência de ≥10% de isquemia do ventrículo esquerdo[48; 49]. Posteriormente, o uso da capacidade de exercício como critério para evitar a realização da CMP foi discutido continuamente. Protocolos provisórios foram estudados para melhor atender os grupos de pacientes que poderiam ser selecionados para essa abordagem e salvos da exposição desnecessária à radiação[50; 51].

Pacientes com DAC conhecida são uma porcentagem importante da coorte comumente referida ao CMP devido ao seu valor prognóstico bem estabelecido, digno de ser utilizado no manejo desses pacientes. Uma associação entre capacidade de exercício e mortalidade geral em pacientes com condições cardiovasculares conhecidas foi demonstrada anteriormente[52]. No entanto, nenhuma investigação adicional foi feita para entender como a carga de trabalho se relaciona com os resultados do CMP em relação à sua capacidade prognóstica ao avaliar esse grupo em particular.

3 Objetivos

Artigo 1: Estabelecer o valor prognóstico de um novo protocolo realizado em menos e tempo e com menor dose de radiação em GC CZT.

Artigo 2: Comparar o valor prognóstico desse novo protocolo de Cintilografia de perfusão miocárdica realizado de forma mais rápida e com menor uso de radiação em GC CZT com aquele realizado em GCs tradicionais.

Artigo 3: Avaliar a contribuição do valor prognóstico da CMP em relação à realização do TE apenas, em pacientes com DAC conhecida que atingiram alta performance aeróbica (>10 METs).

4 Artigos

A pesquisa é apresentada na forma de 3 artigos sucedidos de considerações finais.

Artigo 1: "*Prognostic value of a faster, low-radiation myocardial perfusion SPECT protocol in a CZT camera*"

Este artigo foi publicado na revista *International Journal of Cardiovasc Imaging*.

Lima RSL, Peclat TR, Souza ACAH, Nakamoto AMK, Neves FM, Souza VF, et al. **Prognostic value of a faster, low-radiation myocardial perfusion SPECT protocol in a CZT camera**. Int J Cardiovasc Imaging. 2017;33(12):2049-56.

Artigo 2: "*Comparison of the prognostic value of myocardial perfusion imaging using a CZT-SPECT camera with a conventional anger camera.*"

Esse artigo foi publicado na revista *Journal of Nuclear Cardiology*.

Lima R, Peclat T, Soares T, Ferreira C, Souza AC, Camargo G. **Comparison of the prognostic value of myocardial perfusion imaging using a CZT-SPECT camera with a conventional anger camera**. J Nucl Cardiol. 2017;24(1):245-51.

Artigo 3: "*The additional Prognostic Value of Myocardial Perfusion SPECT in Patients with Known Coronary Artery Disease with high exercise capacity*"

Esse manuscrito foi submetido para a revista *Journal of Nuclear Cardiology*.

5 Referência bibliográfica

[1] SEATTLE; WA: INSTITUTE FOR HEALTH METRICS AND EVALUATION (IHME), U. O.; WASHINGTON. Global Burden of Disease Study 2016. Global Burden of Disease Study 2016 (GBD 2016) results. http://ghdx.healthdata.org/gbd-results-tool, 2016. Acesso em: May 1, 2018.

[2] BENJAMIN, E. J. et al. Heart Disease and Stroke Statistics-2019 Update: A Report From the American Heart Association. **Circulation,** v. 139, n. 10, p. e56-e528, 03 2019. ISSN 1524-4539. Disponível em: < https://www.ncbi.nlm.nih.gov/pubmed/30700139 >.

[3] MURPHY SL, X. J., KOCHANEK KD. **Deaths: final data for 2010. National vital statistics report: from the Centers for Disease Control and Prevention, National Center for Health Statistics, National Vital Statistics System.** 61**:** 1-117 p. 2013.

[4] SANCHIS-GOMAR, F. et al. Epidemiology of coronary heart disease and acute coronary syndrome. **Ann Transl Med,** v. 4, n. 13, p. 256, Jul 2016. ISSN 2305-5839. Disponível em: < https://www.ncbi.nlm.nih.gov/pubmed/27500157 >.

[5] BRANT, L. C. C. et al. Variations and particularities in cardiovascular disease mortality in Brazil and Brazilian states in 1990 and 2015: estimates from the Global Burden of Disease. **Rev Bras Epidemiol,** v. 20Suppl 01, n. Suppl 01, p. 116-128, May 2017. ISSN 1980-5497. Disponível em: < https://www.ncbi.nlm.nih.gov/pubmed/28658377 >.

[6] TEICH, V.; ARAUJO, D. V. **Estimativa de Custo da Síndrome Coronariana Aguda no Brasil**: Rev Bras Cardiol. 24 (2)**:** 85-94 p. 2011.

[7] KNUUTI, J. et al. 2019 ESC Guidelines for the diagnosis and management of chronic coronary syndromes. **Eur Heart J**, Aug 2019. ISSN 1522-9645. Disponível em: < https://www.ncbi.nlm.nih.gov/pubmed/31504439 >.

[8] PATTON, D. D. The birth of nuclear medicine instrumentation: Blumgart and Yens, 1925. **J Nucl Med,** v. 44, n. 8, p. 1362-5, Aug 2003. ISSN 0161-5505. Disponível em: < https://www.ncbi.nlm.nih.gov/pubmed/12902429 >.

[9] ISKANDRIAN, A. E.; GARCIA, E. V. **Nuclear Cardiac Imaging - Principles and Applications**. 4. Oxford university Press, Inc., ISBN 978-0-19-531119-8.

[10] ANGER, H. O. Scintillation camera. v. 29, n. 1, 1958.

[11] BAILEY, I. K. et al. Thallium-201 myocardial perfusion imaging at rest and during exercise. Comparative sensitivity to electrocardiography in coronary artery disease. **Circulation,** v. 55, n. 1, p. 79-87, Jan 1977. ISSN 0009-7322. Disponível em: < https://www.ncbi.nlm.nih.gov/pubmed/830222 >.

[12] RITCHIE, J. L. et al. Myocardial imaging with thallium-201 at rest and during exercise. Comparison with coronary arteriography and resting and stress electrocardiography. **Circulation,** v. 56, n. 1, p. 66-71, Jul 1977. ISSN 0009-7322. Disponível em: < https://www.ncbi.nlm.nih.gov/pubmed/862173 >.

[13] RIGO, P. et al. Stress thallium-201 myocardial scintigraphy for the detection of individual coronary arterial lesions in patients with and without previous myocardial infarction. **Am J Cardiol,** v. 48, n. 2, p. 209-16, Aug 1981. ISSN 0002-9149. Disponível em: < https://www.ncbi.nlm.nih.gov/pubmed/7270430 >.

[14] OKADA, R. D. et al. Exercise radionuclide imaging approaches to coronary artery disease. **Am J Cardiol,** v. 46, n. 7, p. 1188-204, Dec 1980. ISSN 0002-9149. Disponível em: < https://www.ncbi.nlm.nih.gov/pubmed/7006363 >.

[15] PAMELIA, F. X. et al. Prognosis with chest pain and normal thallium-201 exercise scintigrams. **Am J Cardiol,** v. 55, n. 8, p. 920-6, Apr 1985. ISSN 0002-9149. Disponível em: < https://www.ncbi.nlm.nih.gov/pubmed/3984881 >.

16 DES PREZ, R. D. et al. Cost-effectiveness of myocardial perfusion imaging: a summary of the currently available literature. **J Nucl Cardiol,** v. 12, n. 6, p. 750-9, 2005 Nov-Dec 2005. ISSN 1071-3581. Disponível em: < https://www.ncbi.nlm.nih.gov/pubmed/16344238 >.

17 NOTGHI, A.; LOW, C. S. Myocardial perfusion scintigraphy: past, present and future. **Br J Radiol,** v. 84 Spec No 3, p. S229-36, Dec 2011. ISSN 1748-880X. Disponível em: < https://www.ncbi.nlm.nih.gov/pubmed/22723530 >.

18 MULLER, H. J. ARTIFICIAL TRANSMUTATION OF THE GENE. **Science,** v. 66, n. 1699, p. 84-7, Jul 1927. ISSN 0036-8075. Disponível em: < https://www.ncbi.nlm.nih.gov/pubmed/17802387 >.

19 _____. The production of mutations. **J Hered,** v. 38, n. 9, p. 258-70, Sep 1947. ISSN 0022-1503. Disponível em: < https://www.ncbi.nlm.nih.gov/pubmed/18897359 >.

20 CROW, J. F.; ABRAHAMSON, S. Seventy years ago: mutation becomes experimental. **Genetics,** v. 147, n. 4, p. 1491-6, Dec 1997. ISSN 0016-6731. Disponível em: < https://www.ncbi.nlm.nih.gov/pubmed/9409815 >.

21 AGENCY, U. S. E. P. **EPA Radiogenic Cancer Risk Models and Projections for the U.S. Population** April 2011.

22 EFFECTS, U. N. S. C. O. T.; RADIATION, O. A. **SOURCES AND EFFECTS OF IONIZING RADIATION - UNSCEAR 2000 Report to the General Assembly, with Scientific Annexes - Annex G**. 2000

23 SOCIETY, H. P. **Radiation Risk in Perspective - Position Statement of the Health Physics Society**. January 1996

24 KNUUTI, J. et al. Risks and benefits of cardiac imaging: an analysis of risks related to imaging for coronary artery disease. **Eur Heart J,** v. 35, n. 10, p. 633-8, Mar 2014. ISSN 1522-9645. Disponível em: < https://www.ncbi.nlm.nih.gov/pubmed/24375074 >.

25 EINSTEIN, A. J. Effects of radiation exposure from cardiac imaging: how good are the data? **J Am Coll Cardiol,** v. 59, n. 6, p. 553-65, Feb 2012. ISSN 1558-3597. Disponível em: < https://www.ncbi.nlm.nih.gov/pubmed/22300689 >.

26 JEROME, S. D. et al. Nationwide Laboratory Adherence to Myocardial Perfusion Imaging Radiation Dose Reduction Practices: A Report From the Intersocietal Accreditation Commission Data Repository. **JACC Cardiovasc Imaging,** v. 8, n. 10, p. 1170-6, Oct 2015. ISSN 1876-7591. Disponível em: < https://www.ncbi.nlm.nih.gov/pubmed/26363837 >.

[27] MERCURI, M. et al. Comparison of Radiation Doses and Best-Practice Use for Myocardial Perfusion Imaging in US and Non-US Laboratories: Findings From the IAEA (International Atomic Energy Agency) Nuclear Cardiology Protocols Study. **JAMA Intern Med,** v. 176, n. 2, p. 266-9, Feb 2016. ISSN 2168-6114. Disponível em: < https://www.ncbi.nlm.nih.gov/pubmed/26720424 >.

[28] DE LORENZO, A. et al. Comparison between short-acquisition myocardial perfusion SPECT reconstructed with a new algorithm and conventional acquisition with filtered backprojection processing. **Nucl Med Commun,** v. 31, n. 6, p. 552-7, Jun 2010. ISSN 1473-5628. Disponível em: < https://www.ncbi.nlm.nih.gov/pubmed/20300043 >.

[29] BORGES-NETO, S. et al. Clinical results of a novel wide beam reconstruction method for shortening scan time of Tc-99m cardiac SPECT perfusion studies. **J Nucl Cardiol,** v. 14, n. 4, p. 555-65, Jul 2007. ISSN 1532-6551. Disponível em: < https://www.ncbi.nlm.nih.gov/pubmed/17679065 >.

[30] DEPUEY, E. G. et al. Ordered subset expectation maximization and wide beam reconstruction "half-time" gated myocardial perfusion SPECT functional imaging: a comparison to "full-time" filtered backprojection. **J Nucl Cardiol,** v. 15, n. 4, p. 547-63, 2008 Jul-Aug 2008. ISSN 1532-6551. Disponível em: < https://www.ncbi.nlm.nih.gov/pubmed/18674723 >.

[31] LIMA, R. et al. Prognostic value of myocardium perfusion imaging with a new reconstruction algorithm. **J Nucl Cardiol,** v. 21, n. 1, p. 149-57, Feb 2014. ISSN 1532-6551. Disponível em: < http://www.ncbi.nlm.nih.gov/pubmed/24281904 >.

[32] BOCHER, M. et al. A fast cardiac gamma camera with dynamic SPECT capabilities: design, system validation and future potential. **Eur J Nucl Med Mol Imaging,** v. 37, n. 10, p. 1887-902, Oct 2010. ISSN 1619-7089. Disponível em: < https://www.ncbi.nlm.nih.gov/pubmed/20585775 >.

[33] SHARIR, T. et al. High-speed myocardial perfusion imaging initial clinical comparison with conventional dual detector anger camera imaging. **JACC Cardiovasc Imaging,** v. 1, n. 2, p. 156-63, Mar 2008. ISSN 1876-7591. Disponível em: < https://www.ncbi.nlm.nih.gov/pubmed/19356422 >.

[34] HARRISON, S. D.; HARRISON, M. A.; DUVALL, W. L. Stress myocardial perfusion imaging in the emergency department--new techniques for speed and diagnostic accuracy. **Curr Cardiol Rev,** v. 8, n. 2, p. 116-22, May 2012. ISSN 1875-6557. Disponível em: < https://www.ncbi.nlm.nih.gov/pubmed/22708910 >.

[35] DEPUEY, E. G. et al. A comparison of the image quality of full-time myocardial perfusion SPECT vs wide beam reconstruction half-time and half-dose SPECT. **J Nucl Cardiol,** v. 18, n. 2, p. 273-80, Apr 2011. ISSN 1532-6551. Disponível em: < https://www.ncbi.nlm.nih.gov/pubmed/21287370 >.

[36] DUVALL, W. L. et al. Reduced isotope dose with rapid SPECT MPI imaging: initial experience with a CZT SPECT camera. **J Nucl Cardiol,** v. 17, n. 6, p. 1009-14, Dec 2010. ISSN 1532-6551. Disponível em: < https://www.ncbi.nlm.nih.gov/pubmed/21069489 >.

[37] _____. Reduced isotope dose and imaging time with a high-efficiency CZT SPECT camera. **J Nucl Cardiol,** v. 18, n. 5, p. 847-57, Oct 2011. ISSN 1532-6551. Disponível em: < http://www.ncbi.nlm.nih.gov/pubmed/21528422 >.

[38] GIMELLI, A. et al. High diagnostic accuracy of low-dose gated-SPECT with solid-state ultrafast detectors: preliminary clinical results. **Eur J Nucl Med Mol Imaging,** v. 39, n. 1, p. 83-90, Jan 2012. ISSN 1619-7089. Disponível em: < https://www.ncbi.nlm.nih.gov/pubmed/21887532 >.

[39] SLOMKA, P. J. et al. Advances in technical aspects of myocardial perfusion SPECT imaging. **J Nucl Cardiol,** v. 16, n. 2, p. 255-76, 2009 Mar-Apr 2009. ISSN 1532-6551. Disponível em: < https://www.ncbi.nlm.nih.gov/pubmed/19242769 >.

[40] OLDAN, J. D. et al. Prognostic value of the cadmium-zinc-telluride camera: A comparison with a conventional (Anger) camera. **J Nucl Cardiol,** v. 23, n. 6, p. 1280-1287, Dec 2016. ISSN 1532-6551. Disponível em: < https://www.ncbi.nlm.nih.gov/pubmed/26122879 >.

[41] KLOCKE, F. J. et al. ACC/AHA/ASNC guidelines for the clinical use of cardiac radionuclide imaging--executive summary: a report of the American College of Cardiology/American Heart Association Task Force on Practice Guidelines (ACC/AHA/ASNC Committee to Revise the 1995 Guidelines for the Clinical Use of Cardiac Radionuclide Imaging). **J Am Coll Cardiol,** v. 42, n. 7, p. 1318-33, Oct 2003. ISSN 0735-1097. Disponível em: < https://www.ncbi.nlm.nih.gov/pubmed/14522503 >.

[42] PETERSON, P. N. et al. Association of exercise capacity on treadmill with future cardiac events in patients referred for exercise testing. **Arch Intern Med,** v. 168, n. 2, p. 174-9, Jan 2008. ISSN 0003-9926. Disponível em: < https://www.ncbi.nlm.nih.gov/pubmed/18227364 >.

[43] MORISE, A. P.; JALISI, F. Evaluation of pretest and exercise test scores to assess all-cause mortality in unselected patients presenting for exercise testing with symptoms of suspected coronary artery disease. **J Am Coll Cardiol,** v. 42, n. 5, p. 842-50, Sep 2003. ISSN 0735-1097. Disponível em: < https://www.ncbi.nlm.nih.gov/pubmed/12957430 >.

[44] GORAYA, T. Y. et al. Prognostic value of treadmill exercise testing in elderly persons. **Ann Intern Med,** v. 132, n. 11, p. 862-70, Jun 2000. ISSN 0003-4819. Disponível em: < https://www.ncbi.nlm.nih.gov/pubmed/10836912 >.

[45] KODAMA, S. et al. Cardiorespiratory fitness as a quantitative predictor of all-cause mortality and cardiovascular events in healthy men and women: a meta-analysis. **JAMA,** v. 301, n. 19, p. 2024-35, May 2009. ISSN 1538-3598. Disponível em: < https://www.ncbi.nlm.nih.gov/pubmed/19454641 >.

[46] LEE, D. S. et al. Cardiovascular outcomes are predicted by exercise-stress myocardial perfusion imaging: Impact on death, myocardial infarction, and coronary revascularization procedures. **Am Heart J,** v. 161, n. 5, p. 900-7, May 2011. ISSN 1097-6744. Disponível em: < https://www.ncbi.nlm.nih.gov/pubmed/21570520 >.

[47] FASELIS, C. et al. Exercise capacity and all-cause mortality in male veterans with hypertension aged ≥70 years. **Hypertension,** v. 64, n. 1, p. 30-5, Jul 2014. ISSN 1524-4563. Disponível em: < https://www.ncbi.nlm.nih.gov/pubmed/24821944 >.

[48] BOURQUE, J. M. et al. Achieving an exercise workload of > or = 10 metabolic equivalents predicts a very low risk of inducible ischemia: does myocardial perfusion imaging have a role? **J Am Coll Cardiol,** v. 54, n. 6, p. 538-45, Aug 2009. ISSN 1558-3597. Disponível em: < https://www.ncbi.nlm.nih.gov/pubmed/19643316 >.

[49] _____. Prognosis in patients achieving ≥10 METS on exercise stress testing: was SPECT imaging useful? **J Nucl Cardiol,** v. 18, n. 2, p. 230-7, Apr 2011. ISSN 1532-6551. Disponível em: < https://www.ncbi.nlm.nih.gov/pubmed/21132417 >.

[50] SMITH, L. et al. A high exercise workload of ≥ 10 METS predicts a low risk of significant ischemia and cardiac events in older adults. **J Nucl Cardiol**, Jul 2018. ISSN 1532-6551. Disponível em: < https://www.ncbi.nlm.nih.gov/pubmed/30051345 >.

[51] DUVALL, W. L. et al. A hypothetical protocol for the provisional use of perfusion imaging with exercise stress testing. **J Nucl Cardiol,** v. 20, n. 5, p. 739-47, Oct 2013. ISSN 1532-6551. Disponível em: < https://www.ncbi.nlm.nih.gov/pubmed/23737159 >.

[52] HUNG, R. K. et al. Prognostic value of exercise capacity in patients with coronary artery disease: the FIT (Henry Ford ExercIse Testing) project. **Mayo Clin Proc,** v. 89, n. 12, p. 1644-54, Dec 2014. ISSN 1942-5546. Disponível em: < https://www.ncbi.nlm.nih.gov/pubmed/25440889 >.

6 Artigo 1

Prognostic value of a faster, low-radiation myocardial perfusion SPECT protocol in a CZT camera

Ronaldo S. L. Lima; Thaís R. Peclat; Ana Carolina A. H. Souza;
Aline M. K. Nakamoto; Felipe M. Neves; Victor F. Souza; Letícia B. Glerian;
Andrea De Lorenzo

6.1 Abstract

Background and objective: To determine the prognostic value of a new, ultrafast, low dose myocardial perfusion SPECT (MPS) protocol in a cadmium-zinc telluride (CZT) camera. CZT cameras have introduced significant progress in MPS imaging, offering high-quality images despite lower doses and scan time. Yet, it is unknown if, with such protocol changes, the prognostic value of MPS is preserved.

Methods: Patients had a 1-day 99mTc-sestamibi protocol, starting with the rest (185–222 MBq) followed by stress (666–740 MBq). Acquisition times were 6 and 3 min, respectively. MPS were classified as normal or abnormal perfusion scans and summed scores of stress, rest, and difference (SSS, SRS and SDS), calculated.

Results: Patients were followed with 6-month phone calls. Hard events were defined as death or nonfatal myocardial infarction. Late revascularization was that occurring after 60 days of MPS. 2930 patients (age 64.0±12.1 years, 53.3% male) were followed for 30.7±7.5 months. Mean dosimetry was 6 mSv and mean total study time, 48±13 min. The annual hard event and late revascularization rates were higher in

patients with greater extension of defect and ischemia. SSS was higher in patients with hard events compared to those without events (2.6±4.9 vs. 5.0±6.3, p<0.001), as well as the SDS (0.7± 1.9 vs 1.7± 3.4, p<0.001). The same was true for patients with or without late revascularization (SSS: 2.5±4.7 vs. 6.6±7.1; SDS: 0.6±1.7 vs. 2.9±3.8, p<0.01).

Conclusion: A new, faster, low radiation MPS protocol in a CZT camera maintain the ability to stratify patients with increased risk of events, showing that, in the presence of greater extension of defect or ischemia, patients presented higher rates of hard events and late revascularization.

6.2 Introduction

Over the past 30 years, successive technical innovations including, but not limited to, SPECT acquisition, ECG gating, among others, have granted myocardial perfusion imaging the status of a reliable, widely applicable, and increasingly useful technique [1]. The excellent diagnostic and prognostic values of myocardial perfusion SPECT (MPS) have led it to be extensively employed to evaluate patients with suspected or known coronary artery disease (CAD) [2].

Nonetheless, traditional MPS has two important limitations: Prolonged image acquisition time, leading to long procedural times, and relatively large radiation doses. The available literature demonstrates the possibility of high-speed cameras to reduce acquisition times, improving patient's tolerance to the test, and reducing radiation dose [3]. These new cameras rely on a pinhole collimation design and multiple cadmium zinc telluride (CZT) crystal arrays. Compared to the traditional SPECT camera, this type of collimation provides a three- to five-fold increase in photon sensitivity, thereby

reducing imaging times significantly, while providing a 1.7 to 2.5-fold increase in spatial resolution. This makes shorter scans or lower doses (or even both) a reality, without the loss of image quality [3; 4; 5].

However, the prognostic value of MPS imaging with this new protocol is still unknown. This study therefore sought to assess the prognostic value of a new faster, low-radiation MPS protocol performed in a CZT gamma camera (CZT-GC).

6.3 Materials and methods

Consecutive patients who underwent CZT MPS for the assessment of suspected or known CAD at a single laboratory in Rio de Janeiro, Brazil, between November 2011 and December 2012 were prospectively enrolled and followed by 6-month phone calls.

Those who underwent myocardial revascularization (either by coronary angioplasty or coronary artery bypass grafting surgery) < 60 days after MPS were later excluded.

Prior to scanning, patient´s medical history and physical examination data were collected by a team of experienced cardiologists.

All procedures performed were in accordance with the ethical standards of the institutional research committee and with the 1964 Declaration of Helsinki and its later amendments. Informed consent was obtained from all individual participants included in the study.

6.4 Study protocol

Patients were instructed to abstain from any products containing caffeine for 24 h before the test. Beta-blockers, calcium-channel antagonists, and nitrates were terminated 48 h before testing. A 1-day protocol was employed, with 185–222 MBq of 99mTc-sestamibi used for the resting phase and 666–740 MBq for stress. Initially, to determine the best duration for the acquisition of MPS scans, 24 patients (13 men) were selected for a pilot study in which scan acquisition was performed for 6 min in list mode. The scans were then processed using 1–6 min of the total scan time for reconstruction. Images were analyzed by two experienced readers unaware of the time range used for reconstruction, who had their readings evaluated for agreement. The study protocol was then defined according to best combination of reading agreements for stress and rest MPS studies among time ranges.

All patients underwent a 1-day, gated, rest/stress 99mTc-sestamibi protocol. Ten min after tracer injection, image acquisition was performed in the supine position. The second phase was the stress study, in which either symptom-limited exercise treadmill test using the standard Bruce protocol with 13-lead electrocardiographic or pharmacologic stress were performed. Upon 5 min of stress phase completion, patients underwent image acquisition in the supine and prone positions [6; 7]. The CZT-GC (Discovery NM 530c, GE Healthcare, Haifa, Israel) was equipped with a multiple pinhole collimator and 19 stationary cadmium-zinc-telluride detectors simultaneously imaging 19 cardiac views. Each detector contained 32×32 pixelated 5-mm thick (2.46×2.46 mm) elements. The system design enabled high-quality imaging of a three-dimensional volume by all detectors (quality field-of-view), where the patient's heart should be positioned. Once acquisition was initiated, no detector or collimator motion occurred.

6.4.1 Image analysis

All images were interpreted by a consensus of two experienced readers. Image processing was performed using Evolution for Cardiac® software. Images were reconstructed without scatter or attenuation correction. Short axis, vertical and horizontal long-axis tomograms, as well as polar maps, were generated and analyzed. The image reconstruction method used allows extra-cardiac activity to be isolated more easily. Still, two readers analyzed the image before the patient was removed from the camera. The repetition rate of the images was less than 5%. A semi quantitative 17-segment visual interpretation of the gated myocardial perfusion images was performed [8]. Each segment was scored by consensus of the two observers using a standard five-point scoring system [9] (0=normal, 1=equivocal, 2=moderate, 3=severe reduction of uptake, and 4=absence of detectable tracer uptake). Summed stress scores (SSS) were obtained by adding the scores of the 17 segments of the stress images. Summed rest scores (SRS) were obtained by adding scores of the 17 segments of the rest images and a summed difference score (SDS) was calculated by segmental subtraction (SSS-SRS). For evaluating the SSS and the SDS as predictors of events, we performed separate analyses with different cut points for each perfusion variable. We created four groups o SSS and SDS with the purpose of evaluating the prognostic value and the stratification power of this new protocol on a CZT-GC based not only in positive or negative MPI results, but specially, based on the extension of defect and ischemia, which is widely stablished to be achieved by using this type of classification [10; 11]. A normal study was considered when SSS < 3 and SDS < 1.

Post-stress eight frames gated short-axis images were processed using quantitative gated SPECT software (Cedars-Sinai Medical Center, Los Angeles, California). Left ventricular ejection fraction (LVEF), end-systolic and end-diastolic volumes (ESV and EDV, respectively) were automatically calculated.

6.4.2 Follow-up

Follow-up was performed by telephone interview every 6 months after MPS. All-cause death, nonfatal myocardial infarction, or late revascularization (>60 days after MPS) were registered. Evaluation of hospital records and/or review of civil registries confirmed these events. Nonfatal myocardial infarction was defined based on the criteria of typical chest pain, elevated cardiac enzyme levels and typical alterations of the electrocardiogram [12]. Death and nonfatal myocardial infarction were classified as hard events. Late revascularization was studied separately

6.4.3 Statistical analyses

Categorical variables are presented as frequencies and continuous variables as mean ± SD. The annual event rate was calculated as the % of events divided by person-years, and was compared among groups using the log-rank test. Kaplan–Meier curves were generated to visually assess survival in different groups. A Cox proportional hazards analysis was done to evaluate predictors of hard events and late revascularization, using variables with p value< 0.05 in univariable analysis or clinical relevance.

Analyses were performed with SPSS software, version 17.0. A p value< 0.05 was considered significant.

6.5 Results

Among 3265 patients, 235 were excluded due to early revascularization, and 100 were lost to follow-up, leaving 2930 patients who were followed for 30.7±7.5 months. Mean age was 64.0±12.1 years and 53.5% were male. Among these patients, 2072 (70.7%) were asymptomatic. The most frequent indications in asymptomatic patients were a previous treadmill test with intermediate-high risk Duke Score, pre-op risk stratification and a previous calcium score >100. The most prevalent risk factor for CAD was hypertension (61.6%), followed by hypercholesterolemia (52.2%), smoking (36.4%) and family history of CAD (31.2%). Diabetes was present in 22.7% and previous myocardial infarction in 12.5%. From the 2930 patients, 501 (17.1%) had already been submitted to coronary angioplasty and 222 (7.6%) to coronary artery bypass grafting (CABG). About regularly medications, 37.9% was in use of ACE inhibitors, 28.6% was using beta-blocker and 10.9% Calcium receptor blockers. Mean perfusion scores were overall low and mean LVEF was normal with only 6% of patients with a LVEF< 40%. These characteristics are summarized in Table 1.

Table 1 Baseline data

Variables	All patients n (%) or Mean ± SD
Age (years)	64 ± 12.1
Male gender	1568 (53.5%)
Chest pain	865 (29.5%)
Hypertension	1807 (61.6%)
Hypercholesterolemia	1530 (52.2%)
Diabetes Mellitus	667 (22.7%)
Family history of coronary disease	915 (31.2%)
Smoking	1069 (36.4%)
Previous MI	367 (12.5%)
Previous CABG	222 (7.6%)
Previous PCI	501 (17.1%)
Exercise stress	1706 (58.2%)
Pharmacologic test	1224 (41.8%)
ACEi	1112 (37.9%)
Beta-blocker	839 (28.6%)
Calcium receptor blockers	320 (10.9%)
MPS	
SSS	1.7 ± 3.0 (0-26)
SRS	1.1 ± 2.1 (0-23)
SDS	0.6 ± 1.7 (0-18)
LVEF (<40%)	176 (6.0%)
LVEF (%)	62.4 ± 8.1
EDV (ml)	68 ± 17.0
ESV (ml)	26.4 ± 10.6

CABG coronary artery bypass grafting, *MI* myocardial infarction, *MPS* myocardial perfusion SPECT, *PCI* percutaneous coronary intervention, *SDS* summed difference score, *SRS* summed rest score, *SSS* summed stress score

For the definition of optimal scan time, acquired scans were processed using 1, 2, 3, 4, 5 or 6 min of the total list-mode acquisition previously performed for the pilot study. Intra and inter-observer agreement rates of MPS readings among time ranges are shown in Table 2. Based on those, the best combination, which was chosen for the subsequent MPS studies, was 6 min for the rest acquisition, 3 min for post-stress supine acquisition and 1.5 min for post-stress prone acquisition. Figure 1 shows an example of six post-stress images processed using a 6, 5, 4, 3, 2 and 1 min acquisition with a progressive degradation of image quality as we reduced the acquisition time. Considering all MPS studies performed thereafter, mean radiation dose was 6 mSv and mean scan time was 48±13 min.

Table 2 Intra- and interobserver agreement rates of MPS readings using 1 to 6 min time frames

Duration	6 min		5 min		4 min		3 min		2 min		1 min	
Agreement	Inter (%)	Intra (%)	Inter (%)	Intra (%)	Inter (%)	Intra (%)	Inter (%)	Intra (%)	Inter (%)	Intra (%)	Inter (%)	Intra (%)
Stress	100	100	100	100	100	100	100	100	100	96	96	92
Rest	100	100	100	100	100	96	100	92	92	92	92	88

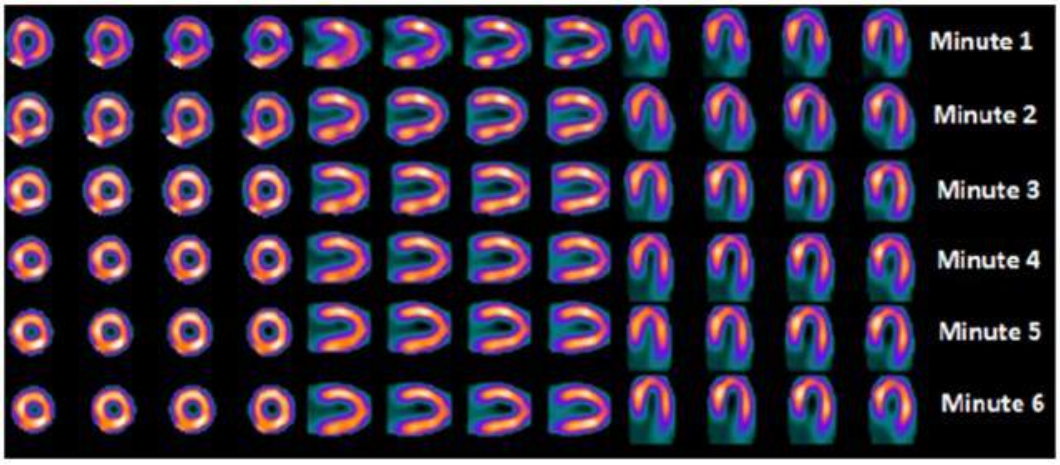

Figure 1 Example of six post-stress short-axis, vertical long axis and longitudinal long axis images processed using a 6, 5, 4, 3, 2 and 1 min acquisition, with a progressive reduction on image quality from to 6 to 1 min.

During follow-up there were 61 deaths, 29 nonfatal infarctions (90 hard events), 148 coronary angioplasty procedures and 22 bypass surgeries (170 late revascularization procedures). Table 3 shows the comparison between patients with or without hard events. The former were older, more frequently male, with prior myocardial infarction or prior CABG and less frequently able to perform exercise stress. Perfusion scores were higher, as well as left ventricular volumes, and LVEF was lower in patients with hard events. In Table 4, comparisons between patients with or without late revascularization are shown. Similarly to patients with hard events, those with late revascularization were older, more frequently male, with cardiovascular risk factors, known coronary artery disease, and less frequently able to perform exercise stress, with higher perfusion scores, left ventricular volumes, and lower LVEF.

Table 3 Characteristics of patients with or without hard events

Variables	Univariate analysis			Cox regression	
	Patients without HE (n= 2844)	Patients with HE (n= 86)	*p* value	HR [95% CI]	*p* value
Age (years)	64.5 ± 11.7	70.7 ± 12.3	< 0.001	1.03 [1.01-1.06]	0.001
Male gender	1515 (53.2%)	57 (66.3%)	<0.01	2.26 [1.33-3.80]	0.030
Chest pain	844 (29.6%)	21 (24.4%)	0.338	1.30 [0.76-2.23]	0.336
Hypertension	1748 (61.4%)	59 (68.6%)	0.173	1.01 [0.61-1.66]	0.955
Hypercholesterolemia	1483 (52.1%)	47 (54.7%)	0.660	1.00 [0.63-1.57]	0.999
Diabetes Mellitus	633 (22.2%)	34 (39.5%)	<0.001	1.69 [1.09-2.62]	0.02
Family history of CAD	887 (31.1%)	28 (32.6%)	0.906		
Smoking	1041 (36.6%)	28 (32.6%)	0.063	0.44 [0.23-1.08]	0.105
Previous MI	347 (12.2%)	20 (23.3%)	<0.01	0.71 [0.42-1.23]	0.229
Previous CABG	208 (7.3%)	14 (16.3%)	<0.01	0.67 [0.36-1.22]	0.196
Previous PCI	480 (16.8%)	21 (24.4%)	0.058	0.88 [0.53-1.45]	0.619
Exercise stress	1682 (59.1%)	24 (27.9%)	<0.01		
Pharmacologic test	1169 (41.1%)	62 (72.1%)	<0.01	2.91 [1.75-4.80]	0.000
MPS					
SSS[a]	2.6 ± 4.9	5.0 ± 6.3	<0.001	1.36 [1.07-1.73]	0.01
SRS	1.9 ± 4.2	3.2 ± 4.8	<0.001		
SDS[a]	0.7 ± 1.9	1.7 ± 3.4	<0.001	1.09 [1.02-1.17]	0.010
LVEF (%)	59.4 ± 11.0	55.5 ± 12.7	<0.01	0.75 [0.39-1.44]	0.392
EDV (ml)	81.4 ± 33.5	87.0 ± 34.6			
ESV (ml)	35.6 ± 25.5	42.0 ± 29.8			

*HE h*ard events; *CABG c* oronary artery bypass graft; *MI* myocardial infarction; *MPS* myocardial perfusion *SPECT; PCI* percutaneous coronary intervention; *SDS* summed difference score; *SRS* summed rest score; *SSS* summed stress score

[a]*SSS* and *SDS* were analyzed separately in the cox regression, each one with other selected variables

Table 4 Characteristics of patients with or without late revascularization

Variables	Univariate analysis			Cox regression	
	Patients w/o late revascularization (n= 2763)	Patients w/ late revascularization (n= 167)	*p* value	HR [95% CI]	*p* value
Age (years)	63.9 ± 12.2	66.4 ± 10.3	< 0.001	1.00 [0.99-1.02]	0.397
Male gender	1462 (52.8%)	110 (65.5%)	<0.01	1.35 [0.97-1.88]	0.068
Chest pain	812 (29.3%)	53 (31.5%)			
Hypertension	1690 (61.0%)	117 (69.6%)	0.044	1.07 [0.75-1.51]	0.689
Hypercholesterolemia	1425 (51.5%)	105 (62.5%)	<0.01	1.47 [1.06-2.04]	0.020
Diabetes Mellitus	598 (21.6%)	69 (41.1%)	<0.001	1.94 [1.41-2.66]	0.000
Family history of CAD	861 (31.1%)	54 (32.1%)			
Smoking	1001 (36.2%)	68 (40.5%)		0.77 [0.46-1.28]	0.314
Previous MI	317 (11.4%)	50 (29.8%)	<0.001	2.01 [1.43-2.83]	0.000
Previous CABG	208 (7.5%)	14 (8.3%)		1.60 [0.92-2.79]	0.095
Previous PCI	429 (15.5%)	72 (42.9%)	<0.001	2.54 [1.76-3.68]	0.000
Exercise stress	1624 (59.0%)	82 (48.8%)	<0.01		
Pharmacologic test	1955 (41.4%)	86 (51.2%)	<0.01	1.20 [0.86-1.67]	0.264
MPS					
SSS[a]	2.5 ± 4.7	6.6 ± 7.1	<0.001	1.06 [1.04-1.08]	0.000
SRS	1.9 ± 4.1	3.7 ± 5.6	<0.001		
SDS[a]	0.6 ± 1.7	2.9 ± 3.8	<0.001	1.22 [1.17-1.26]	0.000
LVEF (%)	59.6 ± 10.9	54.8 ± 12.0	<0.01	1.00 [0.99-1.00]	0.887
EDV (ml)	81.4 ± 33.5	88.5 ± 36.9	<0.01		
ESV (ml)	35.6 ± 25.5	43.0 ± 30.2	<0.01		

CABG coronary artery bypass graft; *MI* myocardial infarction; *MPS* myocardial perfusion *SPECT*; *PCI* percutaneous coronary intervention; *SDS* summed difference score; *SRS* summed rest score; *SSS* summed stress score

[a]*SSS* and *SDS* were analyzed separately in the cox regression, each one with other selected variables

Based on the SSS, 4 patient groups were created: group 1 with SSS values from 0 to 2 [n=2098 (71.6%)]; group 2, SSS values from 3 to 5 [n=430 (14.6%)]; group 3, SSS values from 6 to 11 [n=220 (7.5%)] and group 4, SSS ≥12 [n=182 (6.2%)]. Kaplan–Meier survival curves (Fig. 2a, b) showed that the highest the SSS, the lowest the survival free of hard events (p<0.001) or late revascularization (p<0.001), respectively. Table 5 shows the annualized hard events and late revascularization rates for individual groups of SSS, with highest rates in the group of highest SSS values.

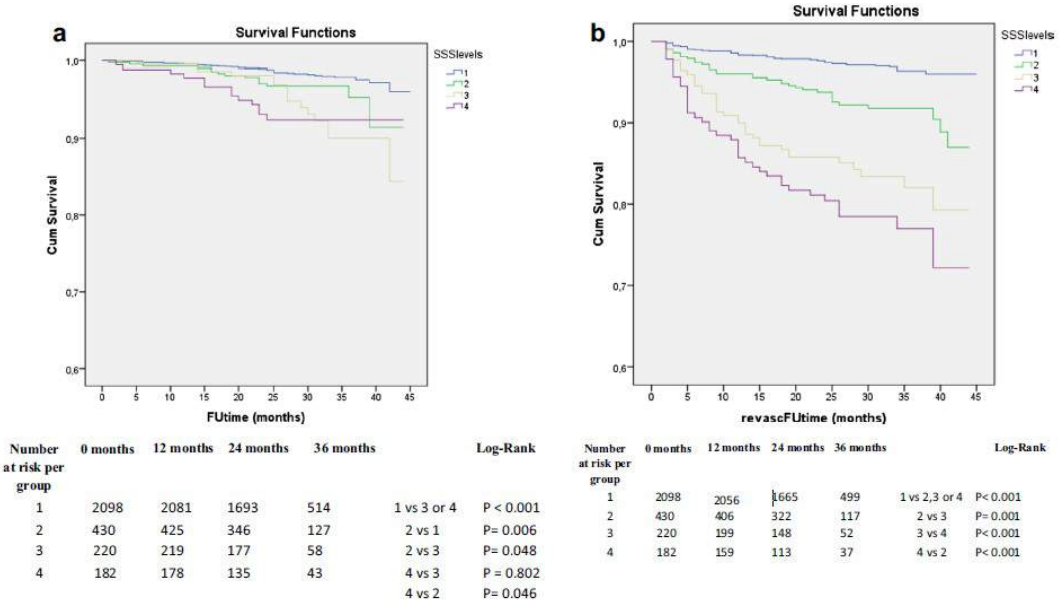

Number at risk per group	0 months	12 months	24 months	36 months		Log-Rank
1	2098	2081	1693	514	1 vs 3 or 4	P < 0.001
2	430	425	346	127	2 vs 1	P= 0.006
3	220	219	177	58	2 vs 3	P= 0.048
4	182	178	135	43	4 vs 3	P = 0.802
					4 vs 2	P= 0.046

Number at risk per group	0 months	12 months	24 months	36 months		Log-Rank
1	2098	2056	1665	499	1 vs 2,3 or 4	P< 0.001
2	430	406	322	117	2 vs 3	P= 0.001
3	220	199	148	52	3 vs 4	P< 0.001
4	182	159	113	37	4 vs 2	P< 0.001

Figure 2 Kaplan-Meier curves of hard events (a) or late revascularization (b) according to SSS categories. Blue line SSS 0-2, green line SSS 3-5; yellow line SSS 6-11; purple line SSS ≥12

Table 5 Annualized hard events and late revascularization rates for

SSS groups	Annualized hard evnt rates	Annualized late revascularizatio rates
1	0.57	0.90
2	1.27	2.45
3	2.06	4.96
4	2.15	6.48

Four groups were also created according to SDS values: group 1 with SDS=0 [n=2334 (79.6.0%)]; group 2, SDS values from 1 to 2 [n=305 (10.4%)]; group 3, SDS from 3 to 5 [n=171 (5.8%)] and group 4, SDS≥6 [n=120 (4.0%)]. Kaplan–Meier survival curves also showed that, with increasing SDS, event-free survival was reduced, both for hard events (Fig 3a) ($p<0.001$) or late revascularization (Fig. 3b) ($p<0.001$). Also, the annualized events rates, both for hard events or late revascularization, showed the same behavior presented on SSS groups for SDS groups, with higher rates in groups

with higher values of SDS (Table 6). For all Kaplan Meier survival curves, p values were demonstrated in a pairwise comparison, below the graphs, to express the statistical differences in events rates between individual groups.

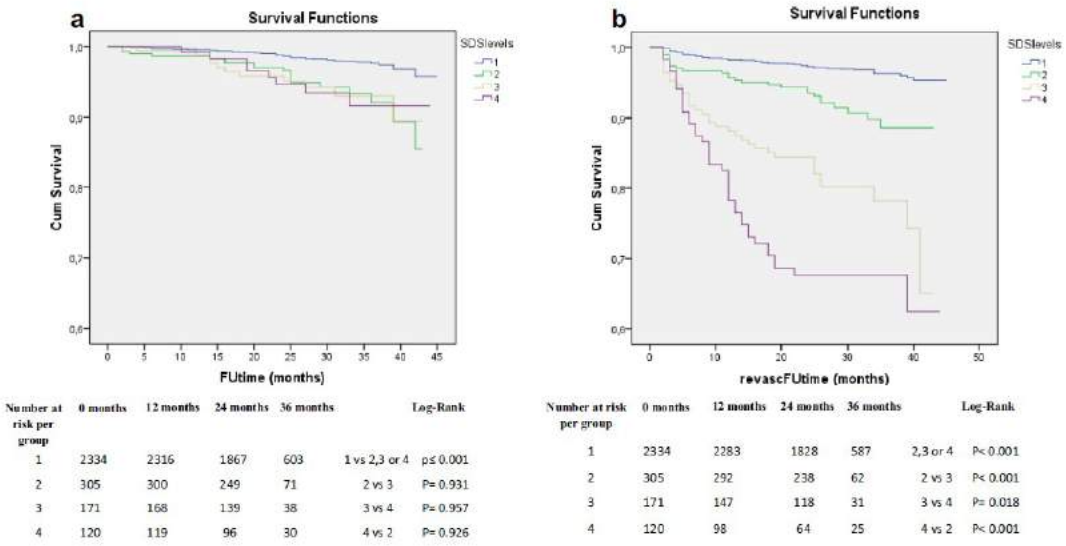

Number at risk per group	0 months	12 months	24 months	36 months		Log-Rank
1	2334	2316	1867	603	1 vs 2,3 or 4	p≤ 0.001
2	305	300	249	71	2 vs 3	P= 0.931
3	171	168	139	38	3 vs 4	P= 0.957
4	120	119	96	30	4 vs 2	P= 0.926

Number at risk per group	0 months	12 months	24 months	36 months		Log-Rank
1	2334	2283	1828	587	2,3 or 4	P< 0.001
2	305	292	238	62	2 vs 3	P< 0.001
3	171	147	118	31	3 vs 4	P= 0.018
4	120	98	64	25	4 vs 2	P< 0.001

Figure 3 Kaplan-Meier curves of hard events (a) or late revascularization (b) according to SDS categories. Blue line SDS 0, green line SDS 1-2; yellow line SDS 3-5; purple line SDS ≥6

Table 6 Annualized hard events and late revascularization rates for individual SDS groups

SDS groups	Annualized hard evnt rates	Annualized late revascularizatio rates
1	0.6	0.96
2	1.87	2.57
3	1.93	6.03
4	2.03	9.84

Finally, in the Cox analysis, male gender (hazard ratio=2.26 [1.33–3.8], p=0.03), age (hazard ratio=1.03 [1.01–1.06], p=0.001), diabetes (hazard ratio=1.69 [1.09–2.62], p=0.02), pharmacologic stress (hazard ratio=2.91 [1.75–4.8], p<0.001) and the SSS (hazard ratio=1.36 [1.07–1.73], p=0.01) were independently associated with hard events. SDS, when substituting SSS in the cox analysis, also showed to be an independent predictor of hard events (hazard ratio=1.09 [1.02–1.17], p=0.01) and maintained the results of the other variables. Table 3 shows all the variables used in the cox regression for hard events, with their respective hazard ratio and confidence interval.

For late revascularization, diabetes (hazard ratio=1.94 [1.41–2.66], p<0.001), prior percutaneous coronary intervention (hazard ratio=2.54 [1.76–3.68], p<0.001) and the SSS (hazard ratio=1.06 [1.04–1.08], p<0.001) were the independent predictors. Again, SDS also showed to be an independent predictor of late revascularization (hazard ratio=1.22 [1.17–1.26], p<0.001) when analyzed substituting the SSS with no modification in the other variables. Table 4 shows the variables used for this cox regression, with their respective hazard ratio and confidence interval.

6.6 Discussion

Previous studies have shown that CZT cameras are able to perform ultrafast and low-dose MPS studies, with even higher sensitivity and image quality when compared to traditional cameras [13]. However, there is still incomplete evidence supporting the prognostic value of MPS performed in CZT cameras. This study shows, in a large patient population, that the prognostic value of a new MPS protocol in a high-speed CZT-GC could be comparable to what literature has shown about the prognostic value traditionally provided by conventional MPS [9]. Our group had already demonstrated the

prognostic value of MPS with a new reconstruction algorithm [11] in traditional Anger cameras, which also allowed faster scans. However, with the advent of CZT technology, it became imperative to define if these new cameras would provide MPS studies with reliable prognostic value, which might be reliably used to manage patients with suspected or known CAD.

Dolan et al. demonstrated the prognostic value of MPS in a CZT camera, but as these authors recognized, they used the conventional dose of radiotracers [14]. The radiation dose used in this study was considerably lower than standard dose used in traditional protocols, and we initially tested different acquisition times to obtain the best possible images with low radiation. Total procedure time was reduced to less than one hour, with imaging time of 6 min for rest and 3 min for stress phase.

After establishing these parameters, we then studied the prognostic value of this protocol. Male gender, increasing age and the use of pharmacologic stress were significant predictors of hard events, as previously described [15; 16]. Diabetes was independently associated both with hard events or late revascularization. Of note, LVEF was not associated with events, what might be explained by the overall normal left ventricular function of the study population. Importantly, the extent and intensity of myocardial ischemia, as expressed by the SDS, was significantly associated with outcomes, what supports the prognostic value of this new protocol.

It is worth noting the characteristics of the study population, composed of outpatients, most asymptomatic (performing MPS as part of a preoperative evaluation or general screening due to cardiac risk factors) with normal left ventricular function. Nonetheless, the prevalence of diabetes was > 20%, and over 10% had a history of myocardial infarction, what increases overall risk and may improve the generalizability

of these results. Therefore, we believe that CZT MPS may be reliably used to evaluate patients for CAD, with the advantages of reduced imaging time and lower radiation dose.

We recognize, as a limitation, that the best method to establish the prognostic value of this new protocol in a CZT-GC would be a comparison between new and traditional cameras, with each patient being studied in both cameras and being control for themselves. However, it assumes that the same protocol would be used for both cameras [14]. Since the new low radiation dose and acquisition time protocol could not be used for traditional cameras, the study would not verify the protocol that this study aims to establish.

6.7 Conclusion

A new, faster, low-radiation, MPS protocol in a CZT camera was able to maintain the ability of stratifying patients with increased risk of events, showing that, in the presence of greater extension of defect or ischemia, patients presented higher rates of hard events and late revascularization.

Compliance with ethical standards

Conflict of interest: The authors declare that they have no conflict of interest.

6.8 References

[1] VERBERNE, H. J. et al. EANM procedural guidelines for radionuclide myocardial perfusion imaging with SPECT and SPECT/CT: 2015 revision. **Eur J Nucl Med Mol Imaging,** v. 42, n. 12, p. 1929-40, Nov 2015. ISSN 1619-7089. Disponível em: < https://www.ncbi.nlm.nih.gov/pubmed/26290421 >.

[2] HANSEN, C. L. et al. Myocardial perfusion and function: single photon emission computed tomography. **J Nucl Cardiol,** v. 14, n. 6, p. e39-60, 2007 Nov-Dec 2007. ISSN 1532-6551. Disponível em: < http://www.ncbi.nlm.nih.gov/pubmed/18022099 >.

[3] ODDSTIG, J. et al. Reduced administered activity, reduced acquisition time, and preserved image quality for the new CZT camera. **J Nucl Cardiol,** v. 20, n. 1, p. 38-44, Feb 2013. ISSN 1532-6551. Disponível em: < http://www.ncbi.nlm.nih.gov/pubmed/23143809 >.

[4] DUVALL, W. L. et al. Reduced stress dose with rapid acquisition CZT SPECT MPI in a non-obese clinical population: comparison to coronary angiography. **J Nucl Cardiol,** v. 19, n. 1, p. 19-27, Feb 2012. ISSN 1532-6551. Disponível em: < http://www.ncbi.nlm.nih.gov/pubmed/22147617 >.

[5] MOUDEN, M. et al. Impact of a new ultrafast CZT SPECT camera for myocardial perfusion imaging: fewer equivocal results and lower radiation dose. **Eur J Nucl Med Mol Imaging,** v. 39, n. 6, p. 1048-55, Jun 2012. ISSN 1619-7089. Disponível em: < http://www.ncbi.nlm.nih.gov/pubmed/22426827 >.

[6] HAYES, S. W. et al. Prognostic implications of combined prone and supine acquisitions in patients with equivocal or abnormal supine myocardial perfusion SPECT. **J Nucl Med,** v. 44, n. 10, p. 1633-40, Oct 2003. ISSN 0161-5505. Disponível em: < https://www.ncbi.nlm.nih.gov/pubmed/14530478 >.

[7] BURRELL, S.; MACDONALD, A. Artifacts and pitfalls in myocardial perfusion imaging. **J Nucl Med Technol,** v. 34, n. 4, p. 193-211; quiz 212-4, Dec 2006. ISSN 0091-4916. Disponível em: < https://www.ncbi.nlm.nih.gov/pubmed/17146108 >.

[8] BERMAN, D. S. et al. Comparative prognostic value of automatic quantitative analysis versus semiquantitative visual analysis of exercise myocardial perfusion single-photon emission computed tomography. **J Am Coll Cardiol,** v. 32, n. 7, p. 1987-95, Dec 1998. ISSN 0735-1097. Disponível em: < https://www.ncbi.nlm.nih.gov/pubmed/9857883 >.

[9] _____. Incremental value of prognostic testing in patients with known or suspected ischemic heart disease: a basis for optimal utilization of exercise technetium-99m sestamibi myocardial perfusion single-photon emission computed tomography. **J Am Coll Cardiol,** v. 26, n. 3, p. 639-47, Sep 1995. ISSN 0735-1097. Disponível em: < https://www.ncbi.nlm.nih.gov/pubmed/7642853 >.

[10] HACHAMOVITCH, R. et al. Incremental prognostic value of myocardial perfusion single photon emission computed tomography for the prediction of cardiac death: differential stratification for risk of cardiac death and myocardial infarction. **Circulation,** v. 97, n. 6, p. 535-43, Feb 1998. ISSN 0009-7322. Disponível em: < https://www.ncbi.nlm.nih.gov/pubmed/9494023 >.

[11] LIMA, R. et al. Prognostic value of myocardium perfusion imaging with a new reconstruction algorithm. **J Nucl Cardiol,** v. 21, n. 1, p. 149-57, Feb 2014. ISSN 1532-6551. Disponível em: < http://www.ncbi.nlm.nih.gov/pubmed/24281904 >.

[12] THYGESEN, K. et al. Universal definition of myocardial infarction. **J Am Coll Cardiol,** v. 50, n. 22, p. 2173-95, Nov 2007. ISSN 1558-3597. Disponível em: < https://www.ncbi.nlm.nih.gov/pubmed/18036459 >.

[13] DUVALL, W. L. et al. Reduced isotope dose and imaging time with a high-efficiency CZT SPECT camera. **J Nucl Cardiol,** v. 18, n. 5, p. 847-57, Oct 2011. ISSN 1532-6551. Disponível em: < http://www.ncbi.nlm.nih.gov/pubmed/21528422 >.

[14] OLDAN, J. D. et al. Prognostic value of the cadmium-zinc-telluride camera: A comparison with a conventional (Anger) camera. **J Nucl Cardiol,** v. 23, n. 6, p. 1280-1287, Dec 2016. ISSN 1532-6551. Disponível em: < https://www.ncbi.nlm.nih.gov/pubmed/26122879 >.

[15] HACHAMOVITCH, R. et al. Effective risk stratification using exercise myocardial perfusion SPECT in women: gender-related differences in prognostic nuclear testing. **J Am Coll Cardiol,** v. 28, n. 1, p. 34-44, Jul 1996. ISSN 0735-1097. Disponível em: < https://www.ncbi.nlm.nih.gov/pubmed/8752792 >.

[16] NAVARE, S. M. et al. Comparison of risk stratification with pharmacologic and exercise stress myocardial perfusion imaging: a meta-analysis. **J Nucl Cardiol,** v. 11, n. 5, p. 551-61, 2004 Sep-Oct 2004. ISSN 1071-3581. Disponível em: < https://www.ncbi.nlm.nih.gov/pubmed/15472640 >.

7 Artigo 2

Comparison of the prognostic value of myocardial perfusion imaging using a CZT-SPECT camera with a conventional anger camera

Ronaldo Lima; Thais Peclat; Thalita Soares; Caio Ferreira; Ana Carolina Souza; Gabriel Camargo

7.1 Abstract

Background: Recent studies have shown that myocardial perfusion imaging (MPI) in cadmium-zinc-telluride (CZT) cameras allow faster exams with less radiation dose but there are little data comparing its prognosis information with that of dedicated cardiac Na-I SPECT cameras

Objective: The objective of this study is to compare the prognostic value of MPI using an ultrafast protocol with low radiation dose in a CZT-SPECT and a traditional one.

Methods: Group 1 was submitted to a two-day MIBI protocol in a conventional camera, and group 2 was submitted to a 1-day MIBI protocol in CZT camera. MPI were classified as normal or abnormal, and perfusion scores were calculated. Propensity score matching methods were performed

Results: 3554 patients were followed during 33±8 months. Groups 1 and 2 had similar distribution of age, gender, body mass index, risk factors, previous revascularization, and use of pharmacological stress. Group 1 had more abnormal scans, higher scores than group 2. Annualized hard events rate was higher in group 1 with normal scans but frequency of revascularization was similar to normal group 2. Patients with abnormal scans had similar event rates in both groups

Conclusion: New protocol of MPI in CZT-SPECT showed similar prognostic results to those obtained in dedicated cardiac Na-I SPECT camera, with lower prevalence of hard events in patients with normal scan.

(J Nucl Cardiol 2016)

Key Words: myocardial perfusion imaging ; coronary artery disease; SPECT

7.2 Introduction

It is well known that myocardial perfusion imaging (MPI) with stress testing is an independent predictor of prognosis in patients with suspected or known coronary artery disease (CAD). The gated single-photon emission computed tomography (SPECT) appears to be the best predictor of cardiac event-free survival in this population.[1] Also, compared with other methods such as stress-ECG and coronary angiography, SPECT-based strategies seem to be more cost-effective.[2]

Over time, numerous technological advances have increased MPI's performance, with the most meaningful being the introduction of tomographic imaging and, later, of the multi-detector gamma cameras. Recent developments have allowed for reductions in scan time and radiation dose used to its acquisition.[3] Specifically, new multipinhole cameras with cadmium-zinc-telluride solid state detectors (CZT-SPECT) technology allow for faster image acquisition and lower radiation doses in comparison with traditional Sodium-Iodine Anger cameras. This allows for 1-day stress/rest MPI protocols, preserving diagnostic image quality and diagnostic accuracy.[4; 5] The CZT technology improves the energy and spatial resolutions, while using simultaneously acquired views improves the overall sensitivity, resulting in high-quality images.[6]

Previous examination of the prognostic value in specific groups, like the obese, demonstrated that CZT SPECT provides adequate risk stratification.[7] However, there is little data comparing the prognostic value between ultrafast protocol CZT-SPECT and dedicated cardiac Na-I SPECT cameras. That could impair the broad use of this technology. Our objective is to compare the prognostic value of MPI using these two camera protocols.

7.3 Methods

7.3.1 Population and Study Design

We analyzed two different groups of patients clinically referred to a SPECT-MPI in an outpatient clinic between 2008 and 2012. Patients in group 1 were scanned in Na-I SPECT cameras from 2008 to 2010, and in group 2 were scanned using CZTSPECT from 2011 to 2012.

Ninety-nine patients who underwent revascularization in the first 60 days after nuclear testing were excluded. History of significant cardiac valve disease or severe nonischemic cardiomyopathy (33 patients) or any condition which might adversely affect short-term prognosis were also considered exclusion criteria (Figure 1). Three patients were excluded because the images acquired in gamma camera CZT were inadequate for interpretation (BMI>45). The research was approved by the institutional review board, and all subjects signed informed consent.

Prior to scanning, a team of cardiologists collected information on the presence of categorical cardiac risk factors in each individual including hypertension, diabetes, hypercholesterolemia, smoking, and family history of CAD using a standard questionnaire.

Cardiac symptoms were based on Diamond and Forrester criteria,[8] divided as asymptomatic, non-anginal pain, atypical angina, typical angina, and shortness of breath.

From a total of 6128 patients meeting inclusion criteria, follow-up was complete in 5828 (95.1% of the total). We selected 3554 using propensity score matching based on sex, age, body mass index (BMI), symptoms, cardiac risk factors, history of coronary events, and type of stress used. A 1 to 1 nearest neighbor matching with no replacement was performed to produce two groups with 1777 individuals in each, divided according to the type of gamma camera used.

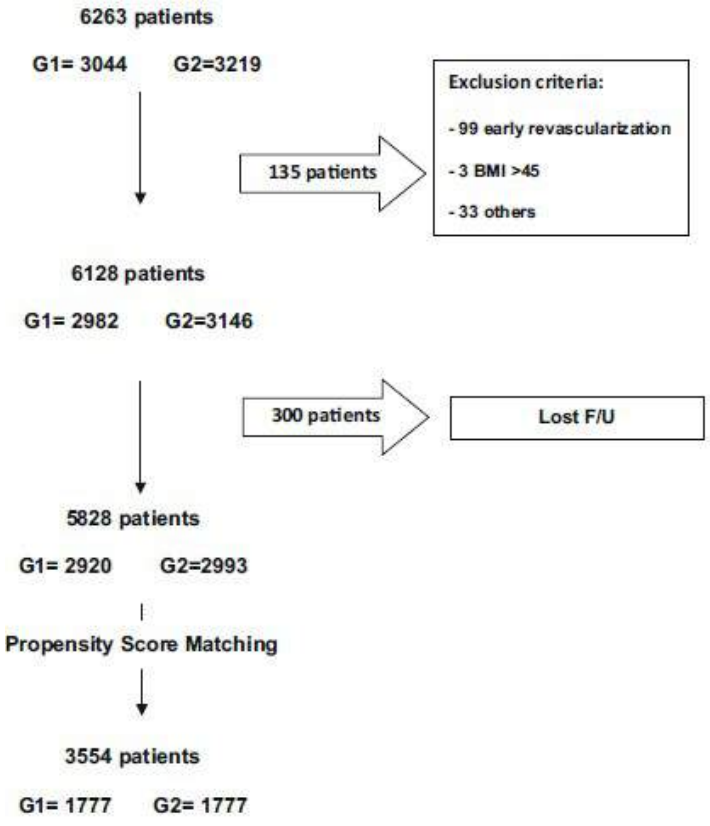

Figure 4 Flow diagram of the study

7.3.2 Cardiac Imaging and Stress Protocol

Patients were instructed to abstain from any products containing caffeine for 24 hours before the test. Beta-blockers and calcium-channel antagonists were terminated 48 hours before testing, and nitrates were withheld for at least 6 hours before testing. Stress testing was performed with a symptom limited Bruce treadmill exercise protocol or pharmacologic protocol (dipyridamole or dobutamine). In general, stress using dipyridamole was the first choice, while dobutamine was reserved for patients with contraindications to vasodilator stress (mainly bronchospastic airway disease).

Patients in group 1 underwent 2-day 99mTc-sestamibi (near-maximal exercise, 10-12 mCi was injected intravenously, and exercise was continued at maximal workload for at least 1 minute) gated MPS with scan time of 6 minutes stress and rest studies (15-18 mCi). Mean radiation dose was 9.5 mSv. Stress-only imaging was not performed due to reimbursement issues. Three minutes prone images were acquired in all male patients but gating was not performed. All supine images were gated. The full protocols used have been previously described.[9] MPI studies were classified as normal or abnormal, and perfusion scores (SSS, SRS, and SDS) were calculated. Images were acquired using a two-headed gamma camera equipped with 90◦-angled detectors (Ventri, GE Healthcare, Waukesha, WI, USA) equipped with a low-energy, high-resolution collimator, and 30 stops in a 64 x 64 matrix. Image acquisition began 15-45 minutes after tracer injection. Scans were reconstructed with Evolution for Cardiac^{TM} (GE healthcare), using 12 iterations. Post stress gated short-axis images were processed using quantitative gated SPECT software (QGS; Cedars-Sinai Medical Center, Los Angeles, California), and left ventricular ejection fraction (LVEF) was automatically calculated after inspection of myocardial contours.

Patients in group 2 underwent treadmill exercise or pharmacological stress using standard dipyridamole or dobutamine infusion protocols,[10] Exercise testing was performed using a symptom-limited Bruce protocol. A 1-day 99m-TcMIBI, rest/stress protocol was used, starting with rest study (injection of 5 mCi) followed by stress (15 mCi) in a CZT camera. Mean radiation dose was 6 mSv. The MPI were also classified as normal or abnormal and perfusion scores (SSS, SRS, and SDS) were also calculated. Post-stress prone acquisitions were performed in all patients. CZT-SPECT was performed using a camera with multipinhole collimator (Discovery 530, GE Healthcare, Milwaukee, USA). The system design allows acquisition without detector or collimator motion. Images were acquired in 6, 3, and 1 minute, respectively, for rest, supine stress and prone stress, as previously described[11]. A 10% symmetric energy window at 140 keV was used. Images were reconstructed on a dedicated Xeleris workstation (GE Healthcare) applying an iterative reconstruction algorithm with maximum-likelihood expectation maximization. Assessment of image quality and perfusion abnormalities was performed visually by two experienced nuclear cardiologists blinded to patient characteristics. Post-stress left ventricular volumes and ejection fraction were calculated from the post-stress-gated images using commercially available software (QGS, Cedars-Sinai Medical Center, Los Angeles, California, USA).

In both groups, semiquantitative visual interpretation of MPI images was performed with short-axis and vertical long axis tomograms divided into 17 segments.[10] Each segment was scored by consensus of two expert observers (aware of clinical and stress data) using a 5-point scale (0 = normal; 1 = equivocal; 2 = moderate; 3 = severe reduction of tracer uptake; 4 = the absence of detectable radiotracer activity in a segment). Then, perfusion scores were calculated to express the extent and severity of myocardial perfusion abnormalities. The summed stress score (SSS, a measure of the

total post-stress perfusion defect) and summed rest score (SRS, a measure of rest defect or myocardial fibrosis) were obtained by means of adding the scores for the 17 segments of the stress and rest images, respectively. The difference between the SSS and SRS was defined as the summed difference score (SDS, a measure of reversible defect or myocardial ischemia). For the purpose of evaluating the SSS and the SDS as predictors of events, we performed separate analyses with different cut points for each perfusion variable. We classified SSS as abnormal when it was >3 and SDS when it was >1.

7.3.3 Follow-Up

Follow-up was performed by telephone interview every 6 months after MPI. Events were defined as all-cause death and nonfatal myocardial infarction (classified as hard events) and late revascularization (>60 days after MPI), by percutaneous coronary intervention (PCI) or bypass surgery (CABG). Events were confirmed through review of hospital charts or physician's records. Nonfatal myocardial infarction was defined based on the criteria of typical chest pain, elevated cardiac enzyme levels, and typical alterations of the electrocardiogram.[12]

7.3.4 Statistical Analysis

All statistical calculations were performed using SPSS (Version 17). Categorical variables are presented as frequencies and continuous variables as mean ± SD. Variables were compared with Pearson Chi-squared test for categorical variables and by Student's two sample t test for continuous variables. Event-free survival curves were constructed using the Kaplan-Meier methods to account for censored survival times and were compared with the log-rank test.

7.4 Results

Patients were divided into group 1 and 2, each with of 1777 subjects, and its overall baseline characteristics are summarized in Table 1. There were no statistically significant differences between groups in regard of gender, prevalence of hypertension, diabetes, smoking, hypercholesterolemia, previous revascularization, and use of pharmacological stress. The more frequent indications in asymptomatic patients were a previous treadmill test with intermediate-high risk Duke Score, pre-op risk stratification and a previous calcium score >100. Patients with previous MI or revascularization were considered to have known CAD. The mean follow-up interval was 34 ± 9 months in group 1 and 33 ± 8 months in group 2.

Comparing the two groups, the classification as normal or abnormal scans and the perfusion scores (SSS, SRS, and SDS) were statistically different. Group 1 had more abnormal scans (27.4% vs 21.6%; $p<0.001$) and higher SSS, SRS, and SDS than group 2. Scan results, perfusion scores, left ventricle ejection fraction, and ventricular volumes of both groups are summarized in Table 2.

Table 7 Baseline characteristics

Baseline Characteristics	Total (6128)	Select (3554)	Group 1 (1777)	Group 2 (1777)	*p* value
Age (years)	63.0 ± 12.3	62.8 ± 12.0	62 ± 12.0	62.9 ± 12.0	1
Male	3370 (55.0%)	1920 (54.0%)	949 (53.4%)	971 (54.6%)	0.46
Weight (kg)	78.5 ± 17.7	78.1 ± 16.6	77.9 ± 16.3	78.2 ± 165.9	0.47
BMI	28.0 ± 6.1	27.8 ± 5.9	27.7 ± 6.0	27.9 ± 6.0	0.26
Asynptomatic	4221 (68.9%)	2377 (66.9%)	1171 (65.9%)	1206 (67.9%)	0.21
Diabetes	1396 (22.8%)	815 (22.9%)	390 (21.9%)	425 (23.9%)	0.16
Hypertension	3908 (63.8%)	2165 (60.9%)	1081 (60.8%)	1084 (61.0%)	0.92
Hypercholesterolemia	3166 (51.7%)	1764 (49.8%)	885 (49.6%)	879 (49.5%)	0.84
Beta-blockers	1782 (29.1%)	1074 (30.2%)	541 (30.4%)	533 (30%)	0.39
ACEi	3247 ((38.6%)	1365 (38.4%)	400 (22.5%)	410 (23.1%)	0.3
Statins	3062 (50.0%)	1777 (50.0%)	886 (49.9%)	891 (50.1%)	0.78
Previous MI	767 (12.5%)	439 (12.4%)	225 (12.7%)	214 (12.0%)	0.31
Previous PCI	1195 (19.5%)	628 (17.7%)	314 (17.7%)	314 (17.7%)	1
Previous CABG	550 (9.0%)	302 (8.5%)	159 (9.0%)	143 (8.0%)	0.34
Pharmacological stress	2566 (41.9%)	1458 (41.0%)	752 (42.3%)	706 (39.7%)	0.13

p value comparison between Group 1 and 2: n (%) or mean ± Standard deviation
ACEi angiotensin-converting enzyme inhibitor; *BMI* body mass index; *CABG* coronary artery bypass graft; *MI* myocardial infarction; *PCI* percutaneous coronary intervention

Table 8 Scans results, perfusion scores, and gated SPECT measurements

	Group 1 (1777)	Group 2 (1777)	*p* value
Abnormal scans	487 (27.4%)	383 (21.6%)	<0.001
Reversible	237 (13.3%)	154 (8.7%)	
Fixed	126 (7.1%)	128 (7.2%)	
Mixed defect	124 (7.0%)	101 (5.7%)	
SSS	2 (0-4)	1 (0-3)	<0.01
SRS	1 (1-3)	0 (0-2)	<0.01
SDS	0 (0-1)	0 (0-0)	<0.01
LVEF stress	58.5 ± 11.9	59.3 ± 13.0	0.07
EDV stress	80.1 ± 33.9	82.1 ± 33.5	0.1
ESV stress	36.4 ± 28.3	36.1 ± 26.5	0.7

EDV end diastolic volume; *ESV* end systolic volume; *LVEF* left ventricle ejection fraction; *SSS* summed stress score; *SRS* summed rest score; *SDS* summed difference score
Perfusion scores are expressed as median and interquantile 25 and 75

During follow-up, 98 deaths and 48 myocardial infarctions, 188 percutaneous coronary interventions, and 48 coronary artery bypass graft surgeries occurred. Assessing data from patients with normal scans, it was found that the annualized hard events rate was higher in patients of Group 1 (1.0%/year vs 0.5%/year; p<0.01), but the percentage of PCI and CABG were not different (0.9% vs 0.8%; 0.3% vs 0.1%, respectively; p = NS) comparing with Group 2. However, patients with abnormal scans had no significant difference between the two groups in regard of both annualized hard events (3.3%/year and 3.2%/year; p = NS) and percentage of revascularization (6.6% vs 6.3%, p = NS). Event rates comparison between two groups are demonstrated in Table 3. Kaplan-Meier cumulative survival comparing group 1 and 2 with normal or abnormal scan are shown in Figure 2 (hard events) and Figure 3 (late revascularization).

Table 9 Annualized event rate (%/year)

Variables	Group 1		Group 2	
	Normal scan (n=1290)	Abnormal scan (n= 487)	Normal scan (n=1394)	Abnormal scan (n= 383)
Hard events	1.0* (41)	3.3 (54)	0.5* (18)	3.2 (33)
Late Revascularization	1.2* (46)	4.2 (92)	0.7* (33)	3.3 (65)
Death	0.7* (26)	2.3 (33)	0.5* (16)	2.4 (23)
MI	0.4* (15)	1.5 (21)	0.06* (2)	1.0 (10)
PCI	0.9* (36)	5.0 (72)	0.8* (30)	5.1 (50)
CABG	0.3* (10)	1.6 (20)	0.1* (3)	1.2 (15)

*Significant difference between normal and abnormal scan
Significant difference between Group 1 and Group 2; (number of events)
CABG coronary artery bypass graft; *MI* myocardial infarction; *PCI* percutaneous coronary intervention

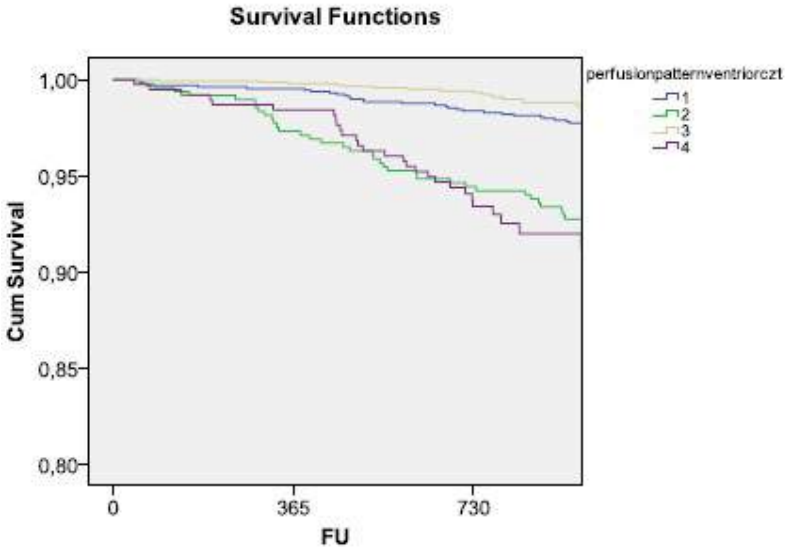

Number at risk				Log-rank
1291	1283	1260	1 vs 2	0.001
486	472	425	3 vs 4	0.001
1396	1392	1344	1 vs 3	0.38
381	375	345	2 vs 4	0.413

Figure 5 Kaplan-Meier curves for hard events. (1) Blue: Ventri normal scans; (2) Green: Ventri-abnormal scans; (3) Yellow: CZT normal scans; and (4) Purple: CZT abnormal scans.

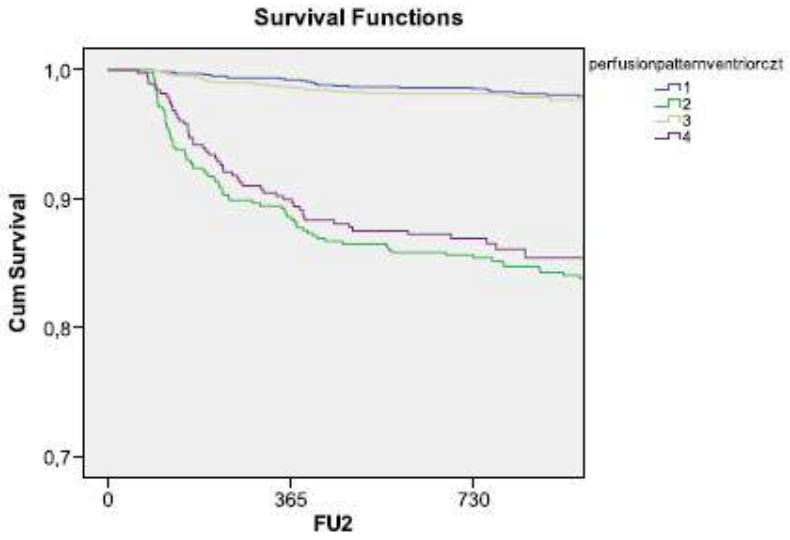

Number at risk				Log-rank
1291	1273	1242	1 vs 2	0.001
486	419	340	3 vs 4	0.001
1396	1372	1325	1 vs 3	0.292
381	336	269	2 vs 4	0.355

Figure 6 Kaplan-Meier curves for late revascularization. (1) Blue: Ventri normal scans; (2) Green: Ventri-abnormal scans; (3) Yellow: CZT normal scans; and (4) Purple: CZT abnormal scans.

7.5 Discussion

MPI is an established method for diagnostic and prognostic evaluation of patients with CAD.[1] However, two considerable limitations of this method are the prolonged time required to scan acquisition and the radiation dose.[13] New high-speed SPECT cameras using cadmium-zinc-telluride detectors are a new technology of gamma camera that allows shorter acquisition time and lower tracer doses.[14] Nevertheless, the prognostic value of this ultrafast, low-dose radiation, protocol is not yet established and has not been compared with the protocol in dedicated cardiac Na-I SPECT cameras.[15; 16; 17]

In an attempt to do this comparison, we studied two different groups with 1777 patients. They were standard to each other through a propensity score matching with the purpose of showing the association, in both groups, between scan results and the hard events rate. As can be seen in Table 1, the strict matching parameter we used produced two groups with very similar exposition to factors that could influence results.

Statistically significant differences in the distribution of perfusion scores (SSS, SRS, and SDS) and the classification as normal and abnormal scans were noted between the CZT camera and the conventional camera. The CZT camera had, on average, 6% less abnormal scans and lower SSS, SDS, and SRS as previously demonstrated by Oldan et al.[16] Results showed that the rate of events and myocardial revascularization was not higher in group 1. Someone might argue that the more frequently abnormal tests in Group 1 could mean greater accuracy of traditional equipment. In this case, a larger number of false negative tests should have occurred in Group 2, which did not happen. In fact patients with normal examination evaluated in CZT cameras showed a lower percentage of events.

In the follow-up data, our study has found that among patients with normal scans, the annualized hard events rate was higher in patients from traditional Na-I camera. The difference among hard event rate between both cameras may be an objective representation of the already known higher sensitivity for these new cameras, reflecting in a higher negative predicted value. In the follow-up of patients with abnormal scans, the study has shown no significant difference between the two groups in regard of both annualized hard events and percentage of revascularization. These data support that in patients with a higher probability of disease; both cameras were totally able to stratify the risk of events and thereby definitely established the MPI good prognostic value for patients with CAD.

There has been controversy regarding the diagnostic value of SPECT-MPI using CZT cameras in obese patients,[7] therefore the weight and BMI were included in the propensity score. As described in Population section, three patients were excluded because the images acquired in gamma camera CZT were inadequate for interpretation but more than 300 patients with at least 220 pounds were included in group 2. De Lorenzo et al demonstrated that in obese patients CZT-SPECT camera provides prognostic discrimination with high image quality This is consistent with the results of the present study.

Our study was a retrospective analysis of outpatients who underwent CZT-SPECT or traditional Anger camera for clinical indications which carries the obvious and inherent bias of this type of study design. This is also a single-institution study and thus may not be applicable to others institutions and others types of camera designs, both CZT and conventional. Beyond that, reviewers were not blinded to clinical data. While this is necessary to clinical interpretation of scan results, it can bias the interpretation for research purposes. However, we can assume that any bias introduced by use of clinical information should affect both cameras in the same degree. Finally, it is important to mention that while the propensity score matching was successful in producing groups with similar baseline characteristics that could bias the results, there could be other potential unknown sources of bias that may not have been balanced in our two groups using this approach.

Analyzing the few data produced by similar studies,[15; 16; 17] we concluded that our study also showed a pattern of maintenance of the prognostic value of CZT comparing with traditional cameras. However, we had the opportunity to use a larger population that was matched in baseline characteristics and exposed to two totally different protocols. We used a standard protocol as mentioned before to dedicated Na-I

cameras and a faster, lower-dose protocol in CZT-SPECT, something pioneer to this type of study.

7.6 New Knowledge Gained

The CZT camera has similar utility for prognostication to conventional Anger cameras even when they are using smaller radiation doses and shorter acquisition time.

7.7 Conclusion

In our study, a new protocol of MPI in CZT-SPECT camera showed similar prognostic results to those obtained in dedicated cardiac Na-I SPECT camera, with lower prevalence of hard events in patients with normal scan. According to these data, we can assume that the new ultrafast protocol, using considerable lower dose of radiation, has a reliable prognostic value and is non-inferior to traditional cameras.

7.8 Acknowledgments

The authors had no financial support for this research.

The authors would like to thanks Dr. Ilan Gottlieb for his review and valuable suggestions.

7.9 Compliance with Ethical Standards

7.9.1 Disclosure

The authors declare that they have no conflict of interest.

7.9.2 Ethical standards

All procedures performed in studies involving human participants were in accordance with the ethical standards of the institutional and/or national research committee and with the 1964 Helsinki declaration and its later amendments of comparable ethical standards.

7.9.3 Informed consent

Informed consent was obtained from all individual participants included in the study.

7.10 References

[1] GIMELLI, A. et al. Stress/Rest Myocardial Perfusion Abnormalities by Gated SPECT: Still the Best Predictor of Cardiac Events in Stable Ischemic Heart Disease. **J Nucl Med,** v. 50, n. 4, p. 546-53, Apr 2009. ISSN 0161-5505. Disponível em: < https://www.ncbi.nlm.nih.gov/pubmed/19289433 >.

[2] UNDERWOOD, S. R. et al. Economics of myocardial perfusion imaging in Europe--the EMPIRE Study. **Eur Heart J,** v. 20, n. 2, p. 157-66, Jan 1999. ISSN 0195-668X. Disponível em: < https://www.ncbi.nlm.nih.gov/pubmed/10099913 >.

[3] DEPUEY, E. G. Advances in SPECT camera software and hardware: currently available and new on the horizon. **J Nucl Cardiol,** v. 19, n. 3, p. 551-81; quiz 585, Jun 2012. ISSN 1532-6551. Disponível em: < https://www.ncbi.nlm.nih.gov/pubmed/22456968 >.

[4] DUVALL, W. L. et al. Reduced isotope dose and imaging time with a high-efficiency CZT SPECT camera. **J Nucl Cardiol,** v. 18, n. 5, p. 847-57, Oct 2011. ISSN 1532-6551. Disponível em: < http://www.ncbi.nlm.nih.gov/pubmed/21528422 >.

[5] HERZOG, B. A. et al. Nuclear myocardial perfusion imaging with a cadmium-zinc-telluride detector technique: optimized protocol for scan time reduction. **J Nucl Med,** v. 51, n. 1, p. 46-51, Jan 2010. ISSN 1535-5667. Disponível em: < https://www.ncbi.nlm.nih.gov/pubmed/20008999 >.

[6] SLOMKA, P. J. et al. Advances in technical aspects of myocardial perfusion SPECT imaging. **J Nucl Cardiol,** v. 16, n. 2, p. 255-76, 2009 Mar-Apr 2009. ISSN 1532-6551. Disponível em: < https://www.ncbi.nlm.nih.gov/pubmed/19242769 >.

[7] DE LORENZO, A. et al. Prognostic evaluation in obese patients using a dedicated multipinhole cadmium-zinc telluride SPECT camera. **Int J Cardiovasc Imaging,** v. 32, n. 2, p. 355-361, Feb 2016. ISSN 1875-8312. Disponível em: < https://www.ncbi.nlm.nih.gov/pubmed/26424491 >.

[8] DIAMOND, G. A. et al. Application of conditional probability analysis to the clinical diagnosis of coronary artery disease. **J Clin Invest,** v. 65, n. 5, p. 1210-21, May 1980. ISSN 0021-9738. Disponível em: < https://www.ncbi.nlm.nih.gov/pubmed/6767741 >.

[9] LIMA, R. et al. Prognostic value of myocardium perfusion imaging with a new reconstruction algorithm. **J Nucl Cardiol,** v. 21, n. 1, p. 149-57, Feb 2014. ISSN 1532-6551. Disponível em: < https://www.ncbi.nlm.nih.gov/pubmed/24281904 >.

[10] HENZLOVA, M. J. et al. ASNC imaging guidelines for SPECT nuclear cardiology procedures: Stress, protocols, and tracers. **J Nucl Cardiol,** v. 23, n. 3, p. 606-39, Jun 2016. ISSN 1532-6551. Disponível em: < https://www.ncbi.nlm.nih.gov/pubmed/26914678 >.

[11] LIMA R, P. T., AMARAL AC, NAKAMOTO A, LAVAGNOLI D, DE; A., L. **Preliminary data on the prognostic value of a new protocol of ultra-fast myocardial scintigraphy with less radiation in CZT gamma camera.** Arq Bras Cardiol: Im Cardiov. 29 (1)**:** 11-16 p. 2016.

[12] THYGESEN, K. et al. Universal definition of myocardial infarction. **J Am Coll Cardiol,** v. 50, n. 22, p. 2173-95, Nov 2007. ISSN 1558-3597. Disponível em: < https://www.ncbi.nlm.nih.gov/pubmed/18036459 >.

[13] DOUGLAS, P. S. et al. ACCF/ACR/AHA/ASE/ASNC/HRS/NASCI/RSNA/SAIP/SCAI/SCCT/SCMR 2008 Health Policy Statement on Structured Reporting in Cardiovascular Imaging. **J Am Coll Cardiol,** v. 53, n. 1, p. 76-90, Jan 2009. ISSN 1558-3597. Disponível em: < https://www.ncbi.nlm.nih.gov/pubmed/19118730 >.

[14] SHARIR, T. et al. Comparison of the diagnostic accuracies of very low stress-dose with standard-dose myocardial perfusion imaging: Automated quantification of one-day, stress-first SPECT using a CZT camera. **J Nucl Cardiol,** v. 23, n. 1, p. 11-20, Feb 2016. ISSN 1532-6551. Disponível em: < https://www.ncbi.nlm.nih.gov/pubmed/26012642 >.

[15] GIMELLI, A. et al. Comparison between ultrafast and standard single-photon emission CT in patients with coronary artery disease: a pilot study. **Circ Cardiovasc Imaging,** v. 4, n. 1, p. 51-8, Jan 2011. ISSN 1942-0080. Disponível em: < https://www.ncbi.nlm.nih.gov/pubmed/21068188 >.

[16] OLDAN, J. D. et al. Prognostic value of the cadmium-zinc-telluride camera: A comparison with a conventional (Anger) camera. **J Nucl Cardiol,** v. 23, n. 6, p. 1280-1287, Dec 2016. ISSN 1532-6551. Disponível em: < https://www.ncbi.nlm.nih.gov/pubmed/26122879 >.

[17] YOKOTA, S. et al. Prognostic value of normal stress-only myocardial perfusion imaging: a comparison between conventional and CZT-based SPECT. **Eur J Nucl Med Mol Imaging,** v. 43, n. 2, p. 296-301, Feb 2016. ISSN 1619-7089. Disponível em: < https://www.ncbi.nlm.nih.gov/pubmed/26392197 >.

8 Artigo 3

The additional Prognostic Value of Myocardial Perfusion SPECT in Patients with Known Coronary Artery Disease with high exercise capacity

Thais R. Peclat, Victor F. Souza, Ana Carolina A.H. Souza, Aline K. M. Nakamoto, Felipe M. Neves, Ronaldo Lima

8.1 Abstract

Background: Previous studies have questioned myocardial perfusion imaging with single photon emission computed tomography (MPI SPECT) cost-effectiveness in patients achieving ≥10 Metabolic Equivalents (METs) in the exercise electrocardiography (ECG) stress test. Nevertheless, it is still unknown the additional prognostic contribution of MPI in a population with known coronary artery disease (CAD), which represents a growing audience for this imaging method.

Objective: To determine the additional MPI prognostic value over ECG stress testing alone in patients with known CAD who achieved high exercise capacity (≥10 METs). **Methods:** We evaluated 4187 consecutive patients with known or suspected CAD referred for clinically-indicated MPI with exercise stress in an outpatient clinic in Rio de Janeiro, Brazil, between March 2008 and October 2012. They were classified in

those who reached ≥10 METs and <10 METs. Baseline characteristics, ECG stress test findings and MPI results were compared between groups. Patients were followed with 6-month phone calls and events were confirmed through review of hospital charts or death certification. Hard events were defined as death or nonfatal myocardial infarction (MI). Late revascularization was that occurring after 60 days of MPI.

Results: Patients were followed for a mean of 32.4 ± 9.7 months. Those achieving ≥10 METs were younger, more often male, and had statistically significant lower rates of hypertension, diabetes mellitus, and obesity. This group also had a greater prevalence of patients achieving their maximum age-predicted heart rate (82.8% vs 74.1%, p=0.002). Patients reaching ≥ 10 METs had lower annualized rate of hard events when compared to those achieving <10 METs (1.13 %/year vs 3.95 %/year, p<0.001). Patients who achieved ≥ 10 METs with an abnormal scan had a higher annualized rate of hard events compared to those in the same group with normal scans (3.37 %/year vs 0.57 %/year, p=0.023). There was also a stepwise increase in the rate of events according to SSS groups (p=0.01). Cardiac workload lower than 10 METs (2.72 [1.28-5.77], p=0.009) and an abnormal MPI scan (1.9 [1.15-3.39], p=0.01) were independently associated with hard events. There was no significant difference between groups of workload in the survival free of late revascularizations.

Conclusions: MPI was able to stratify the risk for all-cause mortality and nonfatal myocardial infarction in patients with known CAD achieving ≥ 10 METs in the exercise ECG stress test.

8.2 Introduction

Coronary artery disease (CAD) remains as the leading cause of death in adults in the United States, accounting for about one-third of all deaths in subjects over age 35 [1]. In patients with known or suspected CAD, accurate risk stratification and management guidance is of great value to improve outcomes.

Exercise electrocardiography (ECG) stress test and myocardial perfusion imaging with single photon emission computed tomography (MPI SPECT) are both well-known and established tests for risk stratification in stable CAD [2; 3]. It is known that MPI has higher sensitivity over exercise ECG stress test for detection of ischemia in patients with an intermediate pretest likelihood of CAD [4]. Moreover, MPI may provide additional clinical information on cardiac function and regional perfusion.

Exercise capacity is an established predictor of mortality [5; 6; 7; 8; 9; 10] and along the past two decades several authors have brought to discussion if this parameter would be sufficient to support clinical decision. Patients achieving ≥10 metabolic equivalents (METS) were shown to have excellent prognosis, with low rates of cardiovascular events and low prevalence of ≥10% LV ischemia regardless of peak exercise heart rate, questioning the usefulness of adding MPI-derived information [11; 12]. Later, the use of exercise capacity as criteria to skip the imaging injection protocol was continuously discussed and provisional protocols created to better address the groups of patients that could be selected for this approach and saved from unnecessary radiation exposure [13; 14].

Patients with known CAD are an important percent of the cohort commonly referred to MPI due to its well-established prognostic value, worthy to be used in the management of those patients. An association between exercise capacity and overall mortality in patients with known cardiovascular conditions was previously

demonstrated [15]. However, no further investigation was done to understand how the workload relates to MPI results regarding the ability to predict outcomes when evaluating this group in particular.

The aim of this study is to determine the additional MPI prognostic value over ECG stress testing alone in patients with known CAD who achieved high exercise capacity (≥10 METs).

8.3 Methods

8.3.1 Study Cohort

We evaluated 4187 consecutive patients with known or suspected CAD referred for clinically-indicated MPI with exercise stress in an outpatient clinic in Rio de Janeiro, Brazil, between March 2008 and October 2012. Patients with suspected CAD, who underwent early revascularization (coronary angioplasty or coronary artery bypass grafting surgery occurring < 60 days after MPI), with history of significant cardiac valve disease, severe non-ischemic cardiomyopathy or any condition which might affect short-term prognosis were excluded.

Patients were classified as having known CAD by a reported medical history of myocardial infarction (MI); coronary artery bypass graft (CABG) or percutaneous coronary intervention (PCI). From 948 patients meeting all criteria, follow-up was completed in 926 (97.6% of the total). Study cohort flowchart is showed on figure 1.

Prior to the scan, patients' medical history and physical examination data were collected in a standard questionnaire by a team of experienced cardiologists. Categorical cardiac risk factors including hypertension, diabetes, hypercholesterolemia, smoking, obesity and family history of CAD were collected. Cardiac symptoms were based on

Diamond and Forrester criteria[16] and classified as asymptomatic, non-cardiac pain, atypical angina, typical angina, and shortness of breath.

All study procedures were in accordance with the ethical standards of the institutional research committee. Informed consent was obtained from all individual participants included in the study.

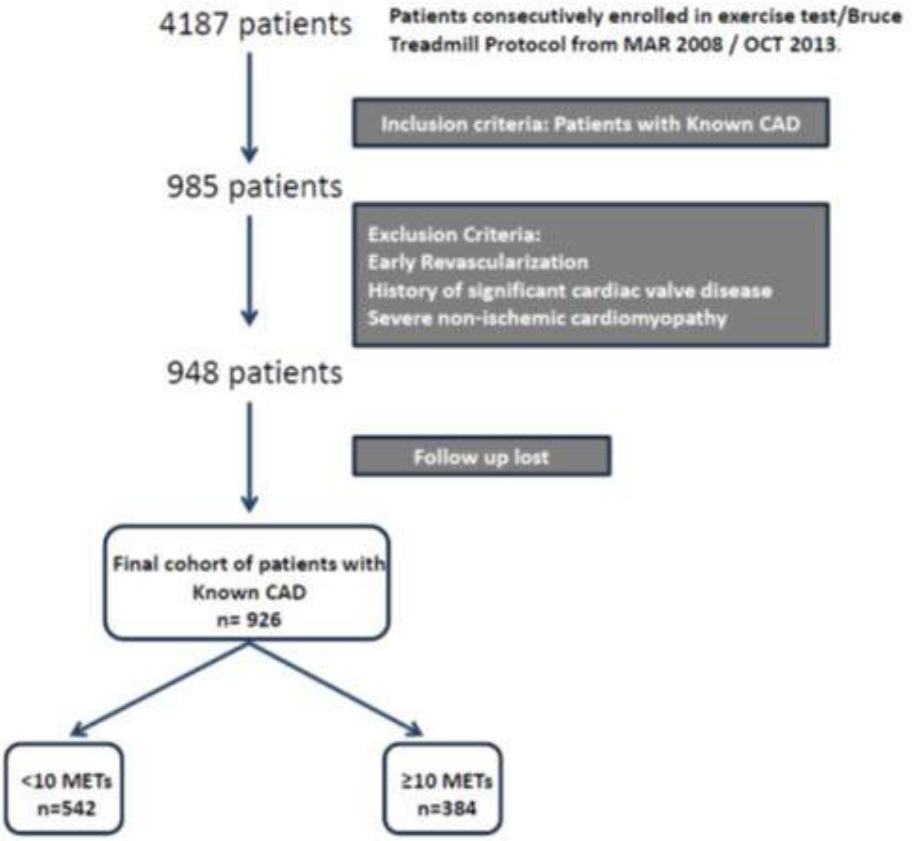

Figure 7 Study cohort derivation flowchart

8.3.2 Study Protocol

8.3.2.1 Exercise Testing

Stress ECG test was performed based on a symptom-limited Bruce treadmill protocol. Exercise workload was defined by the total METs achieved. Ischemic ST segment depression was defined as a horizontal or down-sloping depression of the ST segment with ≥1 mm present ≥80 ms after the J-point for 3 consecutive beats.

8.3.2.2 SPECT Imaging

The SPECT imaging protocols have been previously described and validated [17; 18; 19], and will be summarized here. Patients underwent either a 2-day or 1-day Tc-99m-Sestamibi gated MPI protocol. For the 2-day protocol, in the resting phase, a dose of 15-18mCi ^{99m}Tc-sestamibi was injected with acquisition of the images after 15 to 40 minutes. In the stress phase a dose of 10-12mCi of ^{99}mTc-sestamibi was injected near maximal exercise, which was continued at maximal workload for at least 1 minute. Image acquisition was performed after 15 to 30 minutes. MPI images were acquired through the gated-SPECT technique using a two-headed gamma camera (Ventri, GE Healthcare, Waukesha, WI, USA).

The 1-day 99mTc-sestamibi rest/stress protocol was also used, starting with rest study (injection of 5 mCi) followed by stress (15 mCi) in a CZT camera. CZT-SPECT was performed using a camera with multipinhole collimator (Discovery 530, GE Healthcare, Milwaukee, USA). Images were acquired in 6, 3, and 1 minute, respectively, for rest, supine stress and prone stress.

8.3.3 Imaging Interpretation

All images were interpreted by two experienced cardiologists. Image processing was performed with the software Evolution for Cardiac® using 12 iterations. Images were reconstructed without scatter or attenuation correction. Post-stress gated short axis, vertical and horizontal long-axis tomograms as well as polar maps were generated and analyzed.

A semi quantitative 17-segment visual interpretation of the gated myocardial perfusion images was performed [20; 21]. Each segment was scored by consensus using a standard five-point scoring system [22] (0 = normal, 1 = equivocal, 2 = moderate, 3 = severe reduction of uptake, and 4 = absence of detectable tracer uptake) and each reader chose a score based on both quantitative perfusion data and qualitative visual assessment. Summed stress scores (SSS) were obtained by adding the scores of the 17 segments of the stress images. Summed rest scores (SRS) were obtained by adding scores of the 17 segments of the rest images and a summed difference score (SDS) was calculated by segmental subtraction (SSS-SRS).

For evaluating the correlation of SSS and the SDS with outcomes, we performed separate analyses with different cut points for each perfusion variable. We created four groups o SSS and SDS with the purpose of evaluating the prognostic value and the stratification power based on the extent of defect and ischemia which is widely established to be achieved by using this type of classification [17; 23].

We converted SSS into percentage of left ventricle total perfusion defect (TPD). An abnormal scan was considered as having an SSS ≥ 4 or TPD $\geq 5\%$

Left ventricular ejection fraction (LVEF), end-systolic and end-diastolic volumes (ESV and EDV, respectively) were automatically calculated (Cedars-Sinai Medical Center, Los Angeles, California).

8.3.4 Follow-up

Follow-up was performed by telephone interview every 6 months after MPI. All-cause death, nonfatal myocardial infarction (MI), and late revascularization (>60 days after MPI) were registered. Events were confirmed through review of hospital charts, physician's records and death certification. Nonfatal MI was defined based on the criteria of typical chest pain, elevated cardiac enzyme levels and typical alterations of the electrocardiogram [24]. All-cause death and nonfatal myocardial infarction were classified as hard events and time to first event was considered. Late revascularization was analyzed separately.

8.3.5 Statistical analyses

Categorical variables are presented as frequencies and were calculated using the Pearson Chi-Square or Fisher's Exact Test. Continuous variables are presented as mean ± SD or median and percentiles and were calculated using nonparametric test for independent samples. The annual event rate was calculated as the % of events divided by person-years, and was compared among groups using the log-rank test. Kaplan-Meier curves were generated to visually assess survival in different groups. A cox regression model was used for testing predictors of all-cause mortality and non-fatal MI and variables with a p value <0.05 in the univariate analysis or with clinical significance were considered in the model. All analyses were performed with IBM SPSS statistics version 22.0 and the alpha level of significance was 0.05.

8.4 Results

8.4.1 Cohort baseline Characteristics

A total of 926 patients were followed for a mean 32.4 ± 9.7 months. The clinical characteristics of this study cohort are summarized in table 1. Patients were divided into two groups: Those who achieved ≥10 METs (41.5%), here named group 1, and <10 METs (58.5%), named group 2. Patients achieving higher workloads were younger, more often male, and had lower rates of hypertension, diabetes mellitus and obesity. There was no significant difference between groups concerning the presence of angina.

Table 10 Baseline Characteristics relative to cardiac workload

Baseline Characteristics	Group 1 ≥ 10 METs 384 (41.5%)	Group 2 < 10 METs 542 (58.5%)	Entire cohort n=926	*p* Value*
Age	59.6 (9)	66.7 (9.2)		<0.001
Male	363 (94.5%)	379 (69.9%)	742 (80.1%)	<0.001
Symptoms:				
Asymptomatic	286 (74.5%)	396 (73.1%)	682 (73.6%)	0.630
Typical Angina	16 (4.2%)	24 (4.4%)	40 (4.3%)	0.847
Atypical angina	64 (16.7%)	93 (17.2%)	157 (16.9%)	0.844
Hypertension	216 (56.3%)	345 (63.7%)	561 (60.5%)	0.023
Diabetes Mellitus	67 (17.4%)	162 (29.9%)	229 (24.7%)	<0.001
Hyperlipidemia	220 (57.3%)	327 (60.3%)	547 (59%)	0.354
BMI ≥ 30	65 (17.6%)	123 (24%)	188 (20.3%)	0.023
History of tobacco use	140 (36.4%)	202 (37.3%)	342 (36.9%)	0.968
Previous MI	158 (41.1%)	240 (44.3%)	398 (42.9%)	0.342
Previous CABG	174 (32.1%)	107 (27.9%)	281 (30.3%)	0.095
Previous PCI	356 (65.7%)	253 (65.9%)	609 (65.7%)	0.503
Family History of CAD	177 (46.1%)	225 (41.5%)	402 (43.4%)	0.166

BMI Body Mass Index; *MI* Myocardial Infarction; *CABG* Coronary Artery Bypass Graft; *PCI* Percutaneous Coronary Intervention; *CAD* Coronary Artery Disease.
* Values < 0.05 are considered statistically significant

8.4.2 Stress-ECG Test and SPECT Findings

Table 2 present findings on the stress-ECG test and SPECT imaging stratified by groups of workload achievement. Maximum heart rate achieved during the test was higher in the group of patients achieving ≥ 10 METs (148 vs 137, $p<0.001$), as well the prevalence of patients achieving ≥ 85% of their Maximum age-predicted Heart Rate (MAPHR) (82.8% vs 74.1%, $p=0.002$). The prevalence of chest pain during the ECG stress was lower in group 1 for both typical (2.3% vs 7.4%, $p=0.003$) and atypical angina (1.8% vs 2.4%, $p=0.003$) compared to group 2. There was no significant difference in the prevalence of exercise ST depression between groups.

Table 11 Exercise test and SPECT parameters relative to cardiac workload

Tests Parameters	Group 1 ≥ 10 METs n=384	Group 2 < 10 METs n=542	*p* Value *
Stress-ECG Test:			
Exercise ST depression [n(%)]	35 (9.1%)	47 (8.7%)	0.815
Maximum HR (bpm) (Median(25th, 75th)	148 (138,162)	137 (126,149)	<0.001
>85% MAPHR	303 (82.8%)	380 (74.1%)	0.002
Chest pain during stress [n(%)]			
Typical angina [n(%)]	9 (2.3%)	40 (7.4%)	0.003
Atypical angina [n(%)]	7 (1.8%)	13 (2.4%)	0.003
SPECT imaging:			
Abnormal Scans (%)	74 (19.3%)	119 (22%)	0.322
Mean of SSS (±SD)	2.69 (4.5)	2.97 (5)	0.824
Mean of SDS (±SD)	0.69 (1.8)	0.87 (2.2)	0.424
Mean % TPD (±SD)	3.9 (0.33)	4.3 (0.31)	0.824
LV TPD n (%)			
< 5%	310 (80.7%)	423 (78%)	0.678
5-7 %	18 (4.7%)	29 (5.4%)	0.678
8-9%	10 (2.6%)	12 (2.2%)	0.678
≥ 10%	46 (12%)	78 (14.4%)	0.678
EF < 40% [n(%)]	24 (6.3%)	63 (11.7%)	0.006

HR Hear Rate; *MAPHR* Maximum Age-Predicted Heart Rate; *SSS* Summed Stress Score; *SDS* Summed Difference Score; *LV TPD* Left ventricle total perfusion defect; *LVEF* Left ventricle ejection fraction

* Values < 0.05 are considered statistically significant

When comparing exercise capacity to SPECT imaging results there was no significant difference between groups 1 and 2, respectively, on mean SSS (2.69 vs 2.97), SDS (0.69 vs 0.87) or TPD (3.9 vs 4.3).The prevalence of patients with significant left ventricular dysfunction (EF<40%) was lower in those reaching higher cardiac workloads (6.3% vs 11.7% p=0.006).

8.4.3 Outcomes

A total of 42 deaths (4.5%) and 20 nonfatal myocardial infarction (2.1%) (58 hard events) occurred during the follow-up period, as shown on table 3. The group of patients achieving ≥10 METs had a lower annualized rate of hard events when compared to group 2 (1.13 %/year vs 3.95 %/year, p<0.001). The difference in cumulative survival free of hard events according to cardiac workload achievement is shown in the Kaplan-Meier survival curve (p<0.001) (Figure 2).

Table 12 Prevalence of outcomes relative to cardiac workload

Event	Group 1 ≥ 10 METs n=384	Group 2 < 10 METs n=542	Entire cohort n=926	*p* Value*
Hard events	10 (2.6%)	48 (8.9%)	58 (6.3%)	<0.001
All-cause mortality	6 (1.6%)	36 (6.6%)	42 (4.5%)	<0.001
Non-fatal MI	4 (1%)	16 (3%)	20 (2.1%)	0.04
Late revascularization	22 (5.7%)	40 (7.4%)	62 (6.7%)	0.322

MI Myocardial Infarction
* Values < 0.05 are considered statistically significant

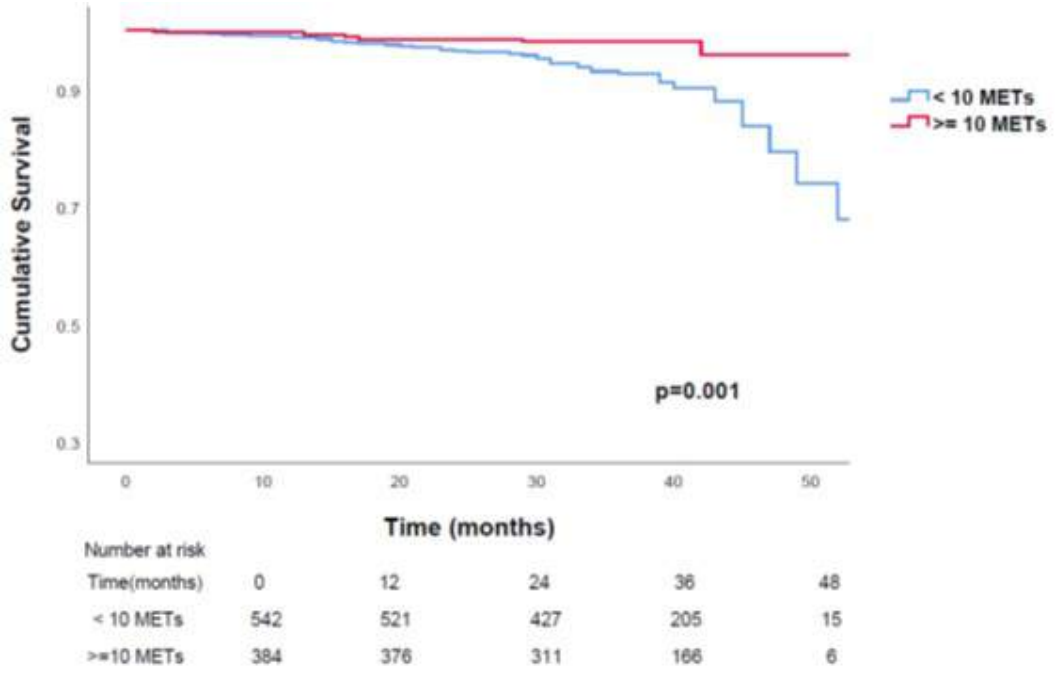

Figure 8 Survival free of hard events stratified by cardiac workload. Blue line Patients reaching < 10 METs. Red line Patients reaching ≥ 10 METs.

In order to evaluate the MPI prognostic contribution for patients with high exercise capacity, we analyzed survival only in patients achieving ≥ 10 METs, stratified for scan results, SSS, and SDS groups. Patients who reached ≥ 10 METs with an abnormal scan had a higher annualized rate of hard events compared to those who reached ≥ 10 METs with normal scans (3.37 %/year vs 0.57 %/year, p=0.023) (Figure 3). There was also a stepwise increase in the rate of events according to SSS groups (figure 4). Kaplan-Meier curves (figures 5 and 6) show cumulative survival curves among patients achieving ≥10 METs based in scan results and SSS groups, respectively. There was no difference in the prevalence of these events when stratifying this same subgroup according to SDS groups.

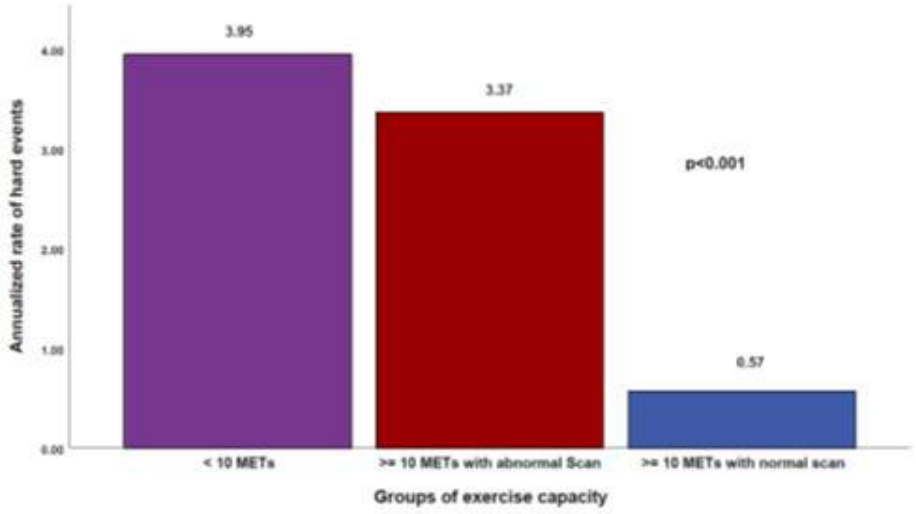

Figure 9 Annualized rate of hard events per group of cardiac workload and scan results in %/year.

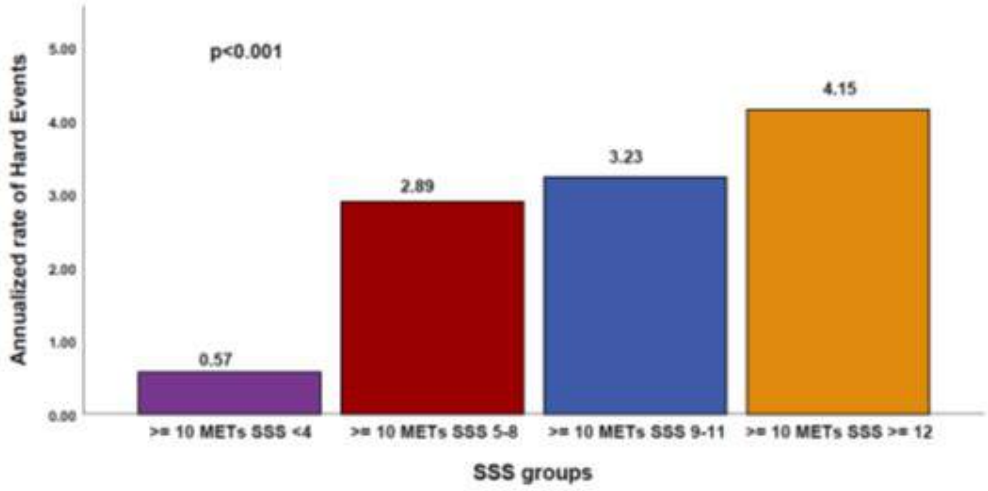

Figure 10 Annualized rate of hard events in patients achieving ≥10 METs per group of SSS in %/year.

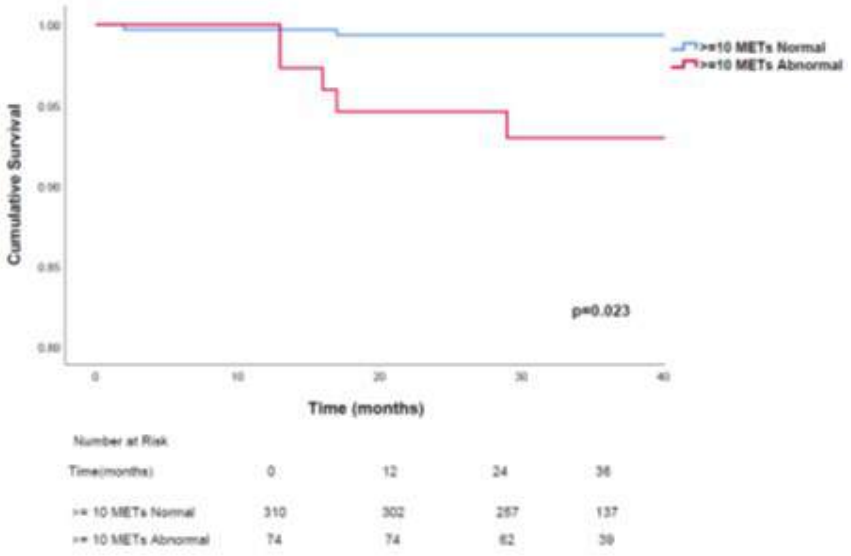

Figure 11 Survival free of hard events stratified by Scan Results in patients achieving ≥10 METs. Blue line Patients reaching ≥10 METs with normal scans; Red line Patients reaching ≥10 METs with abnormal scans.

METs. *Blue line* Patients reaching ≥10 METs with normal scans; *Red line* Patients reaching ≥10 METs with abnormal scans.

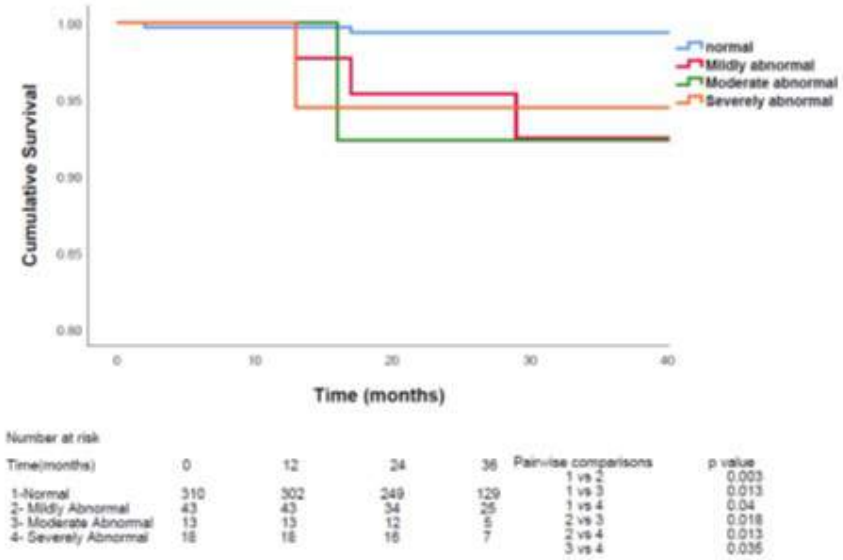

Figure 12 Survival free of hard events stratified by SSS groups in patients achieving ≥10 METs. (1) Blue line - Normal (SSS <4); (2) Red line – Mildly abnormal (SSS 4-8); (3) Green Line – Moderate Abnormal (SSS 9-11); (4) Orange line - Severely abnormal (SSS≥12)

When focusing exclusively on late revascularization as the outcome of interest there were 55 PCI and 7 CABG (62 late revascularizations) (Table 3). Annualized rate of late revascularization was not different between groups 1 and 2 (2.1%/year vs 2.8%/year, respectively). Figure 7 shows the cumulative survival free of late revascularization when comparing cardiac workload. Also, when comparing the annual rate of these events on patients who reached ≥10 METs based on MPI results there is no difference between groups (2.07 %/year normal scans vs 2.79%/year abnormal scans). The annual rates found in our study for these events are higher them previously described in studies with similar cohort sizes.

Finally, in the Cox regression analysis, cardiac workload achievement <10 METs (2.72 [1.28-5.77], p=0.009) and an abnormal MPI result (1.9 [1.15-3.39], p=0.01) were independently associated with hard events.

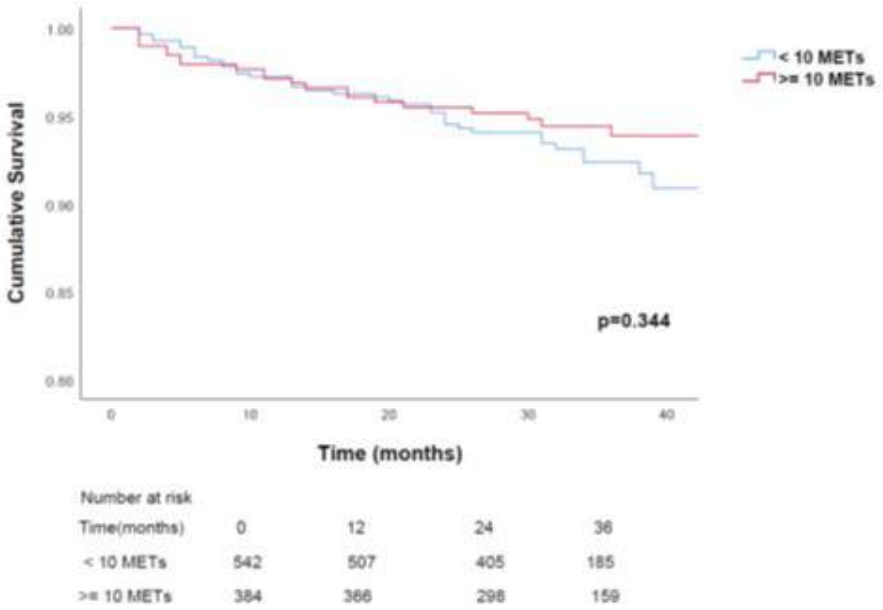

Figure 13 Survival free of Late Revascularizations stratified by workload achievement. Blue line Patients reaching <10 METs. Red line Patients reaching ≥10 METs.

8.5 Discussion

The clinical application of exercise capacity testing as a gatekeeper for nuclear imaging has been a debated topic along the last decade. MPI cost-effectiveness, procedure cost and related benefits are growing challenges in an era of advanced cardiac imaging technologies [3]. On that context, it is crucial to reassure the risk stratification ability of each method in specific populations.

It is established that patients achieving ≥10 METs have low rates of cardiovascular events and low prevalence of ≥ 10% LV ischemia on MPI regardless of peak exercise heart rate [11; 12]. Duvall et al attempted to create a hypothetical provisional injection protocol, applying the ≥10 METs cut-off as criteria to abstain from the injection. However, groups such as older adults and patients with known CAD were excluded [14]. More recently, Smith et al described that exercise capacity also influences outcomes in patients with ≥65 years-old and it is associated to a low rate of significant ischemia in MPI [13]. Nonetheless, it is still not clear if patients with known CAD would show similar results.

Here, we addressed how the achievement of high exercise capacity (≥10 METs) is associated with mortality and cardiovascular events in a population comprised of patients with known CAD referred for exercise ECG-stress MPI. Of most importance, we tried to determine the additional contribution of MPI prognostic value in that specific population.

We showed that patients attaining higher workloads were younger, more often male, and had significant lower rates of hypertension, diabetes mellitus and obesity. Approximately 70% of the population was asymptomatic before the test with no difference between groups 1 and 2 in the prevalence of pre-test symptoms. It indicates

that the main reason for scan referral was to follow up their known CAD, for prognostic assessment and treatment management.

There was no significant difference in the prevalence of ST depression between groups 1 and 2. Also, there was no difference in the prevalence of abnormal scans or extent of ischemia in patients with ST depression compared to those without ST depression.

Survival analyses showed that patients with known CAD achieving ≥10 METs had a significantly better prognosis compared to those attaining <10 METs for all-cause mortality and non-fatal MI, with a lower annualized rate of hard events when compared to those reaching <10 METs (1.13 %/year vs 3.95 %/year, $p<0.001$). This finding is similar to what has been previously described.

However, to further understand how scan results predicted hard events in the study population, we analyzed survival only in patients attaining ≥10 METs. Those with abnormal scans had a significant higher annualized rate of events. Furthermore, the increase in the annualized rate of hard event is directly proportional to the extent of defect based on the increase in SSS values. It shows that although a higher exercise capacity is associated with a lower prevalence of all-cause mortality and non-fatal MI, there is a prognostic difference based on MPS result. These findings were corroborated by Cox regression analysis, showing that both exercise capacity and scan results were independently associated to hard event.

We found no difference in the rate of late revascularization neither between workload groups or between groups of patients with higher cardiac workload divided by scan result. This finding is similar to what has been described in the literature, which has shown a lower annual rate of these events with no difference based on cardiac workload [12; 13].

Nevertheless, our study shows grater annualized rates of revascularization for patients reaching ≥10 METs when compared to previous studies having similar cohort sizes. Bourque et al demonstrated an annualized rate of late revascularization of 0.1%/year in a cohort of 463 patients with suspected and known CAD achieving ≥10 METs [12]. In another study comprised of older adults (mean age of 70 years-old) with suspected and known CAD, the annual rate in those achieving higher cardiac workload was 1.4%/year[13]. It is still lower than what we found in a population of known CAD with a mean age of 60 years-old.

These results may contribute to better determine appropriate referral criteria to MPI in patients with known CAD who achieved high exercise capacity in stress-ECG test.

8.6 Limitations

Our study has some limitations, including its retrospective, observational and single-institution nature. It is worth to notice that despite having a large sample size, the prevalence of events in the group with higher exercise capacity is low and it might have limited further subgroup analyses.

8.7 Conclusion

MPI was able to stratify the risk for all-cause mortality and nonfatal myocardial infarction in patients with known CAD achieving ≥ 10 METs in the exercise ECG stress test.

8.8 References

[1] SANCHIS-GOMAR, F. et al. Epidemiology of coronary heart disease and acute coronary syndrome. **Ann Transl Med,** v. 4, n. 13, p. 256, Jul 2016. ISSN 2305-5839. Disponível em: < https://www.ncbi.nlm.nih.gov/pubmed/27500157 >.

[2] HANSEN, C. L. et al. Myocardial perfusion and function: single photon emission computed tomography. **J Nucl Cardiol,** v. 14, n. 6, p. e39-60, 2007 Nov-Dec 2007. ISSN 1532-6551. Disponível em: < http://www.ncbi.nlm.nih.gov/pubmed/18022099 >.

[3] BOURQUE, J. M.; BELLER, G. A. Value of Exercise ECG for Risk Stratification in Suspected or Known CAD in the Era of Advanced Imaging Technologies. **JACC Cardiovasc Imaging,** v. 8, n. 11, p. 1309-21, Nov 2015. ISSN 1876-7591. Disponível em: < https://www.ncbi.nlm.nih.gov/pubmed/26563861 >.

[4] KLOCKE, F. J. et al. ACC/AHA/ASNC guidelines for the clinical use of cardiac radionuclide imaging--executive summary: a report of the American College of Cardiology/American Heart Association Task Force on Practice Guidelines (ACC/AHA/ASNC Committee to Revise the 1995 Guidelines for the Clinical Use of Cardiac Radionuclide Imaging). **J Am Coll Cardiol,** v. 42, n. 7, p. 1318-33, Oct 2003. ISSN 0735-1097. Disponível em: < https://www.ncbi.nlm.nih.gov/pubmed/14522503 >.

[5] PETERSON, P. N. et al. Association of exercise capacity on treadmill with future cardiac events in patients referred for exercise testing. **Arch Intern Med,** v. 168, n. 2, p. 174-9, Jan 2008. ISSN 0003-9926. Disponível em: < https://www.ncbi.nlm.nih.gov/pubmed/18227364 >.

[6] MORISE, A. P.; JALISI, F. Evaluation of pretest and exercise test scores to assess all-cause mortality in unselected patients presenting for exercise testing with symptoms of suspected coronary artery disease. **J Am Coll Cardiol,** v. 42, n. 5, p. 842-50, Sep 2003. ISSN 0735-1097. Disponível em: < https://www.ncbi.nlm.nih.gov/pubmed/12957430 >.

[7] GORAYA, T. Y. et al. Prognostic value of treadmill exercise testing in elderly persons. **Ann Intern Med,** v. 132, n. 11, p. 862-70, Jun 2000. ISSN 0003-4819. Disponível em: < https://www.ncbi.nlm.nih.gov/pubmed/10836912 >.

[8] KODAMA, S. et al. Cardiorespiratory fitness as a quantitative predictor of all-cause mortality and cardiovascular events in healthy men and women: a meta-analysis. **JAMA,** v. 301, n. 19, p. 2024-35, May 2009. ISSN 1538-3598. Disponível em: < https://www.ncbi.nlm.nih.gov/pubmed/19454641 >.

[9] LEE, D. S. et al. Cardiovascular outcomes are predicted by exercise-stress myocardial perfusion imaging: Impact on death, myocardial infarction, and coronary

revascularization procedures. **Am Heart J,** v. 161, n. 5, p. 900-7, May 2011. ISSN 1097-6744. Disponível em: < https://www.ncbi.nlm.nih.gov/pubmed/21570520 >.

10 FASELIS, C. et al. Exercise capacity and all-cause mortality in male veterans with hypertension aged ≥70 years. **Hypertension,** v. 64, n. 1, p. 30-5, Jul 2014. ISSN 1524-4563. Disponível em: < https://www.ncbi.nlm.nih.gov/pubmed/24821944 >.

11 BOURQUE, J. M. et al. Achieving an exercise workload of > or = 10 metabolic equivalents predicts a very low risk of inducible ischemia: does myocardial perfusion imaging have a role? **J Am Coll Cardiol,** v. 54, n. 6, p. 538-45, Aug 2009. ISSN 1558-3597. Disponível em: < https://www.ncbi.nlm.nih.gov/pubmed/19643316 >.

12 _____. Prognosis in patients achieving ≥10 METS on exercise stress testing: was SPECT imaging useful? **J Nucl Cardiol,** v. 18, n. 2, p. 230-7, Apr 2011. ISSN 1532-6551. Disponível em: < https://www.ncbi.nlm.nih.gov/pubmed/21132417 >.

13 SMITH, L. et al. A high exercise workload of ≥ 10 METS predicts a low risk of significant ischemia and cardiac events in older adults. **J Nucl Cardiol**, Jul 2018. ISSN 1532-6551. Disponível em: < https://www.ncbi.nlm.nih.gov/pubmed/30051345 >.

14 DUVALL, W. L. et al. A hypothetical protocol for the provisional use of perfusion imaging with exercise stress testing. **J Nucl Cardiol,** v. 20, n. 5, p. 739-47, Oct 2013. ISSN 1532-6551. Disponível em: < https://www.ncbi.nlm.nih.gov/pubmed/23737159 >.

15 HUNG, R. K. et al. Prognostic value of exercise capacity in patients with coronary artery disease: the FIT (Henry Ford ExercIse Testing) project. **Mayo Clin Proc,** v. 89, n. 12, p. 1644-54, Dec 2014. ISSN 1942-5546. Disponível em: < https://www.ncbi.nlm.nih.gov/pubmed/25440889 >.

16 DIAMOND, G. A. et al. Application of conditional probability analysis to the clinical diagnosis of coronary artery disease. **J Clin Invest,** v. 65, n. 5, p. 1210-21, May 1980. ISSN 0021-9738. Disponível em: < https://www.ncbi.nlm.nih.gov/pubmed/6767741 >.

17 LIMA, R. et al. Prognostic value of myocardium perfusion imaging with a new reconstruction algorithm. **J Nucl Cardiol,** v. 21, n. 1, p. 149-57, Feb 2014. ISSN 1532-6551. Disponível em: < https://www.ncbi.nlm.nih.gov/pubmed/24281904 >.

18 LIMA, R. S. L. et al. Prognostic value of a faster, low-radiation myocardial perfusion SPECT protocol in a CZT camera. **Int J Cardiovasc Imaging,** v. 33, n. 12, p. 2049-2056, Dec 2017. ISSN 1875-8312. Disponível em: < https://www.ncbi.nlm.nih.gov/pubmed/28664482 >.

19 LIMA, R. et al. Comparison of the prognostic value of myocardial perfusion imaging using a CZT-SPECT camera with a conventional anger camera. **J Nucl Cardiol,** v. 24, n. 1,

p. 245-251, 02 2017. ISSN 1532-6551. Disponível em: < https://www.ncbi.nlm.nih.gov/pubmed/27510176 >.

[20] BERMAN, D. S. et al. Comparative prognostic value of automatic quantitative analysis versus semiquantitative visual analysis of exercise myocardial perfusion single-photon emission computed tomography. **J Am Coll Cardiol,** v. 32, n. 7, p. 1987-95, Dec 1998. ISSN 0735-1097. Disponível em: < https://www.ncbi.nlm.nih.gov/pubmed/9857883 >.

[21] HENZLOVA, M. J. et al. ASNC imaging guidelines for SPECT nuclear cardiology procedures: Stress, protocols, and tracers. **J Nucl Cardiol,** v. 23, n. 3, p. 606-39, Jun 2016. ISSN 1532-6551. Disponível em: < https://www.ncbi.nlm.nih.gov/pubmed/26914678 >.

[22] BERMAN, D. S. et al. Incremental value of prognostic testing in patients with known or suspected ischemic heart disease: a basis for optimal utilization of exercise technetium-99m sestamibi myocardial perfusion single-photon emission computed tomography. **J Am Coll Cardiol,** v. 26, n. 3, p. 639-47, Sep 1995. ISSN 0735-1097. Disponível em: < https://www.ncbi.nlm.nih.gov/pubmed/7642853 >.

[23] HACHAMOVITCH, R. et al. Incremental prognostic value of myocardial perfusion single photon emission computed tomography for the prediction of cardiac death: differential stratification for risk of cardiac death and myocardial infarction. **Circulation,** v. 97, n. 6, p. 535-43, Feb 1998. ISSN 0009-7322. Disponível em: < https://www.ncbi.nlm.nih.gov/pubmed/9494023 >.

[24] THYGESEN, K. et al. Universal definition of myocardial infarction. **J Am Coll Cardiol,** v. 50, n. 22, p. 2173-95, Nov 2007. ISSN 1558-3597. Disponível em: < https://www.ncbi.nlm.nih.gov/pubmed/18036459 >.

9 Considerações Finais

Neste trabalho foram avaliadas estratégias para a redução da exposição à radiação advindas da cintilografia miocárdica de perfusão. Baseando-se nos resultados encontrados na análise dessa coorte retrospectiva , pudemos concluir que é possível a aplicação de um protocolo com redução de dose e tempo em GC CZT sem comprometer o valor prognóstico da CMP. Sendo este não inferior ao valor prognóstico do método quando utilizadas as GCs tradicionais.

Além disso, em face da importância na certificação da indicação dos pacientes à CMP, exploramos a contribuição do valor prognóstico deste método em relação ao TE em pacientes com DAC conhecida que alcançaram ≥ 10 METs. Nossos resultados mostraram que a CMP possui valor na estratificação deste grupo de pacientes, ao contrário do que a literatura tem indicado em relação a outros subgrupos, em atingindo alta capacidade de exercício. Esta evidência acrescenta embasamento para uma melhor utilização do método ajustado a diferentes tipos de pacientes e situações.

10 Anexos

ANEXO A - Produção Científica

Artigo 1:

1. Publicado na revista International Journal of Cardiovascular Imaging. Lima RSL, Peclat TR, Souza ACAH, Nakamoto AMK, Neves FM, Souza VF, et al. Prognostic value of a faster, low-radiation myocardial perfusion SPECT protocol in a CZT camera. Int J Cardiovasc Imaging. 2017;33(12):2049-56.
2. Publicado na revista do departamento de Imagem Cardiovascular (DIC) da Sociedade Brasileira de Cardiologia. Revista DIC, n 3, vol 28.
3. Poster apresentado na International Conference on Integrated Medical Imaging in Cardiovascular Diseases, International Atomic Energy Agency (IAEA), em Vienna, Austria.
4. Prêmio de melhor poster no Congresso do Departamento de Imagem Cardiovascular da Sociedade Brasileira de Cardiologia.

Artigo 2:

1. Publicado na revista Journal of Nuclear Cardiology. Lima R, Peclat T, Soares T, Ferreira C, Souza AC, Camargo G. Comparison of the prognostic value of myocardial perfusion imaging using a CZT-SPECT camera with a conventional anger camera. J Nucl Cardiol. 2017;24(1):245-51.

ANEXO B – Artigo 1

Int J Cardiovasc Imaging
DOI 10.1007/s10554-017-1202-3

ORIGINAL PAPER

Prognostic value of a faster, low-radiation myocardial perfusion SPECT protocol in a CZT camera

Ronaldo S. L. Lima[1,2] · Thaís R. Peclat[2] · Ana Carolina A. H. Souza[2] · Aline M. K. Nakamoto[2] · Felipe M. Neves[2] · Victor F. Souza[2] · Letícia B. Glerian[2] · Andrea De Lorenzo[1,2]

Received: 19 February 2017 / Accepted: 22 June 2017

Abstract To determine the prognostic value of a new, ultrafast, low dose myocardial perfusion SPECT (MPS) protocol in a cadmium-zinc telluride (CZT) camera. CZT cameras have introduced significant progress in MPS imaging, offering high-quality images despite lower doses and scan time. Yet, it is unknown if, with such protocol changes, the prognostic value of MPS is preserved. Patients had a 1-day 99 m-Tc-sestamibi protocol, starting with the rest (185–222 MBq) followed by stress (666–740 MBq). Acquisition times were 6 and 3 min, respectively. MPS were classified as normal or abnormal perfusion scans and summed scores of stress, rest, and difference (SSS, SRS and SDS), calculated. Patients were followed with 6-month phone calls. Hard events were defined as death or nonfatal myocardial infarction. Late revascularization was that occurring after 60 days of MPS. 2930 patients (age 64.0 ± 12.1 years, 53.3% male) were followed for 30.7 ± 7.5 months. Mean dosimetry was 6 mSv and mean total study time, 48 ± 13 min. The annual hard event and late revascularization rate were higher in patients with greater extension of defect and ischemia. SSS was higher in patients with hard events compared to those without events (2.6 ± 4.9 vs. 5.0 ± 6.3, $p < 0.001$), as well as the SDS (0.7 ± 1.9 vs. 1.7 ± 3.4, $p < 0.00$). The same was true for patients with or without late revascularization (SSS: 2.5 ± 4.7 vs. 6.6 ± 7.1; SDS: 0.6 ± 1.7 vs. 2.9 ± 3.8, $p < 0.01$). A new, faster, low-radiation, MPS protocol in a CZT camera maintain the ability to stratify patients with increased risk of events, showing that, in the presence of greater extension of defect or ischemia, patients presented higher rates of hard events and late revascularization.

Keywords Myocardial perfusion SPECT · Prognosis · CZT camera · Coronary artery disease

Introduction

Over the past 30 years, successive technical innovations-including, but not limited to, SPECT acquisition, ECG gating, among others- have granted myocardial perfusion imaging the status of a reliable, widely applicable, and increasingly useful technique [1]. The excellent diagnostic and prognostic values of myocardial perfusion SPECT (MPS) have led it to be extensively employed to evaluate patients with suspected or known coronary artery disease (CAD) [2].

Nonetheless, traditional MPS has two important limitations: Prolonged image acquisition time, leading to long procedural times, and relatively large radiation doses. The available literature demonstrates the possibility of high-speed cameras to reduce acquisition times, improving patient's tolerance to the test, and reducing radiation dose [3]. These new cameras rely on a pinhole collimation design and multiple cadmium zinc telluride (CZT) crystal arrays. Compared to the traditional SPECT camera, this type of collimation provides a three- to five-fold increase in photon sensitivity, thereby reducing imaging times significantly, while providing a 1.7 to 2.5-fold increase in spatial resolution. This makes shorter scans or lower doses (or even both) a reality, without the loss of image quality [3–5].

✉ Ronaldo S. L. Lima
ronlima@hotmail.com

[1] Clínica de Diagnóstico por Imagem, Av. Ataulfo de Paiva 669, Leblon, Rio de Janeiro, RJ, Brazil

[2] Universidade Federal do Rio de Janeiro, Rio de Janeiro, Brazil

Published online: 29 June 2017

However, the prognostic value of MPS imaging with this new protocol is still unknown. This study therefore sought to assess the prognostic value of a new faster, low-radiation MPS protocol performed in a CZT gamma camera (CZT-GC).

Materials and methods

Consecutive patients who underwent CZT MPS for the assessment of suspected or known CAD at a single laboratory in Rio de Janeiro, Brazil, between November 2011 and December 2012 were prospectively enrolled and followed by 6-month phone calls.

Those who underwent myocardial revascularization (either by coronary angioplasty or coronary artery by pass grafting surgery) <60 days after MPS were later excluded.

Prior to scanning, patient´s medical history and physical examination data were collected by a team of experienced cardiologists.

All procedures performed were in accordance with the ethical standards of the institutional research committee and with the 1964 Declaration of Helsinki and its later amendments. Informed consent was obtained from all individual participants included in the study.

Study protocol

The patients were instructed to abstain from any products containing caffeine for 24 h before the test. Beta-blockers, calcium-channel antagonists, and nitrates were terminated 48 h before testing. A 1-day protocol was employed, with 185–222 MBq of 99 m-Tc-sestamibi used for the resting phase and 666–740 MBq for stress. Initially, to determine the best duration for the acquisition of the MPS scan, 24 patients (13 men) were selected for a pilot study in which scan acquisition was performed for 6 min in list mode. The scans were then processed using 1–6 min of the total scan time for reconstruction, and images were analyzed by two experienced readers unaware of the time range used for reconstruction, who had their readings evaluated for agreement. The study protocol was then defined according to best combination of reading agreements for stress and rest MPS studies among time ranges.

All patients underwent a 1-day, gated, rest/stress 99 m-Tc-sestamibi protocol. 10 min after tracer injection, image acquisition was performed in the supine position. The second phase was the stress study, in which either symptom-limited exercise treadmill test using the standard Bruce protocol with 13-lead electrocardiographic or pharmacologic stress were performed. Upon 5 min of stress phase completion, patients underwent image acquisition in the supine and prone positions [6, 7]. The CZT-GC (Discovery NM 530c, GE Healthcare, Haifa, Israel) was equipped with a multiple pinhole collimator and 19 stationary cadmium-zinc-telluride detectors simultaneously imaging 19 cardiac views. Each detector contained 32×32 pixelated 5-mm thick (2.46×2.46 mm) elements. The system design enabled high-quality imaging of a three-dimensional volume by all detectors (quality field-of-view), where the patient's heart should be positioned. Once acquisition was initiated, no detector or collimator motion occurred.

Image analysis

All images were interpreted by a consensus of two experienced readers. Image processing was performed using Evolution for Cardiac® software. Images were reconstructed without scatter or attenuation correction. Short-axis, vertical and horizontal long-axis tomograms, as well as polar maps, were generated and analyzed. The image reconstruction method used allows extra-cardiac activity to be isolated more easily. Still, two readers analyzed the image before the patient was removed from the camera. The repetition rate of the images was less than 5%. A semi quantitative 17-segment visual interpretation of the gated myocardial perfusion images was performed [8]. Each segment was scored by consensus of the two observers using a standard five-point scoring system [9] (0 = normal, 1 = equivocal, 2 = moderate, 3 = severe reduction of uptake, and 4 = absence of detectable tracer uptake). Summed stress scores (SSS) were obtained by adding the scores of the 17 segments of the stress images. Summed rest scores (SRS) were obtained by adding scores of the 17 segments of the rest images and a summed difference score (SDS) was calculated by segmental subtraction (SSS-SRS). For evaluating the SSS and the SDS as predictors of events, we performed separate analyses with different cut points for each perfusion variable. We created four groups o SSS and SDS with the purpose of evaluating the prognostic value and the stratification power of this new protocol on a CZT-GC based not only in positive or negative MPI results, but specially, based on the extension of defect and ischemia, which is widely stablished to be achieved by using this type of classification [10, 11]. A normal study was considered when SSS < 3 and SDS < 1.

Post-stress eight frames gated short-axis images were processed using quantitative gated SPECT software (Cedars-Sinai Medical Center, Los Angeles, California), and left ventricular ejection fraction (LVEF), end-systolic and end-diastolic volumes (ESV and EDV, respectively) were automatically calculated.

Follow-up

Follow-up was performed by telephone interview every 6 months after MPI. All-cause death, nonfatal myocardial infarction, or late revascularization (>60 days after MPS) were registered. Evaluation of hospital records and/or review of civil registries confirmed these events. Nonfatal myocardial infarction was defined based on the criteria of typical chest pain, elevated cardiac enzyme levels and typical alterations of the electrocardiogram [12]. Death or nonfatal myocardial infarction were classified as hard events. Late revascularization was studied separately.

Statistical analyses

Categorical variables are presented as frequencies and continuous variables as mean ± SD. The annual event rate was calculated as the % of events divided by person-years, and was compared among groups using the log-rank test. Kaplan–Meier curves were generated to visually assess survival in different groups. A Cox proportional hazards analysis was done to evaluate predictors of hard events and late revascularization, using variables with p value <0.05 in univariable analysis or clinical relevance.

Analyses were performed with SPSS software, version 17.0. A p value <0.05 was considered significant.

Results

Among 3265 patients, 235 were excluded due to early revascularization, and 100 were lost to follow-up, leaving 2930 patients who were followed for 30.7 ± 7.5 months. Mean age was 64.0 ± 12.1 years and 53.5% were male. Among these patients, 2072 (70.7%) were asymptomatic. The most frequent indications in asymptomatic patients were a previous treadmill test with intermediate-high risk Duke score, pre-op risk stratification and a previous calcium score >100. The most prevalent risk factor for CAD was hypertension (61.6%), followed by hypercholesterolemia (52.2%), smoking (36.4%) and family history of CAD (31.2%). Diabetes was present in 22.7% and previous myocardial infarction in 12.5%. From the 2930 patients, 501 (17.1%) had already been submitted to coronary angioplasty and 222 (7.6%) to coronary artery bypass grafting (CABG). About regularly medications, 37.9% was in use of ACE inhibitors, 28.6% was using beta-blocker and 10.9% Calcium receptor blockers. Mean perfusion scores were overall low and mean LVEF was normal with only 6% of patients with a LVEF <40%. These characteristics are summarized in Table 1.

For the definition of optimal scan time, acquired scans were processed using 1, 2, 3, 4, 5 or 6 min of the total list-mode acquisition previously performed for the pilot study. Intra and inter-observer agreement rates of MPS readings among time ranges are shown in Table 2. Based on those, the best combination, which was chosen for the subsequent MPS studies, was 6 min for the rest acquisition, 3 min for post-stress supine acquisition and 1.5 min for post-stress prone acquisition. Figure 1 shows an example of six post-stress images processed using a 6, 5, 4, 3, 2 and 1 min acquisition with a progressive degradation of image quality as we reduced the acquisition time. Considering all MPS studies performed thereafter, mean radiation dose was 6 mSv and mean scan time was 48 ± 13 min.

During follow-up, there were 61 deaths, 29 nonfatal infarctions (90 hard events), 148 coronary angioplasty procedures and 22 bypass surgeries (170 late revascularization procedures). Table 3 shows the comparison between patients with or without hard events. The former were older, more frequently male, with prior myocardial infarction or prior CABG and less frequently able to perform

Table 1 Baseline data

Variables	All patients N (%) or mean ± SD
Age (years)	64.0 ± 12.1
Male gender	1568 (53.5%)
Chest pain	865 (29.5%)
Hypertension	1807 (61.6%)
Hypercholesterolemia	1530 (52.2%)
Diabetes mellitus	667 (22.7%)
Family history of coronary disease	915 (31.2%)
Smoking	1069 (36.4%)
Previous MI	367 (12.5%)
Previous CABG	222 (7.6%)
Previous PCI	501 (17.1%)
Exercise stress	1706 (58.2%)
Pharmacologic test	1224 (41.8%)
ACEi	1112 (37.9%)
Beta-blocker	839 (28.6%)
Calcium receptor blockers	320 (10.9%)
MPS	
SSS	1.7 ± 3.0 (0–26)
SRS	1.1 ± 2.1 (0–23)
SDS	0.6 ± 1.7 (0–18)
LVEF (<40%)	176 (6.0%)
LVEF (%)	62.4 ± 8.1
EDV (ml)	68.0 ± 17.0
ESV (ml)	26.4 ± 10.6

CABG coronary artery bypass grafting, *MI* myocardial infarction, *MPS* myocardial perfusion SPECT, *PCI* percutaneous coronary intervention, *SDS* summed difference score, *SRS* summed rest score, *SSS* summed stress score

Table 2 Intra- and interobserver agreement rates of MPS readings using 1 to 6 min time frames

Duration	6 min		5 min		4 min		3 min		2 min		1 min	
Agreement	Inter (%)	Intra (%)	Inter (%)	Intra (%)	Inter (%)	Intra (%)	Inter (%)	Intra (%)	Inter (%)	Intra (%)	Inter (%)	Intra (%)
Stress	100	100	100	100	100	100	100	100	100	96	96	92
Rest	100	100	100	100	100	96	100	92	92	92	92	88

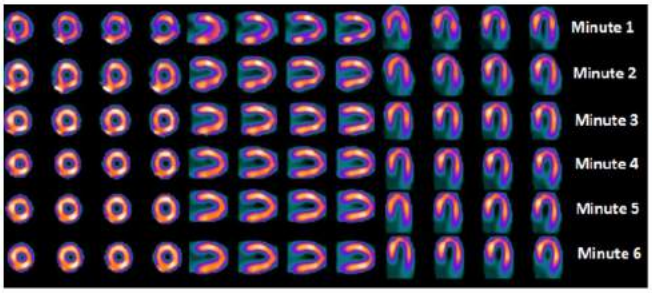

Fig. 1 Example of six post-stress short-axis, vertical long axis and longitudinal long axis images processed using a 6, 5, 4, 3, 2 and 1 min acquisition, with a progressive reduction on image quality from 6 to 1 min

exercise stress. Perfusion scores were higher, as well as left ventricular volumes, and LVEF was lower in patients with hard events. In Table 4, comparisons between patients with or without late revascularization are shown. Similarly to patients with hard events, those with late revascularization were older, more frequently male, with cardiovascular risk factors, known coronary artery disease, and less frequently able to perform exercise stress, with higher perfusion scores, left ventricular volumes, and lower LVEF.

Based on the SSS, 4 patient groups were created: group 1 with SSS values from 0 to 2 [n = 2098 (71.6%)]; group 2, SSS values from 3 to 5 [n = 430 (14.6%)]; group 3, SSS values from 6 to 11 [n = 220 (7.5%)] and group 4, SSS ≥ 12 [n = 182 (6.2%)]. Kaplan–Meier survival curves (Fig. 2a, b) showed that the highest the SSS, the lowest the survival free of hard events ($p < 0.001$) or late revascularization ($p < 0.001$), respectively. Table 5 shows the annualized hard events and late revascularization rates for individual groups of SSS, with highest rates in the group of highest SSS values. Four groups were also created according to SDS values: group 1 with SDS = 0 [n = 2334 (79.6.0%)]; group 2, SDS values from 1 to 2 [n = 305 (10.4%)]; group 3, SDS from 3 to 5 [n = 171 (5.8%)] and group 4, SDS ≥ 6 [n = 120 (4.0%)]. Kaplan–Meier survival curves also showed that, with increasing SDS, event-free survival was reduced, both for hard events (Fig. 3a) ($p < 0.001$) or late revascularization (Fig. 3b) ($p < 0.001$). Also, the annualized events rates, both for hard events or late revascularization, showed the same behavior presented on SSS groups for SDS groups, with higher rates in groups with higher values of SDS (Table 6). For all Kaplan Meier survival curves, p values were demonstrated in a pairwise comparison, below the graphs, to express the statistical differences in events rates between individual groups.

Finally, in the Cox analysis, male gender (hazard ratio = 2.26 [1.33–3.8], $p = 0.03$), age (hazard ratio = 1.03 [1.01–1.06], $p = 0.001$), diabetes (hazard ratio = 1.69 [1.09–2.62], $p = 0.02$), pharmacologic stress (hazard ratio = 2.91 [1.75–4.8], $p < 0.001$) and the SSS (hazard ratio = 1.36 [1.07–1.73], $p = 0.01$). were independently associated with hard events. SDS, when substituting SSS in the cox analysis, also showed to be an independent predictor of hard events (hazard ratio = 1.09 [1.02–1.17], $p = 0.01$) and maintained the results of the other variables. Table 3 shows all the variables used in the cox regression for hard events, with their respective hazard ratio and confidence interval.

For late revascularization, diabetes (hazard ratio = 1.94 [1.41–2.66], $p < 0.001$), prior percutaneous coronary intervention (hazard ratio = 2.54 [1.76–3.68], $p < 0.001$), and the SSS (hazard ratio = 1.06 [1.04–1.08], $p < 0.001$) were the independent predictors. Again, SDS also showed to be an independent predictor of late revascularization (hazard ratio = 1.22 [1.17–1.26], $p < 0.001$) when analyzed substituting the SSS with no modification in

Table 3 Characteristics of patients with or without hard events

Variables	Univariate analysis			Cox regression	
	Patients without HE (n = 2844)	Patients with HE (n = 86)	p value	HR [95% CI]	p value
Age (years)	64.5 ± 11.7	70.7 ± 12.3	<0.001	1.03 [1.01–1.06]	0.001
Male gender	1515 (53.2%)	57 (66.3%)	<0.01	2.26 [1.33–3.80]	0.030
Chest pain	844 (29.6%)	21 (24.4%)	0.338	1.30 [0.76–2.23]	0.336
Hypertension	1748 (61.4%)	59 (68.6%)	0.173	1.01 [0.61–1.66]	0.955
Hypercholesterolemia	1483 (52.1%)	47 (54.7%)	0.660	1.00 [0.63–1.57]	0.999
Diabetes mellitus	633 (22.2%)	34 (39.5%)	<0.001	1.69 [1.09–2.62]	0.020
Family history of CAD	887 (31.1%)	28 (32.6%)	0.906		
Smoking	1041 (36.6%)	28 (32.6%)	0.063	0.44 [0.23–1.08]	0.105
Previous MI	347 (12.2%)	20 (23.3%)	<0.01	0.71 [0.42–1.23]	0.229
Previous CABG	208 (7.3%)	14 (16.3%)	<0.01	0.67 [0.36–1.22]	0.196
Previous PCI	480 (16.8%)	21 (24.4%)	0.058	0.88 [0.53–1.45]	0.619
Exercise stress	1682 (59.1%)	24 (27.9%)	<0.01		
Pharmacologic test	1169 (41.1%)	62 (72.1%)	<0.01	2.91 [1.75–4.80]	0.000
MPS					
SSS[a]	2.6 ± 4.9	5.0 ± 6.3	<0.001	1.36 [1.07–1.73]	0.01
SRS	1.9 ± 4.2	3.2 ± 4.8	<0.001		
SDS[a]	0.7 ± 1.9	1.7 ± 3.4	<0.001	1.09 [1.02–1.17]	0.010
LVEF (%)	59.4 ± 11.0	55.5 ± 12.7	<0.01	0.75 [0.39–1.44]	0.392
EDV (ml)	81.4 ± 33.5	87.0 ± 34.6			
ESV (ml)	35.6 ± 25.5	42.0 ± 29.8			

HE hard events, *CABG* coronary artery bypass grafting, *MI* myocardial infarction, *MPS* myocardial perfusion SPECT, *PCI* percutaneous coronary intervention, *SDS* summed difference score, *SRS* summed rest score, *SSS* summed stress score

[a]SSS and SDS were analyzed separately in the cox regression, each one with all other selected variables

the other variables. Table 4 shows the variables used for this cox regression, with their respective hazard ratio and confidence interval.

Discussion

Previous studies have shown that CZT cameras are able to perform ultrafast and low-dose MPS studies, with even higher sensitivity and image quality when compared to traditional cameras [13]. However, there is still incomplete evidence supporting the prognostic value of MPS performed in CZT cameras. This study shows, in a large patient population, that the prognostic value of a new MPS protocol in a high-speed CZT-GC could be comparable to what literature has shown about the prognostic value traditionally provided by conventional MPS [9]. Our group had already demonstrated the prognostic value of MPS with a new reconstruction algorithm [11] in traditional Anger cameras, which also allowed faster scans. However, with the advent of CZT technology, it became imperative to define if these new cameras would provide MPS studies with reliable prognostic value, which might be reliably used to manage patients with suspected or known CAD.

Dolan et al. demonstrated the prognostic value of MPS in a CZT camera, but as these authors recognized, they used the conventional dose of radiotracers [14]. The radiation dose used in this study was considerably lower than standard dose used in traditional protocols, and we initially tested different acquisition times to obtain the best possible images with low radiation. Total procedure time was reduced to less than one hour, with imaging time of 6 min for rest and 3 min for stress phase.

After establishing these parameters, we then studied the prognostic value of this protocol. Male gender, increasing age, the use of pharmacologic stress were significant predictors of hard events, as previously described [15, 16]. Diabetes was independently associated both with hard events or late revascularization. Of note, LVEF was not associated with events, what might be explained by the overall normal left ventricular function of the study population. Importantly, the extent and intensity of myocardial ischemia, as expressed by the SDS, was significantly

Table 4 Characteristics of patients with or without late revascularization

Variables	Univariate analysis			Cox regression	
	Patients w/o late revascularization (n = 2763)	Patients w/late revascularization (n = 167)	p value	HR [95% CI]	p value
Age (years)	63.9 ± 12.2	66.4 ± 10.3	<0.001	1.00 [0.99–1.02]	0.397
Male gender	1462 (52.8%)	110 (65.5%)	<0.01	1.35 [0.97–1.88]	0.068
Chest pain	812 (29.3%)	53 (31.5%)			
Hypertension	1690 (61.0%)	117 (69.6%)	0.044	1.07 [0.75–1.51]	0.689
Hypercholesterolemia	1425 (51.5%)	105 (62.5%)	<0.01	1.47 [1.06–2.04]	0.020
Diabetes mellitus	598 (21.6%)	69 (41.1%)	<0.001	1.94 [1.41–2.66]	0.000
Family history of CAD	861 (31.1%)	54 (32.1%)			
Smoking	1001 (36.2%)	68 (40.5%)		0.77 [0.46–1.28]	0.314
Previous MI	317 (11.4%)	50 (29.8%)	<0.001	2.01 [1.43–2.83]	0.000
Previous CABG	208 (7.5%)	14 (8.3%)		1.60 [0.92–2.79]	0.095
Previous PCI	429 (15.5%)	72 (42.9%)	<0.001	2.54 [1.76–3.68]	0.000
Exercise stress	1624 (59.0%)	82 (48.8%)	<0.01		
Pharmacologic test	1955 (41.4%)	86 (51.2%)	<0.01	1.20 [0.86–1.67]	0.264
MPS					
SSS[a]	2.5 ± 4.7	6.6 ± 7.1	<0.001	1.06 [1.04–1.08]	0.000
SRS	1.9 ± 4.1	3.7 ± 5.6	<0.001		
SDS[a]	0.6 ± 1.7	2.9 ± 3.8	<0.001	1.22 [1.17–1.26]	0.000
LVEF (%)	59.6 ± 10.9	54.8 ± 12.0	<0.01	1.00 [0.99–1.00]	0.887
EDV (ml)	81.1 ± 33.3	88.5 ± 36.9	<0.01		
ESV (ml)	35.3 ± 25.3	43.0 ± 30.2	<0.01		

CABG coronary artery bypass grafting, *MI* myocardial infarction, *MPS* myocardial perfusion SPECT, *PCI* percutaneous coronary intervention, *SDS* summed difference score, *SRS* summed rest score, *SSS* summed stress score

[a]SSS and SDS were analyzed separately in the cox regression, each one with all other selected variables

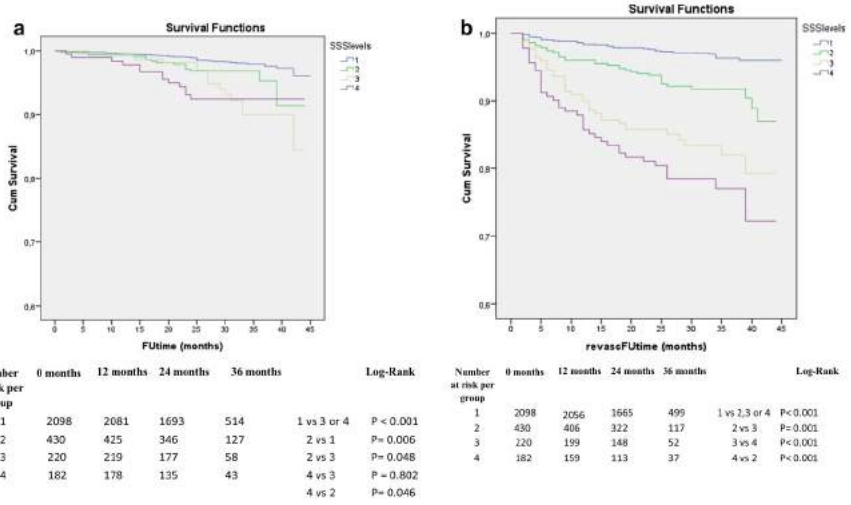

Number at risk per group	0 months	12 months	24 months	36 months		Log-Rank
1	2098	2081	1693	514	1 vs 3 or 4	P < 0.001
2	430	425	346	127	2 vs 1	P= 0.006
3	220	219	177	58	2 vs 3	P= 0.048
4	182	178	135	43	4 vs 3	P = 0.802
					4 vs 2	P= 0.046

Number at risk per group	0 months	12 months	24 months	36 months		Log-Rank
1	2098	2056	1665	499	1 vs 2,3 or 4	P<0.001
2	430	406	322	117	2 vs 3	P=0.001
3	220	199	148	52	3 vs 4	P<0.001
4	182	159	113	37	4 vs 2	P<0.001

Fig. 2 Kaplan–Meier curves of hard events (**a**) or late revascularization (**b**) according to SSS categories. *Blue line* SSS 0–2; *green line* SSS 3–5; *yellow line* SSS 6–11; *purple line* SSS ≥ 12

Table 5 Annualized hard events and late revascularization rates for individual SSS groups

SSS groups	Annualized hard event rates	Annualized late revascularization rates
1	0.57	0.90
2	1.27	2.45
3	2.06	4.96
4	2.15	6.48

Table 6 Annualized hard events and late revascularization rates for individual SDS groups

SDS groups	Annualized hard event rates	Annualized late revascularization rates
1	0.60	0.96
2	1.87	2.57
3	1.93	6.03
4	2.03	9.84

associated with outcomes, what supports the prognostic value of this new protocol.

It is worth noting the characteristics of the study population, composed of outpatients, most asymptomatic (performing MPS as part of a preoperative evaluation or general screening due to cardiac risk factors) with normal left ventricular function. Nonetheless, the prevalence of diabetes was >20%, and over 10% had a history of myocardial infarction, what increases overall risk and may improve the generalizability of these results. Therefore, we believe that CZT MPS may be reliably used to evaluate patients for CAD, with the advantages of reduced imaging time and lower radiation dose.

We recognize, as a limitation, that the best method to establish the prognostic value of this new protocol in a CZT-GC would be a comparison between new and traditional cameras, with each patient being studied in both cameras and being control for themselves. However, it assumes that the same protocol would be used for both cameras [14]. Since the new low radiation dose and acquisition time protocol could not be used for traditional cameras, the study would not verify the protocol that this study aim to establish.

Conclusion

A new, faster, low-radiation, MPS protocol in a CZT camera was able to maintain the ability of stratifying patients with increased risk of events, showing that, in the presence of greater extension of defect or ischemia, patients presented higher rates of hard events and late revascularization.

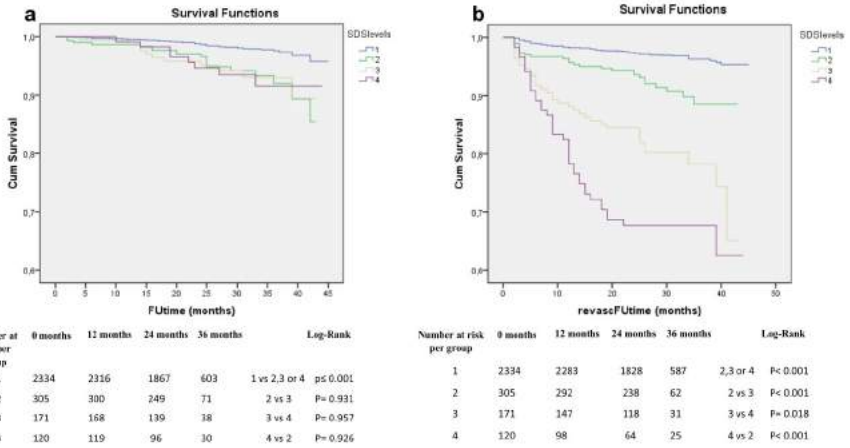

Number at risk per group	0 months	12 months	24 months	36 months		Log-Rank
1	2334	2316	1867	603	1 vs 2,3 or 4	p≤ 0.001
2	305	300	249	71	2 vs 3	P= 0.931
3	171	168	139	18	3 vs 4	P= 0.957
4	120	119	96	30	4 vs 2	P= 0.926

Number at risk per group	0 months	12 months	24 months	36 months		Log-Rank
1	2334	2283	1828	587	2,3 or 4	P< 0.001
2	305	292	238	62	2 vs 3	P< 0.001
3	171	147	118	31	3 vs 4	P= 0.018
4	120	98	64	25	4 vs 2	P< 0.001

Fig. 3 Kaplan–Meier curves of hard events (**a**) or late revascularization (**b**) according to SDS categories. *Blue line* SDS 0; *green line* SDS 1–2; *yellow line* SDS 3–5; *purple line* SDS ≥ 6

Compliance with ethical standards

Conflict of interest The authors declare that they have no conflict of interest.

References

1. Verberne HJ, Acampa W, Anagnostopoulos C, Ballinger J, Bengel F, De Bondt P et al (2015) EANM procedural guidelines for radionuclide myocardial perfusion imaging with SPECT and SPECT/CT: 2015 revision. Eur J Nucl Med Mol Imaging 42(12):1929–1940
2. Hansen CL, Goldstein RA, Akinboboye OO, Berman DS, Botvinick EH, Churchwell KB et al (2007) Myocardial perfusion and function: single photon emission computed tomography. J Nucl Cardiol 14(6):e39–e60
3. Oddstig J, Hedeer F, Jögi J, Carlsson M, Hindorf C, Engblom H (2013) Reduced administered activity, reduced acquisition time, and preserved image quality for the new CZT camera. J Nucl Cardiol 20(1):38–44
4. Duvall WL, Sweeny JM, Croft LB, Ginsberg E, Guma KA, Henzlova MJ (2012) Reduced stress dose with rapid acquisition CZT SPECT MPI in a non-obese clinical population: comparison to coronary angiography. J Nucl Cardiol 19(1):19–27
5. Mouden M, Timmer JR, Ottervanger JP, Reiffers S, Oostdijk AH, Knollema S et al (2012) Impact of a new ultrafast CZT SPECT camera for myocardial perfusion imaging: fewer equivocal results and lower radiation dose. Eur J Nucl Med Mol Imaging 39(6):1048–1055
6. Hayes SW, De Lorenzo A, Hachamovitch R, Dhar SC, Hsu P, Cohen I et al (2003) Prognostic implications of combined prone and supine acquisitions in patients with equivocal or abnormal supine myocardial perfusion SPECT. J Nucl Med 44(10):1633–1640
7. Burrell S, MacDonald A (2006) Artifacts and pitfalls in myocardial perfusion imaging. J Nucl Med Technol 34(4):193–211 (**quiz 2–4**)
8. Berman DS, Kang X, Van Train KF, Lewin HC, Cohen I, Areeda J et al (1998) Comparative prognostic value of automatic quantitative analysis versus semiquantitative visual analysis of exercise myocardial perfusion single-photon emission computed tomography. J Am Coll Cardiol 32(7):1987–1995
9. Berman DS, Hachamovitch R, Kiat H, Cohen I, Cabico JA, Wang FP et al (1995) Incremental value of prognostic testing in patients with known or suspected ischemic heart disease: a basis for optimal utilization of exercise technetium-99m sestamibi myocardial perfusion single-photon emission computed tomography. J Am Coll Cardiol 26(3):639–647
10. Hachamovitch R, Berman DS, Shaw LJ, Kiat H, Cohen I, Cabico JA et al (1998) Incremental prognostic value of myocardial perfusion single photon emission computed tomography for the prediction of cardiac death: differential stratification for risk of cardiac death and myocardial infarction. Circulation 97(6):535–543
11. Lima R, Ronaldo L, De Lorenzo A, Andrea DL, Camargo G, Gabriel C et al (2014) Prognostic value of myocardium perfusion imaging with a new reconstruction algorithm. J Nucl Cardiol 21(1):149–157
12. Thygesen K, Alpert JS, White HD, Joint ESC/ACCF/AHA/WHF Task Force for the Redefinition of Myocardial Infarction (2007) Universal definition of myocardial infarction. J Am Coll Cardiol 50(22):2173–2195
13. Duvall WL, Croft LB, Ginsberg ES, Einstein AJ, Guma KA, George T et al (2011) Reduced isotope dose and imaging time with a high-efficiency CZT SPECT camera. J Nucl Cardiol 18(5):847–857
14. Oldan JD, Shaw LK, Hofmann P, Phelan M, Nelson J, Pagnanelli R et al (2016) Prognostic value of the cadmium-zinc-telluride camera: a comparison with a conventional (Anger) camera. J Nucl Cardiol 23(6):1280–1287
15. Hachamovitch R, Berman DS, Kiat H, Bairey CN, Cohen I, Cabico A et al (1996) Effective risk stratification using exercise myocardial perfusion SPECT in women: gender-related differences in prognostic nuclear testing. J Am Coll Cardiol 28(1):34–44
16. Navare SM, Mather JF, Shaw LJ, Fowler MS, Heller GV (2004) Comparison of risk stratification with pharmacologic and exercise stress myocardial perfusion imaging: a meta-analysis. J Nucl Cardiol 11(5):551–561

ANEXO B – Artigo 2

ORIGINAL ARTICLE

Comparison of the prognostic value of myocardial perfusion imaging using a CZT-SPECT camera with a conventional anger camera

Ronaldo Lima, MD, PhD,[a,b] Thais Peclat, MD,[c] Thalita Soares, BMBS,[c] Caio Ferreira, BMBS,[c] Ana Carolina Souza, BMBS,[c] and Gabriel Camargo, MD[a]

[a] Department of Cardiology, Universidade Federal do Rio de Janeiro, Rio de Janeiro, Brazil
[b] Nuclear Medicine, Clínicade Diagnóstico por Imagem, Rio de Janeiro, Brazil
[c] Universidade Federal do Rio de Janeiro, Rio de Janeiro, Brazil

Received May 21, 2016; accepted Jul 15, 2016
doi:10.1007/s12350-016-0618-9

Background. **Recent studies have shown that myocardial perfusion imaging (MPI) in cadmium-zinc-telluride (CZT) cameras allow faster exams with less radiation dose but there are little data comparing its prognosis information with that of dedicated cardiac Na-I SPECT cameras**

Objective. **The objective of this study is to compare the prognostic value of MPI using an ultrafast protocol with low radiation dose in a CZT-SPECT and a traditional one.**

Methods. **Group 1 was submitted to a two-day MIBI protocol in a conventional camera, and group 2 was submitted to a 1-day MIBI protocol in CZT camera. MPI were classified as normal or abnormal, and perfusion scores were calculated. Propensity score matching methods were performed**

Results. **3554 patients were followed during 33±8 months. Groups 1 and 2 had similar distribution of age, gender, body mass index, risk factors, previous revascularization, and use of pharmacological stress. Group 1 had more abnormal scans, higher scores than group 2. Annualized hard events rate was higher in group 1 with normal scans but frequency of revascularization was similar to normal group 2. Patients with abnormal scans had similar event rates in both groups**

Conclusion. **New protocol of MPI in CZT-SPECT showed similar prognostic results to those obtained in dedicated cardiac Na-I SPECT camera, with lower prevalence of hard events in patients with normal scan. (J Nucl Cardiol 2016)**

Key Words: myocardial perfusion imaging · coronary artery disease · SPECT

Abbreviations			
MPI	Myocardial perfusion imaging	BMI	Body mass index
CAD	Coronary artery disease	PCI	Percutaneous coronary intervention
SPECT	Single-photon emission computed tomography	CABG	Coronary artery bypass surgery
CZT	Cadmium-zinc-telluride		

Electronic supplementary material The online version of this article (doi:10.1007/s12350-016-0618-9) contains supplementary material, which is available to authorized users.

The authors of this article have provided a PowerPoint file, available for download at SpringerLink, which summarises the contents of the paper and is free for re-use at meetings and presentations. Search for the article DOI on http://SpringerLink.com

Reprint requests: Ronaldo Lima, MD, PhD, Cardiology, Universidade Federal do Rio de Janeiro, Cardiology, Rio de Janeiro, Brazil; *ronlima@hotmail.com*

1071-3581/$34.00

Published online: 10 August 2016

See related editorial, doi:10.1007/s12350-016-0640-y.

INTRODUCTION

It is well known that myocardial perfusion imaging (MPI) with stress testing is an independent predictor of prognosis in patients with suspected or known coronary artery disease (CAD). The gated single-photon emission computed tomography (SPECT) appears to be the best predictor of cardiac event-free survival in this population.[1] Also, compared with other methods such as stress-ECG and coronary angiography, SPECT-based strategies seem to be more cost-effective.[2]

Over time, numerous technological advances have increased MPI's performance, with the most meaningful being the introduction of tomographic imaging and, later, of the multidetector gamma cameras. Recent developments have allowed for reductions in scan time and radiation dose used to its acquisition.[3] Specifically, new multipinhole cameras with cadmium-zinc-telluride solid state detectors (CZT-SPECT) technology allow for faster image acquisition and lower radiation doses in comparison with traditional Sodium-Iodine Anger cameras. This allows for 1-day stress/rest MPI protocols, preserving diagnostic image quality and diagnostic accuracy.[4,5] The CZT technology improves the energy and spatial resolutions, while using simultaneously acquired views improves the overall sensitivity, resulting in high-quality images.[6]

Previous examination of the prognostic value in specific groups, like the obese, demonstrated that CZT-SPECT provides adequate risk stratification.[7] However, there are little data comparing the prognostic value between ultrafast protocol CZT-SPECT and dedicated cardiac Na-I SPECT cameras. That could impair the broad use of this technology. Our objective is to compare the prognostic value of MPI using these two camera protocols.

METHODS

Population and Study Design

We analyzed two different groups of patients clinically referred to a SPECT-MPI in an outpatient clinic between 2008 and 2012. Patients in group 1 scanned in Na-I SPECT cameras from 2008 to 2010, and in group 2 were scanned using CZT-SPECT from 2011 to 2012.

Ninety-nine patients who underwent revascularization in the first 60 days after nuclear testing were excluded, and history of significant cardiac valve disease or severe nonischemic cardiomyopathy (33 patients) or any condition which might adversely affect short-term prognosis were also considered exclusion criteria (Figure 1). Three patients were excluded because the images acquired in gamma camera CZT were inadequate for interpretation (BMI > 45). The research was approved by the institutional review board, and all subjects signed informed consent.

Prior to scanning, a team of cardiologists collected information on the presence of categorical cardiac risk factors in each individual including hypertension, diabetes, hypercholesterolemia, smoking, and family history of CAD using a standard questionnaire.

Cardiac symptoms were based on Diamond and Forrester criteria,[8] divided as asymptomatic, nonanginal pain, atypical angina, typical angina, and shortness of breath.

From a total of 6128 patients meeting inclusion criteria, follow-up was complete in 5828 (95.1% of the total); we selected 3554 using propensity score matching based on sex, age, body mass index (BMI), symptoms, cardiac risk factors, history of coronary events, and type of stress used. A 1 to 1 nearest neighbor matching with no replacement was performed to produce two groups with 1777 individuals in each, divided according to the type of gamma camera used.

Cardiac Imaging and Stress Protocol

Patients were instructed to abstain from any products containing caffeine for 24 hours before the test. Beta-blockers and calcium-channel antagonists were terminated 48 hours before testing, and nitrates were withheld for at least 6 hours before testing. Stress testing was performed with a symptom-limited Bruce treadmill exercise protocol or pharmacologic protocol (dipyridamole or dobutamine). In general, stress using dipyridamole was the first choice, while dobutamine was

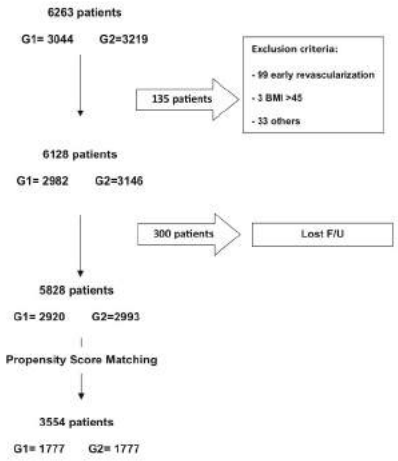

Figure 1. Flow diagram of the study.

reserved for patients with contraindications to vasodilator stress (mainly bronchospastic airway disease).

Patients in group 1 underwent 2-day Tc-99 m sestamibi (near-maximal exercise, 10-12 mCi was injected intravenously, and exercise was continued at maximal workload for at least 1 minute) gated MPS with scan time of 6 minutes stress and rest studies (15-18 mCi). Mean radiation dose was 9.5 mSv. Stress-only imaging was not performed due to reimbursement issues. Three minutes prone images were acquired in all male patients but gating was not performed. All supine images were gated. The full protocols used have been previously described.[9] MPI studies were classified as normal or abnormal, and perfusion scores (SSS, SRS, and SDS) were calculated. Images were acquired using a two-headed gamma camera equipped with 90°-angled detectors (Ventri, GE Healthcare, Waukesha, WI, USA) equipped with a low-energy, high-resolution collimator, and 30 stops in a 64 × 64 matrix. Image acquisition began 15-45 minutes after tracer injection. Scans were reconstructed with Evolution for Cardiac™ (GE healthcare), using 12 iterations. Poststress-gated short-axis images were processed using quantitative-gated SPECT software (QGS; Cedars-Sinai Medical Center, Los Angeles, California), and left ventricular ejection fraction (LVEF) was automatically calculated after inspection of myocardial contours.

Patients in group 2 underwent treadmill exercise or pharmacological stress using standard dipyridamole or dobutamine infusion protocols.[10] Exercise testing was performed using a symptom-limited Bruce protocol. A 1-day 99m-Tc-MIBI, rest/stress protocol was used, starting with rest study (injection of 5 mCi) followed by stress (15 mCi) in a CZT camera. Mean radiation dose was 6 mSv. The MPI were also classified as normal or abnormal and perfusion scores (SSS, SRS, and SDS) were also calculated. Poststress prone acquisitions were performed in all patients. CZT-SPECT was performed using a camera with multipinhole collimator (Discovery 530, GE Healthcare, Milwaukee, USA). The system design allows acquisition without detector or collimator motion. Images were acquired in 6, 3, and 1 minute, respectively, for rest, supine stress and prone stress, as previously described.[11] A 10% symmetric energy window at 140 keV was used. Images were reconstructed on a dedicated Xeleris workstation (GE Healthcare) applying an iterative reconstruction algorithm with maximum-likelihood expectation maximization. Assessment of image quality and perfusion abnormalities was performed visually by two experienced nuclear cardiologists blinded to patient characteristics. Poststress left ventricular volumes and ejection fraction were calculated from the poststress-gated images using commercially available software (QGS, Cedars-Sinai Medical Center, Los Angeles, California, USA).

In both group, semiquantitative visual interpretation of MPI images was performed with short-axis and vertical long-axis tomograms divided into 17 segments.[10] Each segment was scored by consensus of two expert observers (aware of clinical and stress data) using a 5-point scale (0 = normal; 1 = equivocal; 2 = moderate; 3 = severe reduction of tracer uptake; 4 = the absence of detectable radiotracer activity in a segment). Then, perfusion scores were calculated to express the extent and severity of myocardial perfusion abnormalities. The summed stress score (SSS, a measure of the total poststress perfusion defect) and summed rest score (SRS, a measure of rest defect or myocardial fibrosis) were obtained by means of adding the scores for the 17 segments of the stress and rest images, respectively. The difference between the SSS and SRS was defined as the summed difference score (SDS, a measure of reversible defect or myocardial ischemia). For the purpose of evaluating the SSS and the SDS as predictors of events, we performed separate analyses with different cut points for each perfusion variable. We classified SSS as abnormal when it was >3 and SDS when it was >1.

Follow-Up

Follow-up was performed by telephone interview every 6 months after MPI. Events were defined as all-cause death and nonfatal myocardial infarction (classified as hard events) and late revascularization (>60 days after MPI), by percutaneous coronary intervention (PCI) or bypass surgery (CABG). Events were confirmed through review of hospital charts or physician's records. Nonfatal myocardial infarction was defined based on the criteria of typical chest pain, elevated cardiac enzyme levels, and typical alterations of the electrocardiogram.[12]

Statistical Analysis

All statistical calculations were performed using SPSS (Version 17). Categorical variables are presented as frequencies and continuous variables as mean ± SD. Variables were compared with Pearson Chi-squared test for categorical variables and by Student's two sample *t* test for continuous variables. Event-free survival curves were constructed using the Kaplan-Meier methods to account for censored survival times and were compared with the log-rank test.

RESULTS

Patients were divided into group 1 and 2, each with of 1777 subjects, and its overall baseline characteristics are summarized in Table 1. There were no statistically significant differences between groups in regard of gender, prevalence of hypertension, diabetes, smoking, hypercholesterolemia, previous revascularization, and use of pharmacological stress. The more frequent indications in asymptomatic patients were a previous treadmill test with intermediate-high risk Duke score, pre-op risk stratification and a previous calcium score >100. Patients with previous MI or revascularization were considered to have known CAD. The mean follow-up interval was 34 ± 9 months in group 1 and 33 ± 8 months in group 2.

Comparing the two groups, the classification as normal or abnormal scans and the perfusion scores (SSS,

Table 1. Baseline characteristics

	Total (6128)	Select (3554)	Group 1 (1777)	Group 2 (1777)	*p* value
Age (years)	63.0 ± 12.3	62.8 ± 12.0	62. ± 12.0	62.9 ± 12.0	1
Male	3370 (55.0%)	1920 (54.0%)	949 (53.4%)	971 (54.6%)	0.46
Weight (kg)	78.5 ± 17.7	78.1 ± 16.6	77.9 ± 16.3	78.2 ± 16.9	0.47
BMI	28.0 ± 6.1	27.8 ± 5.9	27.7 ± 6.0	27.9 ± 6.0	0.26
Asymptomatic	4221 (68.9%)	2377 (66.9%)	1171 (65.9%)	1206 (67.9%)	0.21
Diabetes	1396 (22.8%)	815 (22.9%)	390 (21.9%)	425 (23.9%)	0.16
Hypertension	3908 (63.8%)	2165 (60.9%)	1081 (60.8%)	1084 (61.0%)	0.92
Hypercholesterolemia	3166 (51.7%)	1764 (49.8%)	885 (49.6%)	879 (49.5%)	0.84
Beta-blockers	1782 (29.1%)	1074 (30.2%)	541 (30.4%)	533 (30.0%)	0.39
ACEI	3247 (38.6%)	1365 (38.4%)	400 (22.5%)	410 (23.1%)	0.3
Statins	3062 (50.0%)	1777 (50.0%)	886 (49.9%)	891 (50.1%)	0.78
Previous MI	767 (12.5%)	439 (12.4%)	225 (12.7%)	214 (12.0%)	0.31
Previous PCI	1195 (19.5%)	628 (17.7%)	314 (17.7%)	314 (17.7%)	1
Previous CABG	550 (9.0%)	302 (8.5%)	159 (9.0%)	143 (8.0%)	0.34
Pharmacological stress	2566 (41.9%)	1458 (41.0%)	752 (42.3%)	706 (39.7%)	0.13

p value comparison between Group 1 and 2; n (%) or mean ± standard deviation
ACEI angiotensin-converting enzyme inhibitor; *BMI* body mass index; *CABG* coronary artery bypass; *MI* myocardial infarction; *PCI* percutaneous coronary intervention

Table 2. Scans results, perfusion scores, and gated SPECT measurements

	Group 1 (1777)	Group 2 (1777)	*p* value
Abnormal Scans	487 (27.4%)	383 (21.6%)	<0.001
Reversible	237 (13.3%)	154 (8.7%)	
Fixed	126 (7.1%)	128 (7.2%)	
Mixed defect	124 (7.0%)	101 (5.7%)	
SSS	2 (0-4)	1 (0-3)	<0.01
SRS	1 (1-3)	0 (0-2)	<0.01
SDS	0 (0-1)	0 (0-0)	<0.01
LVEF stress	58.5 ± 11.9	59.3 ± 13.0	0.07
EDV stress	80.1 ± 33.9	82.1 ± 33.5	0.1
ESV stress	36.4 ± 28.3	36.1 ± 26.5	0.7

EDV end diastolic volume; *ESV* end systolic volume; *LVEF* left ventricle ejection fraction; *SSS* summed stress score; *SRS* summed rest score; *SDS* summed difference score
Perfusion scores are expressed as median and interquintile 25 and 75

SRS, and SDS) were statistically different. Group 1 had more abnormal scans (27.4% vs 21.6%; $p < 0.001$) and higher SSS, SRS, and SDS than group 2. Scan results, perfusion scores, left ventricle ejection fraction, and ventricular volumes of both groups are summarized in Table 2.

During follow-up, 98 deaths and 48 myocardial infarctions, 188 percutaneous coronary interventions, and 48 coronary artery bypass graft surgeries occurred. Assessing data from patients with normal scans, it was found that the annualized hard events rate was higher in patients of Group 1 (1.0%/year vs 0.5%/year; $p < 0.01$), but the percentage of PCI and CABG were not different (0.9% vs 0.8%; 0.3% vs 0.1%, respectively; $p = NS$) comparing with Group 2. However, patients with abnormal scans had no significant difference between the two groups in regard of both annualized hard events (3.3%/year and 3.2%/year; p = NS) and percentage of revascularization (6.6% vs 6.3%, p = NS). Event rates comparison between two groups are demonstrated in Table 3. Kaplan-Meier cumulative survival comparing group 1 and 2 with normal or abnormal scan are shown in Figure 2 (hard events) and Figure 3 (late revascularization).

Table 3. Annualized event rate (%/year)

	Group 1		Group 2	
	Normal scan (*N* = 1290)	**Abnormal scan (*N* = 487)**	**Normal scan (*N* = 1394)**	**Abnormal scan (*N* = 383)**
Hard events	1.0*† (41)	3.3 (54)	0.5* (18)	3.2 (33)
Late Revasc	1.2*† (46)	4.2 (92)	0.7* (33)	3.3 (65)
Death	0.7*† (26)	2.3 (33)	0.5 *(16)	2.4 (23)
MI	0.4*† (15)	1.5 (21)	0.06* (2)	1.0 (10)
PCI	0.9* (36)	5.0 (72)	0.8* (30)	5.1 (50)
CABG	0.3* (10)	1.6 (20)	0.1* (3)	1.2 (15)

*Significant difference between normal and abnormal scan
†Significant difference between Group 1 and Group 2: (number of events)
CABG coronary artery bypass graft; *MI* myocardial infarction; *PCI* percutaneous coronary intervention

DISCUSSION

MPI is an established method for diagnostic and prognostic evaluation of patients with CAD.[1] However, two considerable limitations of this method are the prolonged time required to scan acquisition and the radiation dose.[13] New high-speed SPECT cameras using cadmium-zinc-telluride detectors are a new technology of gamma camera that allows shorter acquisition time and lower tracer doses.[14] Nevertheless, the prognostic value of this ultrafast, low-dose radiation, protocol is not yet established and has not been compared with the protocol in dedicated cardiac Na-I SPECT cameras.[15,17]

In an attempt to do this comparison, we studied two different groups with 1777 patients. They were standard to each other through a propensity score matching with the purpose of showing the association, in both groups, between scan results and the hard events rate. As can be seen in Table 1, the strict matching parameter we used produced two groups with very similar exposition to factors that could influence results.

Statistically significant differences in the distribution of perfusion scores (SSS, SRS, and SDS) and the classification as normal and abnormal scans were noted between the CZT camera and the conventional camera. The CZT camera having, on average, 6% less abnormal scans and lower SSS, SDS, and SRS as previously demonstrated by Oldan et al.[16] Results showed that the rate of events and myocardial revascularization was not higher in group 1. Someone might argue that the more frequently abnormal tests in Group 1 could mean greater accuracy of traditional equipments. In this case, a larger number of false negative tests should have occurred in Group 2, which did not happen. In fact patients with normal examination evaluated in CZT cameras showed a lower percentage of events.

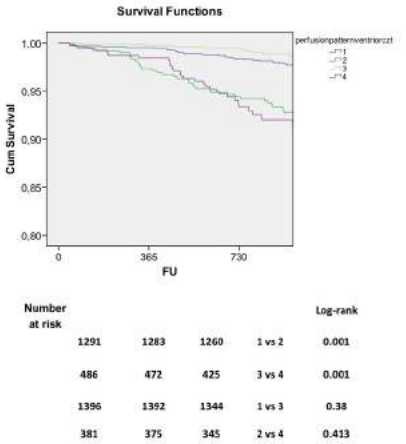

Figure 2. Kaplan-Meier curves for hard events. (1) Blue: Ventri normal scans; (2) Green: Ventri-abnormal scans; (3) Yellow: CZT normal scans; and (4) Purple: CZT abnormal scans.

In the follow-up data, our study has found that among patients with normal scans, the annualized hard events rate was higher in patients from traditional Na-I camera. The difference among hard event rate between both cameras may be an objective representation of the already known higher sensitivity for these new cameras, reflecting in a higher negative predicted value. In the follow-up of patients with abnormal scans, the study has

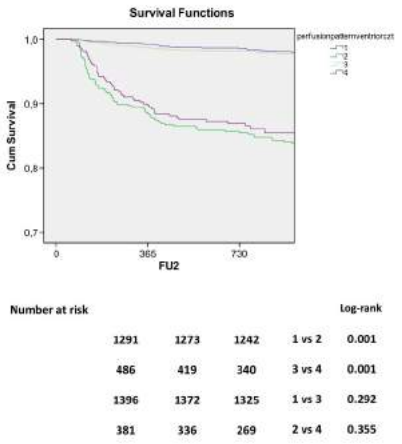

Number at risk				Log-rank
1291	1273	1242	1 vs 2	0.001
486	419	340	3 vs 4	0.001
1396	1372	1325	1 vs 3	0.292
381	336	269	2 vs 4	0.355

Figure 3. Kaplan-Meier curves for late revascularization. (1) Blue: Ventri normal scans; (2) Green: Ventri-abnormal scans; (3) Yellow: CZT normal scans; and (4) Purple: CZT abnormal scans.

shown no significant difference between the two groups in regard of both annualized hard events and percentage of revascularization. These data support that in patients with a higher probability of disease; both cameras were totally able to stratify the risk of events and thereby definitely established the MPI good prognostic value for patients with CAD.

There has been controversy regarding the diagnostic value of SPECT-MPI using CZT cameras in obese patients,[7] therefore the weight and BMI were included in the propensity score. As described in Population section, three patients were excluded because the images acquired in gamma camera CZT were inadequate for interpretation but more than 300 patients with at least 220 pounds were included in group 2. De Lorenzo et al demonstrated that in obese patients CZT-SPECT camera provides prognostic discrimination with high image quality and our data suggest. This is consistent with the results of the present study.

Our study was a retrospective analysis of outpatients who underwent CZT-SPECT or traditional Anger camera for clinical indications which carries the obvious and inherent bias of this type of study design. This is also a single-institution study and thus may not be applicable to others institutions and others types of camera designs, both CZT and conventional. Beyond that, reviewers were not blinded to clinical data. While this is necessary to clinical interpretation of scan results, it can bias the interpretation for research purposes. However, we can assume that any bias introduced by use of clinical information should affect both cameras in the same degree. Finally, it is important to stress that while the propensity score matching was successful in producing groups with similar baseline characteristics that could bias the results, there could be other potential unknown sources of bias that may not have been balanced in our two groups using this approach.

Analyzing the few data produced by similar studies,[15-17] we concluded that our study also showed a pattern of maintenance of the prognostic value of CZT comparing with traditional cameras. However, we had the opportunity to use a larger population that was matched in baseline characteristics and exposed to two totally different protocols. We used a standard protocol as mentioned before to dedicated Na-I cameras and a faster, lower-dose protocol in CZT-SPECT, something pioneer to this type of study.

NEW KNOWLEDGE GAINED

The CZT camera has similar utility for prognostication to conventional Anger cameras even when they are using smaller radiation doses and shorter acquisition time.

CONCLUSION

In our study, a new protocol of MPI in CZT-SPECT camera showed similar prognostic results to those obtained in dedicated cardiac Na-I SPECT camera, with lower prevalence of hard events in patients with normal scan. According to these data, we can assume that the new ultrafast protocol, using considerable lower dose of radiation, has a reliable prognostic value and is noninferior to traditional cameras.

Acknowledgments

The authors had no financial support for this research. The authors would like to thanks Dr. Ilan Gottlieb for his review and valuable suggestions.

Compliance with Ethical Standards

Disclosure *The authors declare that they have no conflict of interest.*

Ethical standards *All procedures performed in studies involving human participants were in accordance with the ethical standards of the institutional and/or national research*

committee and with the 1964 Helsinki declaration and its later amendments of comparable ethical standards.

Informed consent *Informed consent was obtained from all individual participants included in the study.*

References

1. Gimelli A, Rossi G, Landi P, Marzullo P, Iervasi G, L'abbate A, et al. Stress/rest myocardial perfusion abnormalities by gated SPECT: Still the best predictor of cardiac events in stable ischemic heart disease. J Nucl Med. 2009;50(4):546–53.
2. Underwood SR, Godman B, Salyani S, Ogle JR, Ell PJ. Economics of myocardial perfusion imaging in Europe—the EMPIRE Study. Eur Heart J. 1999;20(2):157–66.
3. De Puey EG. Advances in SPECT camera software and hardware: Currently available and new on the horizon. J Nucl Cardiol. 2012;19(3):551–81.
4. Duvall WL, Croft LB, Ginsberg ES, Einstein AJ, Guma KA, George T, et al. Reduced isotope dose and imaging time with a high-efficiency CZT SPECT camera. J Nucl Cardiol. 2011;18(5):847–57.
5. Herzog BA, Buechel RR, Katz R, Brueckner M, Husmann L, Burger IA, et al. Nuclear myocardial perfusion imaging with a cadmium-zinc-telluride detector technique: optimized protocol for scan time reduction. J Nucl Med. 2010;51(1):46–51.
6. Slomka PJ, Patton JA, Berman DS, Germano G. Advances in technical aspects of myocardial perfusion SPECT imaging. J Nucl Cardiol. 2009;16(2):255–76.
7. De Lorenzo A, Peclat T, Amaral AC, Lima RSL. Prognostic evaluation in obese patients using a dedicated multipinhole cadmium-zinc telluride SPECT camera. Int J Cardiovasc Imaging. 2015;2015:1–7.
8. Diamond GA, Forrester JS, Hirsch M, Staniloff HM, Vas R, Berman DS, et al. Application of conditional probability analysis to the clinical diagnosis of coronary artery disease. J Clin Investig. 1980;65(5):1210–21.
9. Lima R, De Lorenzo A, Camargo G, Oliveira G, Reis T, Peclat T, et al. Prognostic value of myocardium perfusion imaging with a new reconstruction algorithm. J Nucl Cardiol. 2014;21(1):149–57.
10. Henzlova MJ, Cerqueira MD, Hansen CL, Taillefer R, Yao S-S. ASNC imaging guidelines for nuclear cardiology procedures: stress protocols and tracers. J Nucl Cardiol. 2009. doi: 10.1007/s12350-009-9062-4.
11. Lima R, Peclat T, Amaral AC, Nakamoto A, Lavagnoli D, De Lorenzo A. Preliminary data on the prognostic value of a new protocol of ultra-fast myocardial scintigraphy with less radiation in CZT gamma camera. Arq Bras Cardiol: Im Cardiov. 2016;29(1):11–6.
12. Thygesen K, Alpert JS, White HD. Universal definitions of myocardial infarction. J Am Coll Cardiol. 2007;50:2173–95.
13. Douglas PS, Hendel RC, Cummings JE, Dent JM, Hodgson JM, Hoffmann U, et al. ACCF/ACR/AHA/ASE/ASNC/HRS/NASCI/RSNA/SAIP/SCAI/SCCT/SCMR 2008 Health Policy Statement on Structured Reporting in Cardiovascular Imaging. J Am Coll Cardiol. 2009;53:76–90.
14. Sharir T, Pinskiy M, Pardes A, Rochman A, Prokhorov V, Kovalski G, et al. Comparison of the diagnostic accuracies of very low stress-dose with standard-dose myocardial perfusion imaging: Automated quantification of one-day, stress-first SPECT using a CZT camera. J Nucl Card. 2016;23(1):11–20.
15. Gimelli A, Bottai M, Giorgetti A, Genovesi D, Kusch A, Ripoli A, et al. Comparison between ultrafast and standard single-photon emission CT in patients with coronary artery disease: a pilot study. Circ Cardiovasc Imaging. 2011;4(1):51–8.
16. Oldan JD, Shaw LK, Hofmann P, Phelan M, Nelson J, Pagnanelli R, et al. Prognostic value of the cadmium-zinc-telluride camera: A comparison with a conventional (Anger) camera. J Nucl Cardiol. 2015. doi:10.1007/s12350-015-0224-2.
17. Yokota S, Mouden M, Ottervanger JP, Engbers E, Knollema S, Timmer JR, et al. Prognostic value of normal stress-only myocardial perfusion imaging: a comparison between conventional and CZT-based SPECT. Eur J Nucl Med Mol Imaging. 2016;43(2):296–301.